

# Varsche Rivier 003: A Middle and Later Stone Age Site with Still Bay and Howiesons Poort Assemblages in Southern Namaqualand, South Africa

TERESA E. STEELE

*Department of Anthropology, One Shields Ave., University of California-Davis, Davis, CA 95616, USA; and, Department of Human Evolution, Max Planck Institute for Evolutionary Anthropology, Deutscher Platz 6, 04103, Leipzig, GERMANY; [testeele@ucdavis.edu](mailto:testeele@ucdavis.edu)*

ALEX MACKAY

*Centre for Archaeological Science, University of Wollongong, NSW 2522, AUSTRALIA; and, Department of Archaeology, University of Cape Town, Rondebosch 7701, SOUTH AFRICA; [amackay@uow.edu.au](mailto:amackay@uow.edu.au)*

KATHRYN E. FITZSIMMONS

*Department of Human Evolution, Max Planck Institute for Evolutionary Anthropology, Deutscher Platz 6, 04103, Leipzig, GERMANY; [Fitzsimmons@mpic.de](mailto:Fitzsimmons@mpic.de)*

MARINA IGREJA

*ENVARCH, CIBIO-INBIO, University of Porto, PORTUGAL; and, LAMPEA UMR 7269, CNRS, Aix-en-Provence, FRANCE; [dearaujo.igreja@mmsch.univ-aix.fr](mailto:dearaujo.igreja@mmsch.univ-aix.fr)*

BEN MARWICK

*Department of Anthropology, Denny Hall 117, Box 353100, University of Washington, Seattle, WA 98195-3100, USA; [bmarwick@uw.edu](mailto:bmarwick@uw.edu)*

JAYSON ORTON

*ASHA Consulting (Pty) Ltd, 6A Scarborough Road, Muizenberg, 7945; Department of Archaeology, University of Cape Town, Rondebosch 7701; and, Department of Anthropology and Archaeology, University of South Africa, Pretoria 003, SOUTH AFRICA; [jayson@asha-consulting.co.za](mailto:jayson@asha-consulting.co.za)*

STEVE SCHWORTZ

*Department of Anthropology, One Shields Ave., University of California-Davis, Davis CA 95616, USA; [schwortz@gmail.com](mailto:schwortz@gmail.com)*

MAREIKE C. STAHLSCHMIDT

*Institute for Archaeological Sciences, University of Tübingen, Rümelinstr. 23, 72070 Tübingen GERMANY; and, School of Archaeology, Newman Building, University College Dublin, Belfield, Dublin 4, IRELAND; [mareike.stahlschmidt@ucd.ie](mailto:mareike.stahlschmidt@ucd.ie)*

*submitted: 20 April 2016; revised: 28 August 2016; accepted 5 September 2016*

## ABSTRACT

Southern Africa presents the best-documented Middle and Later Stone Age (MSA and LSA) records in Africa, and yet significant uncertainties still exist concerning the sequence and timing of behavioral and occupational changes in the region. A recent surge in research has provided a suite of new results that indicate more intricate and complex patterns than those previously considered. This paper describes recent excavations at the archaeological site of Varsche Rivier (VR) 003 located in the poorly-researched southern Namaqualand (Knersvlakte) region of South Africa (Western Cape Province). Two seasons of excavations have revealed a long sequence of MSA and LSA cultural materials, including lithics, fauna, ostrich eggshell, marine mollusks, beads, and pigments; bedrock has yet to be reached anywhere in our excavations. Within the shelter, we have uncovered probable Howiesons Poort material, with overlying late MSA and capped by late Holocene LSA. On the slope, the deepest materials are earlier MSA, overlain by assemblages with affinities to the Still Bay and Howiesons Poort. In addition to providing descriptions of the lithic, faunal, and pigment assemblages, we report on the results of micromorphological analysis of the sediments and optically stimulated luminescence (OSL) and radiocarbon dating of the sequence. Based on the analysis of single-grain samples from both parts of the excavation, OSL age estimates suggest that the putative Howiesons Poort assemblages at VR003 were deposited 45.7–41.7 kya. While our results are stratigraphically consistent, they are substantially younger than any previously published Howiesons Poort chronologies.

We discuss the implications of these results in detail. When presenting the results of our analyses, we compare the VR003 assemblages to those from other sites in the region to address questions concerning lithic technology, stone material exploitation, chronology, ecology, and the significance of “complex” behaviors, such as early bead production and long distance transport of marine mollusks.

## INTRODUCTION

Paleoanthropologists generally agree that modern humans evolved in Africa during the Middle to Late Pleistocene; nevertheless, many critical details about our origins and evolutionary trajectory remain unclear. Using archaeological datasets, we often look to evidence of symbolic, innovative, and culturally transmitted behavior as indicative of modern cognition, and therefore identifying the appearance of these features plays a pivotal role in documenting our behavioral evolution. In southern Africa, the Still Bay (SB) and Howiesons Poort (HP) industries have received a great deal of attention in the discussion of these issues. The SB presents an early example of a dedicated bifacial point industry, including the use of pressure-flaking in point manufacture, as well as providing early evidence of engraving, the use of personal ornaments, and the production of bone tools (d’Errico et al. 2008; Henshilwood et al. 2001; 2002; 2004; Mourre et al. 2010). The HP features the production of standardized microlithic tools from blade blanks, often made using locally-scarce stone materials, and at some sites includes the engraving of ostrich eggshells (OES) with repeated motifs (Henshilwood et al. 2014; Parkington et al. 2006; Soriano et al. 2007; Texier et al. 2010; 2013; Wurz 1999). Both of these industries appear, at minimum, to antedate 60,000 years before present (Jacobs et al. 2008; 2013; Tribolo et al. 2013).

Intriguingly, in spite of their suggestively modern character, both of these industries appear and disappear within the Middle Stone Age (MSA). Subsequent technological developments are in some ways more similar to the earlier parts of the MSA. Moreover, recent research has thrown into question the accepted ages and ranges of the SB and HP (Feather 2015; Galbraith 2015; Guérin et al. 2013; Jacobs et al. 2008; 2013; Jacobs and Roberts 2015; Tribolo et al. 2009; 2013). Part of the problem arises from the paucity of known and well-resolved samples. The five SB sites thus far dated constitute the sum of samples excavated in the last 40 years (Högberg 2014; Porraz et al. 2013b; Villa et al. 2009; Vogel-sang et al. 2010; Wadley 2007). While the HP has been dated at more sites, the number of samples recovered with modern techniques and associated fauna remains small. In both cases, the bulk of known sites occur around the southern periphery of South Africa, resulting in a spatially-skewed understanding of their distribution and inter-regional character. Further complicating our knowledge of the SB and HP is the fact that they rarely occur together in the same site; thus far this succession is best known from Diepkloof (Rigaud et al. 2006) and Sibudu (Wadley 2007), although it has been indicated for Peer’s Cave (as cited in Henshilwood 2012), Apollo 11 (Vogelsang 1998; Vogelsang et al.

2010), and Umhlatuzana (Kaplan 1990). A consequence of these problems is that, despite their high profile, many core questions remain about the causes, nature, and significance of these industries.

The newly excavated site of Varsche Rivier (VR) 003 (southern Namaqualand, Western Cape Province, South Africa) provides an opportunity to investigate the SB and HP, and thus to provide new information on human behavioral evolution in southern Africa. As presented here, VR003 preserves both SB and HP industries within a longer sequence of MSA cultural history and it is outside of the well-documented coastal and montane zones, which account for the preponderance of well-documented MSA samples. In addition to large assemblages of stone artifacts, the site also has faunal preservation throughout the known sequence. Here we report on our findings, focusing on the results from our 2011 field season.

## AN OVERVIEW OF THE SITE

### ENVIRONMENTAL CONTEXT

Namaqualand is a narrow strip (<100km wide) that spans the coastal and hinterland region between the Olifants River in the south and the Orange (or Gariep) River in the north, along the west coast of South Africa (Figure 1). At the southern extremity of Namaqualand is the Knersvlakte, a low-lying quartz-gravel covered basin (created by the proto-Orange River) with low hills and shallow drainages just to the north of the Olifants River and the uplands of Matsikammaberg and to the west of the Bokkeveld Escarpment. These uplands provide sharp topographic relief which marks distinct physical (geological) boundaries that have significant implications for precipitation and vegetation (Desmet 2007). Namaqualand is part of the Succulent Karoo Biome, distinct from the better-known Fynbos Biome to the south. The Succulent Karoo is composed of a large number of leaf succulents and bulbs; within it, the Knersvlakte is biologically unique and best characterized by dwarf succulent shrubland or vygieveld, and tiny stone plants (Cowling and Pierce 1999; Manning 2008). The Succulent Karoo is a hot-spot of global biodiversity (Myers et al. 2000); in Namaqualand, according to Desmet (2007: 580), “18% of the total number of national vegetation types are to be found in less than 4% of the surface area of the country”, and about 25% of Namaqualand’s flora is endemic (Desmet 2007). Currently, the region is considered a desert; it receives less than 150mm of rainfall each year, and as part of southern Africa’s Winter Rainfall Zone (WRZ), this rain is concentrated in the winter months (Cowling and Pierce 1999). However, the rainfall is relatively reliable compared

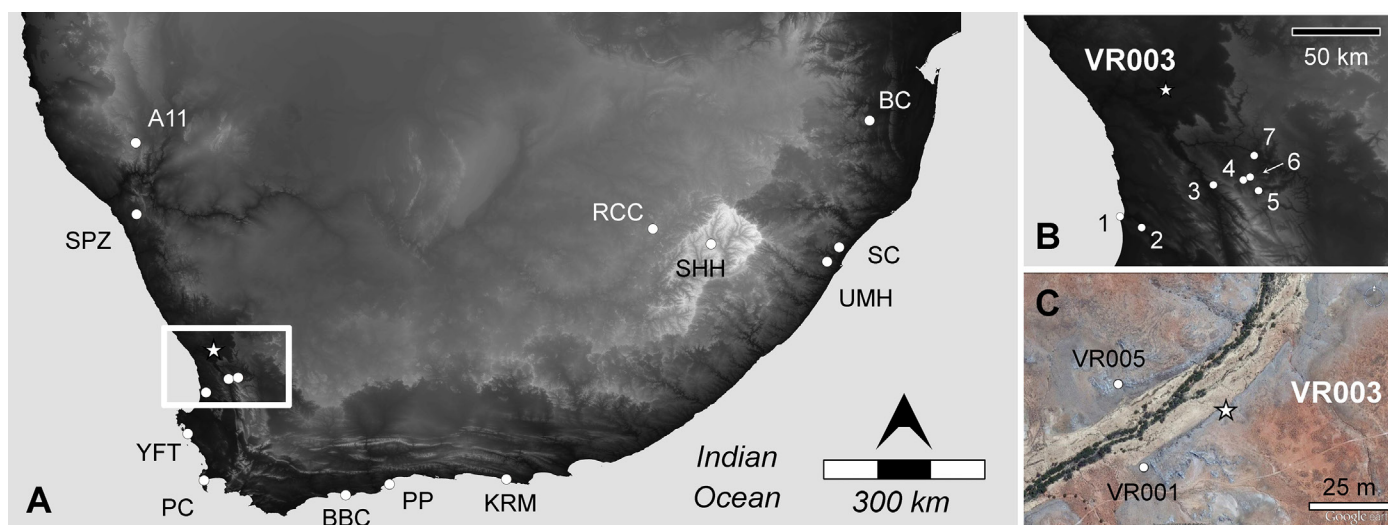


Figure 1. Location of Varsche Rivier (VR) 003 (star). (A) Prominent MSA sites in southern Africa, including Apollo 11 (A11), Blombos Cave (BBC), Border Cave (BC), Klasies River (KRM), Peers Cave (PC), Pinnacle Point (PP), Rose Cottage Cave (RCC), Sehonghong (SHH), Sibudu Cave (SC), Spitzkloof (SPZ), Umhlatuzana (UMH), Ysterfontein 1 (YFT). (B) Other excavated MSA sites near VR003, including Elands Bay Cave (1), Diepkloof Rock Shelter (2; DRS), Klein Kliphuis (3; KKH), Hollow Rock Shelter (4; HRS), Mertenhof Rock Shelter (5; MRS), Klipfonteinrand (6; KFR), and Putslaagte 8 (7; PL8). The borders of panel (B) are represented by the white box in (A). (C) Aerial photo of VR003 and other excavated sites in the kloof, the LSA sites of VR001 (Reception Shelter) and VR005 (Buzz Shelter). Digital elevation data for (A) and (B) from Jarvis et al. (2008); image in (C) courtesy of Google Earth.

to other desert regions (Desmet 2007). Additional moisture is provided by coastal fogs that are brought inland through river valleys and by intermittent rivers and streams that flow after storms when draining the eastern uplands. One of these rivers is the Varsche River, which forms the focus of our study region (Figures 2 and 3). The Varsche Rivier (a.k.a. Varsrivier) begins with the edge of the escarpment about 45km to the east, runs through our study area and then meets with the Sout River just west of VR003. The river continues as the Hol River until it joins the Olifants River; the Olifants continues on its south to north trajectory until it transitions to flow west to the Atlantic Ocean. VR003 is about 45km in a direct line from the current coast, but the distance would be longer following the meandering path of the rivers.

Much of the attention on Namaqualand focuses on the flora, and historically the large mammal communities, while diverse, have been sparse (Cowling and Pierce 1999; Hoffman and Rohde 2007; Skead 1980). Livestock thinly dot the landscape today, but in the recent past springbok (*Antidorcas marsupialis*), gemsbok (*Oryx gazella*), and hartebeest (*Alcelaphus buselaphus*) grazed the coastal plains, with black rhinoceros (*Diceros bicornis*) grazing in the scrubby areas; klipspringer (*Oreotragus oreotragus*), rhebok (*Pelea capreolus*), and mountain zebra (*Equus zebra*) stayed in rockier uplands. Eland (*Taurotragus oryx*) and quagga (*Equus quagga*) were also seen in the region historically. The larger perennial rivers such as the Orange supported megafauna such as giraffe (*Giraffa camelopardalis*), hippopotamus (*Hippopotamus amphibius*), and elephants (*Loxodonta africana*). Steenbok (*Raphicerus campestris*), common duiker (*Sylvicapra grimmia*), and ostrich (*Struthio camelus*) were seen through-

out the region, as well as small animals such as hyrax (*Procavia capensis*), hare (*Lepus* sp.), and tortoises (angulate or South African bowsprit tortoise [*Chersina angulata*], speckled padloper [*Homopus signatus*], and tent tortoise [*Psammobates tentorius*]). A variety of large carnivores roamed the region, including hyenas (brown [*Hyaena brunnea*] and spotted [*Crocuta crocuta*]), jackals (*Canis mesomelas*), caracals (*Caracal caracal*), leopards (*Panthera pardus*), and even lions (*Panthera leo*).

Paleoenvironmental reconstructions, based on the synthesis of multiple proxies, indicate that southern Namaqualand as part of the WRZ experienced increased humidity through increased winter rainfall during the cooler period of the Late Pleistocene (Chase and Meadows 2007), and archaeological records from the Holocene demonstrate the continuance of this pattern (Dewar 2008). Sediment cores from off the coast of Namibia identify increases in precipitation from 86–79 kya (~MIS 5b) and 72–58 kya (MIS 4), the latter of which encompasses the proposed antiquity of the HP and potentially the SB (Chase 2010). It is important to note, though, that while moisture on the landscape increased, the WRZ remained semi- to hyper-arid (Chase and Meadows 2007). However, both the winter and summer rainfall zones experienced aridification with the transition from MIS 4 to MIS 3, at approximately 58 kya.

## EXCAVATION HISTORY

As part of the Southern Namaqualand Archaeology Project (SNAP), in July 2009 we spent three weeks testing rock shelters in the limestone cliffs on the farm Varsche Rivier 260 (the farm name retains the Dutch version of the river name) and conducting surveys of surrounding open-air

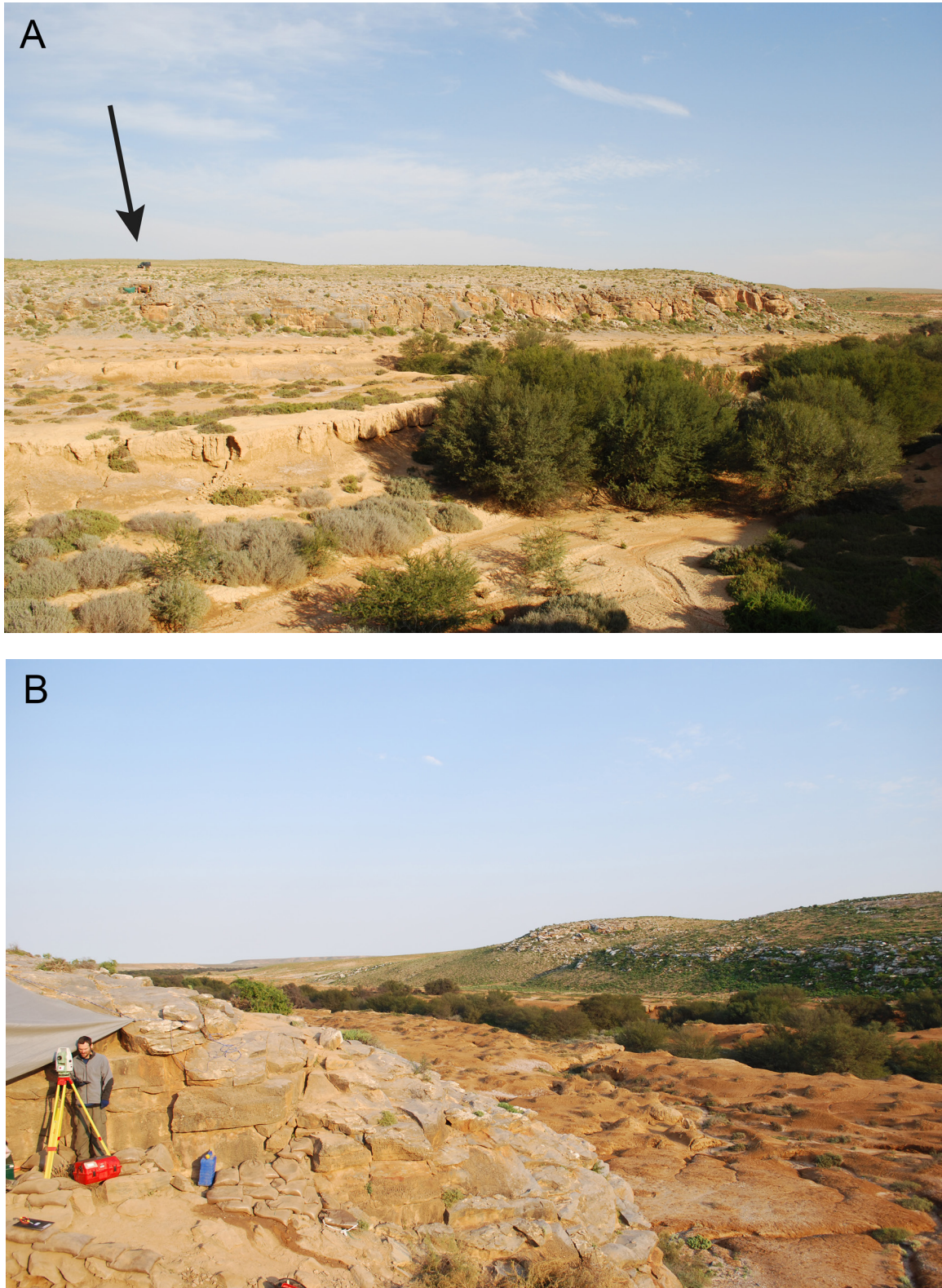


Figure 2. Environmental setting of VR003. In both photos the line of trees indicates the Varsche River valley with its extensive floodplain. (A) The VR003 excavation is visible in the left part of the image, just below the black vehicle (arrow); to the right, at the end of the cliffline, is a small cave, Reception Shelter (VR001), with late Holocene Later Stone Age material. (B) The extent of the Varsche River floodplain with VR003 above it.

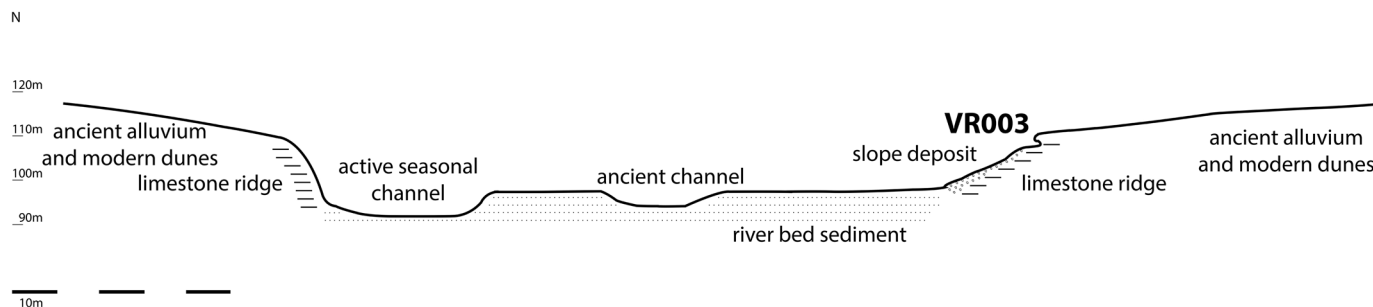


Figure 3. Schematic topographic cross section through the Varsche River valley at the site's location. The site of VR003 is located about 8m above the present river bed elevation. The river cut through the limestone bedrock and the riverbed is about 130m broad in front of the site. Further sediment sources are present on the plateau above the limestone with red sands, clays, soils, silcrete, and quartz outcrops.

sites. Our efforts exposed one MSA (VR003) (Steele et al. 2012) and two Later Stone Age (LSA; VR001=Reception Shelter and VR005=Buzz Shelter) (Orton et al. 2011b) rock shelter sequences and added numerous open-air occurrences to those previously documented (Orton 2012; Orton et al. 2011a), including the open-air bifacial point site of Soutfontein 001 (Mackay et al. 2010). Our 2009 test excavations at VR003 were sufficient to demonstrate the presence of extensive, stratified MSA deposits. VR003 is a rock shelter on top of a 26m long and 8m high slope above the Varsche River. The shelter is associated with a fault in the bedrock and a small 'chimney' connects the shelter with the plateau. Several large limestone boulders on the slope indicate past collapses of the shelter and served to preserve sediments in the shelter. Prior to excavation the shelter was almost filled to the top with sediments, but the depth of deposits beneath the remaining overhang indicate that it was much more accessible in the past. The back and bottom of the shelter have not been reached yet and the actual height, width, and depth of the shelter remain unknown.

During 2009, we opened two test pits (TP), one on the level upper surface of the site (TP-II) and one just downslope (TP-I). However, a large boulder separated the two units, which prevented us from stratigraphically linking the lower layers. We returned to VR003 for a one-month field season in July 2011 and we collected OSL samples in October 2011. During this fieldwork, we opened a long section to the grid west of the current excavation and linked the two previous units into one stratigraphic sequence with a 4m long profile, which we now refer to as the "Main Area" (Figure 4). In the process, our previous layer designations of I-03, II-04, etc. were unified and are now simply Layer 03, 04, etc. In addition, we brought the entire excavation deeper, and we identified eight archaeological layers (Layers 01–07 plus the deeper "s1", labeled as such because it was a 'deep sounding' and not yet clear if the deposits should remain 07 or be designated as 08) in six geological horizons (Figures 5 and 6; Table 1), which span the pre-SB/earlier MSA to post-HP. The site continued to reveal its po-

tential when we opened up a new test unit, "TP-III", inside the small extant rock shelter. This 1m x 1m unit, excavated to 1.2m, revealed 20 archaeological layers in nine geological horizons (Figures 7 and 8; Table 2). The upper fifteen archaeological layers contain mostly *in situ* late Holocene LSA materials. Layers III 16–20 are MSA, and the lowest levels so far excavated contain HP assemblages. We have not yet reached bedrock anywhere in the site. We provide more details about the site's stratigraphy, chronology, and archaeological assemblages as known through the end of the 2011 season below.

## EXCAVATION METHODOLOGY

The site's excavation grid (1m<sup>2</sup>) was established with the y-axis increasing towards the south (we have excavated squares 1022.0 to 1030.4) and the x-axis increasing towards the east (squares 1016.0 to 1018.0) (see Figure 4). All spatial data were recorded using a Leica TS02 PinPoint R400 total station connected to an HP iPAQ Pocket PC using the software developed by Dibble and McPherron (Dibble et al. 2007; Dibble and McPherron 1995; McPherron et al. 2005; McPherron and Dibble 2002). We excavate following the site's identifiable natural stratigraphy, which generally corresponds to our archaeological layers or horizons; we established these from archaeological material (artifact classes, density, etc.) combined with sedimentary characteristics. Geological horizons were defined based on color, texture, and sedimentary components (see Tables 1 and 2). During the test excavations, only cores, retouched pieces, and other notable finds (e.g., pigments, marine shell) were individually plotted, along with spatial data for each bucket of sediment. Each bucket was given a unique number and is considered as representing one "aggregate sample." All sediments were passed through 3mm and 1.5mm screens, using water for the Main Area materials. All these materials have been sorted into their appropriate artifact classes and submitted for analyses. For perpetuity, the assemblages will be curated at Iziko South African Museum (Cape Town).

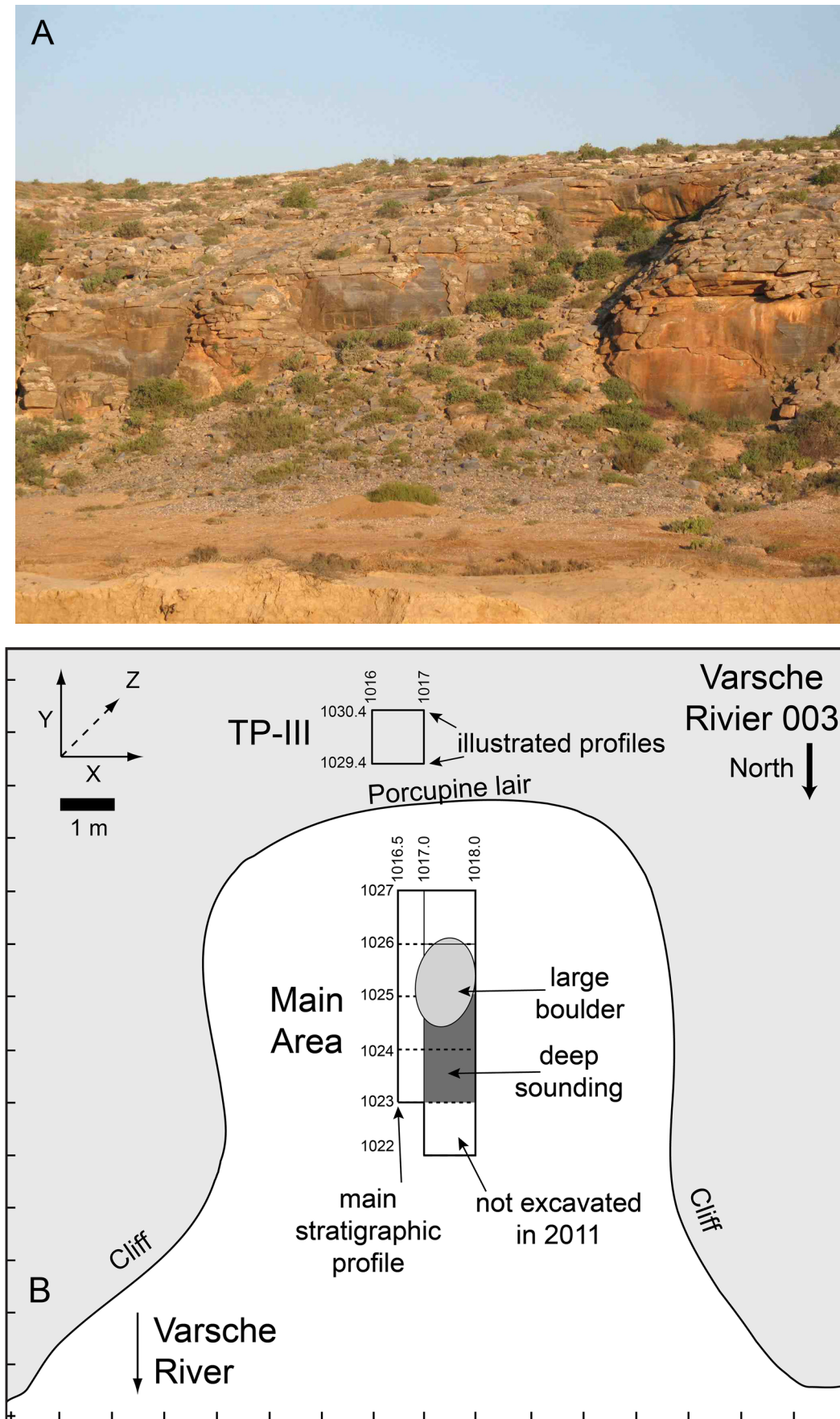


Figure 4. (A) View of VR003 before excavation began with one's back to the Varsche River, facing approximately southeast. (B) Plan view of the VR003 excavation at the end of the 2011 field season.



Figure 5. The Main Area eastern stratigraphic profile, as indicated in Figure 3 ( $y=1016.5$ ). The two notches highlighted in red show the sampling locations of block samples (MiMo) for micromorphological study (MiMo 1–5 is upslope/closer to the shelter and MiMo 6 and 7 are downslope).

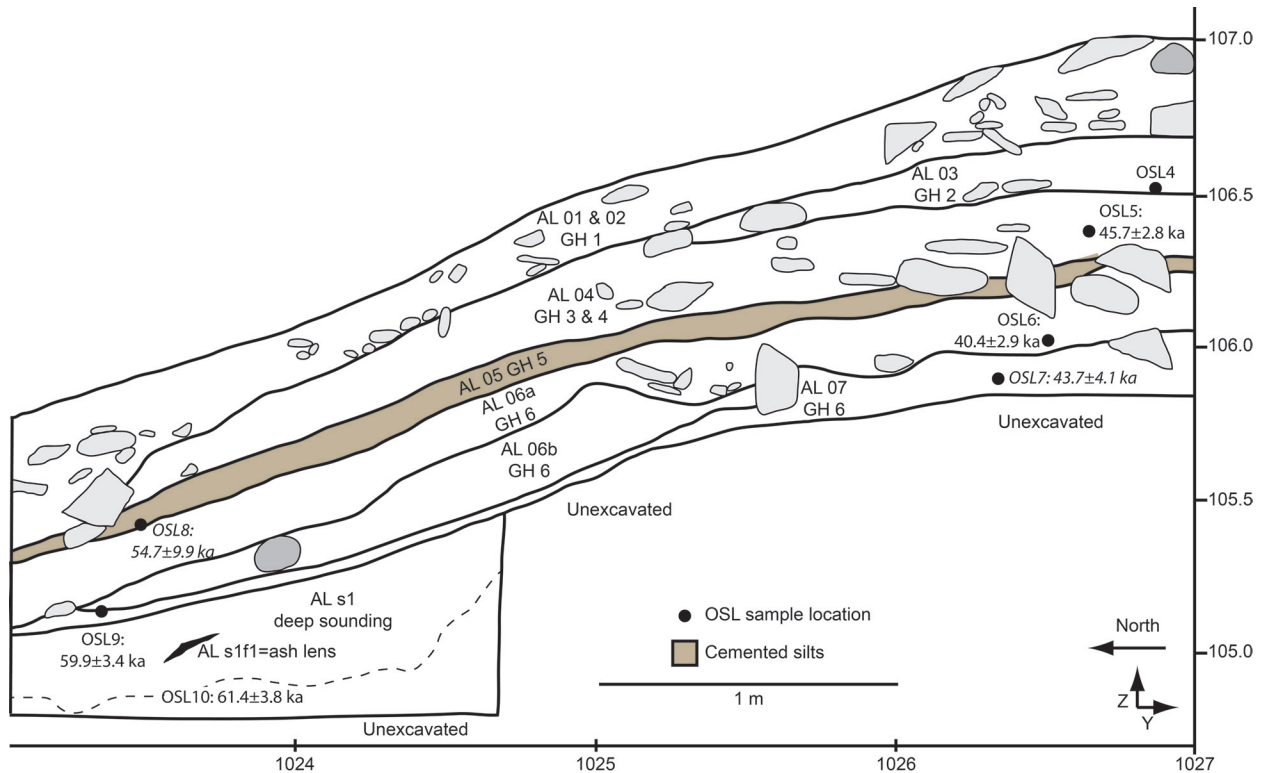


Figure 6. Illustration of the Archaeological Layers (AL) and Geological Horizons (GH) of the VR003 Main Area stratigraphic profile ( $y=1016.5$ ), shown in Figure 5. See Table 1 for descriptions of the sediments. OSL sampling locations and the reliable age estimates also are shown, with the less reliable estimates provided in italics (see Table 5); note that OSL10 was not taken in the illustrated section, but further west on the small  $y=1017$  profile from  $x=1022$  to 1023.

**TABLE 1. MAIN AREA: STRATIGRAPHIC SUMMARY OF THE MAIN EXCAVATION AREA BASED ON THE 2009 (Steele et al. 2012) AND 2011 EXCAVATIONS (published here)\*.**

| Old Archaeological Layer (Steele et al. 2012) | New Archaeological Layer (AL) | Geological Horizon (GH) | Lithostratigraphic Description**   | Archaeological Description  |
|---|-------------------------------|-------------------------|--|---|
| I-01  | 01                            | 1                       | angular limestone rubble with bioturbated silt, 10YR3/4 dark yellowish brown   | Loose disturbed surface otherwise equivalent to more compact Layer 02; large limestone rubble ranging in size from 1cm to 20cm; dark brown silt; organic/humic; significant bioturbation; abundant land snails and roots; about 5cm thick; primarily MSA with a few LSA items   |
| I-02  | 02                            |                         |  | Limestone rubble varying in size from a few mm to 30cm; orientation of the rubble: elongated pieces lying flat with a slight slope-downward dip in downslope part; brown to yellow grey silt; bioturbation; land snails and roots; about 15–25cm thick; primarily MSA with a few LSA items  |
| n/a   | 03<br>04                      | 2                       | angular limestone rubble with dry silt, 10YR4/4 dark yellowish brown   | Limestone rubble varying in size from a few mm to 30cm, increased number of small limestone rubble in up-slope part of the profile; orientation of the rubble: elongated pieces lying flat and in southern part of the profile horizontal while showing a slight slope-downward dip in the northern part; about 10cm thick, thinning out down-slope; abundant stone artifacts including laminar flakes, OES, and tortoise |
| I-03  | 04                            | 3                       | dry silt with angular limestone rubble, intersected by accumulation of larger rocks in the mid-section, 7.5YR4/4 brown | Limestone rubble varying in size from a few mm to 5cm (except mid-section with large limestone rubble), with higher proportion of small pieces; about 15–25cm thick; very rich in stone artifacts, OES, and bones; laminar flakes, backed artifacts, unifacial and bifacial points  |
| I-04  | 05                            | 4                       | dry silt, intersected by accumulation of larger rocks in the mid-section, calcretes, 7.5YR4/4 brown                    | Less and smaller limestone rubble than in the upper layer, except mid-section with big block and other large pieces; mid-section with some local calcretes; horizontal lens of rounded limestone rubble in downslope section; very rich in stone artifacts, OES, and bones; laminar flakes, backed artifacts, unifacial and bifacial points   |
| I-05  | 06<br>07                      | 5                       | layer of cemented silts/calcrete, bioturbated  | Cemented layer/calcrete visible in southern part and mid-section, in northern/down-slope part not visible (undclear if not present or not yet excavated); incorporating some limestone rubble of varying size (15cm to few mm); some bifacial/unifacial points  |
| I-05 (east)                                   | s1                            | 6                       | silt, 10YR3/3 dark brown   | Soft brown silt with very few small pieces of limestone rubble; moist; some cemented clasts present; decrease in artifact density   |
| I-05f1 (east)                                 | s1f1                          | n/a                     | silt, 10YR3/3 dark brown   | Soft brown silt with very few small pieces of limestone rubble; larger fragments of OES with well-preserved surfaces, increase in bone density; early MSA stone artifacts<br><i>Deep Sounding</i> ; fine silty sediment; some large limestone spall; several lenses and concentrations of cemented sediment (crust)   |
|   |                               |                         |  | Cemented ash lens within sounding   |

\*Before the first two excavation units were joined during the 2011 season, the northern end of the Main Excavation was Test Pit I and the southern end was Test Pit II, as indicated in the previous layer designations. Geological horizons (GH) were defined based on color, texture and sedimentary components, and are separate from the archaeological layers (AL), which were defined based on archaeological materials combined with sedimentary characteristics.

\*\*Color described with the Munsell Soil Color Chart after wetting the sample slightly.



Figure 7. Test Pit III: (A) during excavation; (B) the south ( $x=1030.4$ ) profile at the end of the 2011 season.

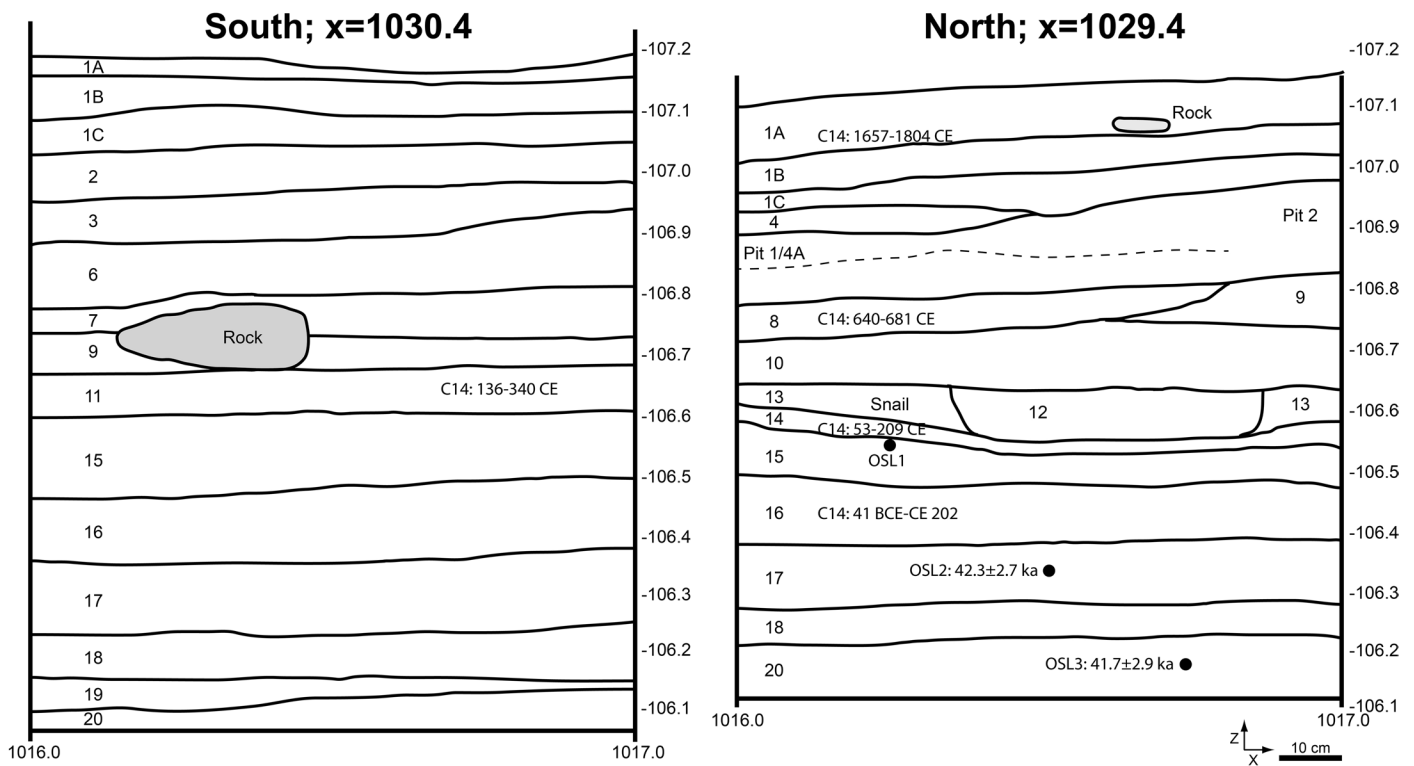


Figure 8. Test Pit III: Illustrations of the (A) deeper into the shelter (south;  $x=1030.4$ ) and (B) closer to the opening (north;  $x=1029.4$ ) stratigraphic profiles. The Archaeological Layers are indicated; Table 2 provides the associated Geological Horizons and sediment descriptions. The Archaeological Layers are not continuously numbered because some layers were only present in one profile and a few layers were not present in either profile. Tables 4 and 5 provide more details of dating samples.

## GEOARCHAEOLOGY

The geoarchaeological research at VR003 is directed at understanding the formation of the site, documenting the stratigraphic succession, connecting the stratigraphic succession of the multiple excavation areas, comparing the formation processes in the shelter and on the slope, analyzing the integrity of the archaeological deposits, and integrating the site into the landscape. For this aim, in the 2011 field season a survey of the surrounding landscape was conducted, a standard stratigraphic description was carried out in both excavation areas, loose samples were collected at the site and the surrounding area, and block samples were taken for micromorphological study.

## MATERIALS AND METHODS

The geoarchaeological research consisted of two parts, an exploration of the surrounding landscape and on-site study of the stratigraphy. To document the landscape, GPS points were taken at prominent points and at different possible sediment sources to the site. At these points, loose sediment samples and rock samples were collected as a reference collection for the landscape and site. Additional points were shot in with a total station for the preparation of a topographic profile from the tip of the limestone ridge above VR003 across the Varsche River bed to the north (see Figure 3). For the on-site study of the stratigraphy, geological horizons (GH) were defined based on color, texture, sedimen-

tary structures and components and are separate from the archaeologically defined horizons, which were defined by sedimentary and archaeological characteristics (see Tables 1 and 2 and Figure 6). Geological and archaeological horizons were numbered from top down, because we have not reached bedrock yet. In addition, 16 loose samples and 12 block samples were collected on site. Block samples were taken for micromorphological analysis, which was the main method of geoarchaeological investigation here. Nine of the 12 blocks were included in this study (MiMo = micromorphology; Table 3; one block produced two samples). Micromorphology is the microscopic study of intact blocks of sediments (see e.g., Courty et al. 1989; Stoops 2003); this technique provides insights into the formation of depositional units and their post-depositional alterations. In the current study, block samples stabilized with plaster were taken in the field. Once they were in the geoarchaeological laboratory in Tübingen, Germany, they were indurated with a mix of unpromoted polyester resin, styrene, and methyl ethyl ketone peroxide. Small blocks were then cut off, glued onto glass slides, and then ground to a thickness of  $30\mu\text{m}$ . Thin section production was conducted by T. Beckmann (Braunschweig, Germany) and P. Kritikakis (Tübingen, Germany) and 14 thin sections were produced for this study. Analysis was performed with a standard petrographic microscope at magnifications of 25x, 50x, 100x, 200x, and 500x using plane- and cross-polarized as well

TABLE 2. STRATIGRAPHIC SUMMARY OF TEST PIT III (TP-III), WHICH IS INSIDE THE SHELTER, BASED ON THE 2011 EXCAVATIONS\*.

| Archaeological Layer (AL) | Geological Horizon (GH) | Lithostratigraphic Description**  | Archaeological Description  |
|---------------------------|-------------------------|---|---|
| III-1A                    | 1                       | loose, bioturbated silt, faecal pellets, 10YR4/4 dark yellowish brown     | Loose surface material. Light orange silty soils with small (<3mm) degraded limestone inclusions. Contains large quantities of bone, twigs, and dassic pellets. Some limestone rocks on and within the matrix (30–400mm).   |
| III-1B                    |                         |   | A "crust" of moderately compact light orange/yellow/grey silts. Varied in thickness from 10mm in south to 80mm in north. OES, bone and some small artifacts.  |
| III-1C                    | 2                       | bioturbated silt with bone, OES and gravels, 10YR4/4 dark yellowish brown | Bedding layer - brown organic rich. Large amounts of bedding 'grass' in varied degrees of degradation, best preserved along the western edge of the excavation. Bone, OES (including some beads and many large unworked fragments), charcoal (flecks to 20mm), large flakes (silcrete, hornfels, quartz), and dassic pellets. |
| III-2                     |                         |   | Light orange/yellow grey silty sands in the northern half of the square. Top of this layer is slightly more compact than rest of layer. Small (<10mm) limestone gravels throughout, but in low densities. Some small (<100mm) dark brown organic rich lenses within the light orange/yellow silts.                            |
| III-3                     |                         |   | Sediment slightly more consolidated and slightly lighter in color (light orange/yellow grey). Inclusions of highly fragmented/degraded bone, bedding throughout, and limestone gravels (<10mm) throughout.  |
| III-4                     | 3                       | dry silt with anthropogenic bedding features, 10R3/6 dark yellowish brown | Patchy darker orange/yellow silt layer with dark brown organic mottled inclusions throughout with darker more intense orange areas that have a burnt appearance. Layer confined to the northern portion of the square. Only a few larger bone and OES fragments, and only a few charcoal inclusions.                          |
| III-4A                    |                         |   | Similar to Layer 1C (bedding layer), although slightly darker brown. This layer starts at the base of Layer 1 and truncates Layers 3, 4, and 5. The bottom half of this layer is much lighter in color than the matrix above, but organic nature of sediment continued.   |
| III-5                     |                         |   | Thin consolidated silt layer; light/moderate orange/yellow in color. Truncated in the north by Layer 4A and not preserved in any of the sections. Some large fragments of bone throughout.  |
| III-6                     |                         |   | Loose fine silty layer with slight variation in color. Very light orange/yellow in SE corner and gradually darkens towards the north. There are tiny fragments (<5mm) of bone and grasses and degraded limestone gravels (<15mm) throughout. Several large OES fragments and larger limestone inclusions occur infrequently.  |
| III-7                     |                         |   | More consolidated with more white mineral flecks present in the east. Large OES fragments and a few small limestone gravels occur throughout. Does not extend in the northern portion of the square. Truncated by Layer 4A and Layer 8.   |
| III-8                     | 4                       | dry silt with white concretions, bones, and OES                           | Brown organic sediment. Large (10–30mm) charcoal inclusions throughout.   |
| III-9                     |                         |   | Large amounts of OES, snail, and bone.  |
| III-10                    | 5                       | dry silt with charcoal, bones and OES, 10YR4/4 dark yellowish brown       | Darker orange/yellow grey silts. Loose/moderate compaction. Speckled white small mineral flecks throughout with a higher concentration in the NE corner. Increase in stone artifact density.  |
| III-11                    |                         |   | Predominantly fine orange/yellow grey silty sand with abundant charcoal flecks and more consolidated black patches around the edges. Ash lens enter the northern section below which the sediments become much greyer.  |
| III-12                    |                         |   | Semi-compacted gritty yellow to brown grey silts with fragments of rock (30–50mm). OES is common but much of it is bedded at different angles.  |
|                           |                         |   | Dark brown sticky sediment. Very organic rich. Possibly part of a burrow/warren. Dense snails; OES and bone also are present. Sharp contact with layer above and below; only occurs in a small area of the northern portion.  |

**TABLE 2. STRATIGRAPHIC SUMMARY OF TEST PIT III (TP-III), WHICH IS INSIDE THE SHELTER, BASED ON THE 2011 EXCAVATIONS (continued)\*.**

| Archaeological Layer (AL) | Geological Horizon (GH) | Lithostratigraphic Description**                                 | Archaeological Description  |
|---------------------------|-------------------------|--|---|
| III-13                    | Snail                   | Horizontal layer of snails, 7.5YR 3/2 dark brown                 | Orange/yellow grey silt defined by large number of complete and fragmented snails. Other organics are present within this layer including OES, bone and charcoal flecks (5–15 mm). Layer 12 truncated Layer 13. |
| III-14                    | 6                       | Compact silt with small limestone rubble, 7.5YR 4/3-4/4 brown    | Light orange/yellow grey fine silt. Sharp transition with layer above and below. Stone artifacts, snail, bone and OES are still present, but occur in lower numbers. Only occurs in the northern portion.       |
| III-15                    |                         |  | Gravelly, brown to orange/yellow grey silt. Calcrete pieces (<200 mm) occur in SW corner; possible root casts. Flat, bedded rocks (100 – 200 mm) occur throughout.  |
| III-16                    | 7                       | Compact silt with medium sized limestone rubble, 7.5YR 4/4 brown | Gravelly brown-orange/yellow grey silts. Gradual transition between layer 15 and 16; defined by an increase in consolidation, increase in density of gravels, and decrease in the number of root casts.         |
| III-17                    | 8                       | Less compact silt, 10YR 3/3 dark brown                           | Similar to Layer 16 but with an increase in the density of stone artifacts and OES, as well as the increase in larger rocks.  |
| III-18                    |                         |  | Loose, patchy brown and orange/yellow grey silts. Small (5–20 mm) gravels in moderate density throughout.   |
| III-19                    |                         |  | Compact orange/yellow grey silty sands. Quite thin and only in the south; thickest in SE. Gravels are cemented throughout the layer. Quite low density of artifacts.  |
| III-20                    | 9                       | Soft silt, 7.5YR 2.5/2 very dark brown                           | Brown very fine silt layer. Darker towards the north. Artifact density increases, many flakes with vertical orientation.  |

\*Geological horizons (GH) were defined based on color, texture, and sedimentary components, and are separate from the archaeological layers (AL), which were defined based on archaeological materials combined with more detailed sedimentary characteristics.

\*\*Color described with the Munsell Soil Color Chart after wetting the sample slightly.

**TABLE 3. LOCATION OF GEOLOGICAL SAMPLES STUDIED FROM THE 2011 FIELD SEASON AT VARSCHE RIVIER 003\*.**

| <b>MICROMORPHOLOGY</b>      |                            |  |                     |                |
|-----------------------------|----------------------------|--|---------------------|----------------|
| <b>Sample blocks (MiMo)</b> | <b>Excavation area</b>     | <b>Geological horizon (GH)<br/>Archaeological layer (AL)</b> | <b>Square (X/Y)</b> | <b>Z-value</b> |
| VR3-11-1                    | Main Area (south)          | GH 2-3 (AL 03-04)  | 1016.5/1025         | 106.48         |
| VR3-11-3                    | Main Area (south)          | GH 4 (AL 05)   | 1016.5/1025         | 106.23         |
| VR3-11-4A                   | Main Area (south)          | GH 4-5 (AL 05)   | 1016.5/1025         | 106.08         |
| VR3-11-4B                   | Main Area (south)          | GH 4-5 (AL 05)   | 1016.5/1025         | 106.06         |
| VR3-11-5                    | Main Area (south)          | GH 6 (AL 07)   | 1016.5/1025         | 105.93         |
| VR3-11-6                    | Main Area (north)          | GH 5-6 (AL 05&7)   | 1016.5/1023         | 105.57         |
| VR3-11-7                    | Main Area (north)          | GH 6 (AL 07)   | 1016.5/1023         | 105.39         |
| VR3-11-8                    | TP-III: Inside the Shelter | GH 6-7 (AL III-15-16)  | 1016.0/1029         | 106.53         |
| VR3-11-10                   | TP-III: Inside the Shelter | GH 8-9 (AL III-17-20)  | 1016.0/1029         | 106.35         |
| VR3-11-11                   | TP-III: Inside the Shelter | GH 9 (AL III-20)   | 1016.0/1029         | 106.2          |

\*For the Main Area, the micromorphology sample (MiMo) locations are shown in Figure 5.

as blue-light florescence. Thin section description follows Courty et al. (1989), Stoops (2003) and Stoops et al. (2010).

## RESULTS

### Macroscopic Analysis

The stratigraphic successions of the Main Excavation Area and TP-III are described in detail in Tables 1 and 2 and illustrated in Figures 6 and 8 and the following presents a summary of macroscopic field observations. In the Main Area, starting from the top, Geological Horizons 1–3 contain a range of unsorted limestone rubble in grey sandy silt matrix with many bioturbation features, such as roots and channels. From Geological Horizon 1, the surface layer, through Geological Horizon 2 to Geological Horizon 3, a decrease in bioturbation features, such as roots and other organic matter, is evident. A huge limestone boulder associated with numerous large limestone debris (see Figures 4 and 5) divides Geological Horizon 3, along with Geological Horizons 4 and 5 below, into upper-slope (south) and down-slope (north) parts; they differ mainly in the more horizontal orientation of limestone rubble in the upper slope part where the boulder served as a sediment trap. Geological Horizons 4 and 5 also consist of limestone rubble in a grey sandy silt matrix, but the limestone rubble has a smaller size than the upper layers. In addition, Geological Horizons 4 and 5 are characterized by horizontal calcareous crust structures. Geological Horizon 5 presents one continuous hardpan structure, which coincides with the bottom of the large limestone boulder mentioned above. In the lower slope part, Geological Horizon 4 and 5 are less expressed. The lowermost Geological Horizon, 6, consists of fine brown silt with much less limestone rubble than above. All geological units show a slight dip down the slope parallel to the modern surface, which is less expressed in upslope Geological Horizons 3–5 (see above).

In the area of the original Test Pit I, we excavated a ‘deep sounding’, which we label Archaeological Layer s1; further excavation will reveal the most appropriate archaeological and geological attributions (see Table 1). Layer s1 incorporates different depositional conditions. The upper parts of the unit are immediately downslope of the large boulder and formed after the boulder was deposited. The lower parts of the unit, however, antedate the deposition of the boulder, and may thus be more strongly related to the general slope of the deposit.

The sedimentary sequence in TP-III, which is inside the shelter, is quite different and it can be divided into an upper, more anthropogenic part with LSA artifacts and a lower, more geogenic part with the MSA components (see Table 2 and Figures 7 and 8). The upper LSA part of the sequence was separated into Geological Horizons 1 to 5. Geological Horizon 1 is the bioturbated surface. Below, Geological Horizon 2 is a grey to brown silt with many organic remains like modern roots, bones, and shells. Geological Horizon 3 is composed of layered organic materials (primarily plant materials), presumably for use as bedding, as has been documented in other recent LSA contexts from the region (Orton et al. 2011b; Parkington and Poggenpoel 1971, 1987; van Rissen and Avery 1992). Geological Horizon 4 is defined by the presence of white calcareous nodules in the brownish grey silt matrix. Geological Horizon 5 is characterized by numerous charcoal fragments and some white possible ash lenses. A horizontal layer of land snail shells in the northern profile separates the upper LSA and lower MSA part of the stratigraphic sequence. The lower MSA part was divided into four geological horizons, Geological Horizon 6 to 9. Geological Horizons 6 and 7 both consist of pebble-sized limestone rubble in yellowish grey sandy silt with Geological Horizon 7 being more compact. Geological Horizon 8 presents a transitional horizon to Geological Horizon 9 and shows a decrease in limestone rubble and

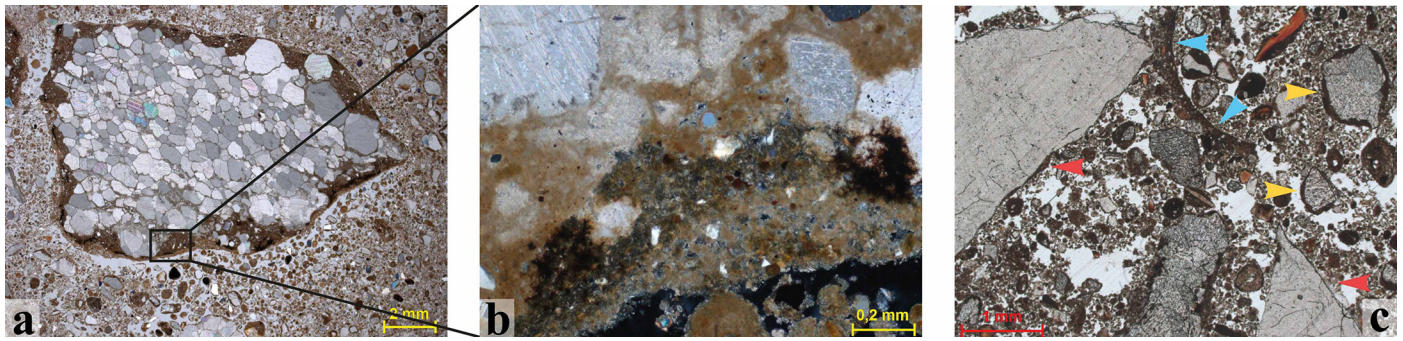


Figure 9. Microphotographs of the coating on coarse grains in the Main Area. (A) Thick coating on coarse grains, here limestone rubble, by fine material in Geological Horizon 3. Note how all the fine material ( $>10\mu\text{m}$ ) is arranged in globular shape. Plane-polarized light (PPL), scale at right bottom 2mm. (B) Zoom onto the coating of the microphotograph 9A showing that the coating often consists of several layers of coating, clayish and calcareous, and incorporates silt sized grains. Cross-polarized light (XPL), scale at right bottom 0.2mm. (C) Coating of all coarse grains (yellow arrows) in Geological Horizon 6, but microdebitage (red arrows) showing only thin to no coating. Note also a circular burrow (blue arrow) as a bioturbation feature. PPL, scale at lower left 1mm.

a slightly brownish grey color. The lowermost horizon, Geological Horizon 9, consists of brown silt similar to the brown silt in the Main Area, Geological Horizon 6, but only few centimeters of this layer were observable at the end of the field season 2011.

### Micromorphological Analysis

Micromorphological analyses were conducted on 14 thin sections, encompassing Geological Horizon 2 to 6 in the Main Area (MiMos in Figure 5) and Geological Horizon 6 to 9 inside the shelter (TP-III), all presenting MSA-bearing horizons. Table S1 provides the detailed results of the micromorphological analyses for each geological horizon, and the following is a summary of the micromorphological highlights.

All analyzed horizons in the Main Area have a calcareous groundmass with a lower clay component. Coarse components are sparry limestone rubble (Figure 9a), sand-sized calcite crystals, sand to silt sized quartz, bone fragments, ostrich eggshell fragments, and geogenic calcite pendant fragments (which form by the precipitation of calcite with percolating water on the lower surface of grains or on walls). Possible microdebitage (Figure 9c) and a few lenticular gypsum crystals are also present. The microstructure is micro-granular and spongy with thick, multilayered coatings of coarse grains by calcareous and clayey fine material (see Figure 9a-c; Figure 12c). Coating of coarse grains is less expressed in the brown sandy silt of Geological Horizon 6 (Figure 11a). Interestingly, only thin or no coatings were observed on angular quartz, quartzite and silcrete microdebitage (see Figure 9c). However, all observed bone fragments show thick coating. Bioturbation features are present in all horizons, e.g., in the form of burrows, channels, rhizoliths, and redox features, and transported soil aggregates are of regular appearance (Figure 12a-c). Translocation processes, like root action, burrows, and channels, caused local movement of fine sediment particles, e.g., quartz grains, and produced some homogenization (granular microstructure) of the layers, but probably did not af-

fect spatial patterning of larger sediment components such as artifacts; note that bioturbation is less intense in the less rocky deposits beneath the overhang (see below).

In Geological Horizon 4 and 5 dense calcareous areas were observed representing the calcareous crust as observed in the field. The calcareous crust is micritic, incorporates coated grains, bone fragments, plant pseudomorphs, and is dissected by some channels and vughs (see Figure 10a-c). No carbonate depletion was observed in the overlying Geological Horizons 4 and 3, while the lower geological horizon shows a lower carbonate content (see below). Burnt remains are present in Geological Horizon 4 to 6 in the form of reddened, predominantly sand-sized bone fragments, few charcoal fragments, and bone char (see Figure 11a, 12b). Geological Horizon 6 is characterized by an increased presence of reddened, sand-sized bone fragments, higher clay content in the matrix compared to the above horizons, and less limestone rubble (see Figure 11a, 12b); it shows the same micro-granular to spongy microstructure and coating, but less thick, as the upper horizons.

The picture is quite different inside the shelter in TP-III, but the analyzed thin sections generally show the same characteristics. The microstructure of Geological Horizons 6 to 8 is predominantly spongy and less micro-granular. The fine material is generally not arranged in coatings (see Figure 11a, c) in contrast to the slope deposits. Bioturbation features are less frequent, whereas transported soil aggregates were regularly observed. Intense gypsum formation was observed in all analyzed horizons (see Figure 11b, c). Otherwise no difference in coarse components was observed. The groundmass is dominantly calcareous in Geological Horizon 6 to 8, but clayish in Geological Horizon 9 (see Figure 11c) and here only calcareous in association with a channel feature.

### DISCUSSION

In the Main Area, on the slope, the most intriguing microscopic sedimentary feature is the round coating of all coarse grains throughout the sequence. Coating on coarse



Figure 10. Microphotographs on the calcareous crust in Geological Horizon 4 and 5 in the Main Area. (A) The calcareous crust shows a dense microfascies dissected by channels with a more granular microstructure. PPL, scale at lower right 1mm. (B) The calcareous crust incorporates coated grains and coated bone fragments (yellow arrows). PPL, scale at upper right 1mm. (C) Zoom into the crust showing a calcitic crystalline *b*-fabric, micritic calcite, a rough microstructure (blue arrow) and some plant pseudomorphs (purple arrows). XPL, scale at lower right 0.1mm.



Figure 11. Brown silt in Geological Horizon 6 in the Main Area and in Geological Horizon 9 in Test Pit III. (A) Brown silt in the main excavation area showing a speckled to calcitic crystalline *b*-fabric with brownish organic staining. Note also the black bone char fragment in the middle of the photograph and the less intense coating on coarse grains. XPL, scale at lower right 0.2mm. (B) Abundant lenticular, secondary gypsum (yellow arrows) forming inside the shelter, in Test Pit III. XPL, scale at lower right 1mm. (C) Brown silt inside the shelter, Test Pit III, shows a dominantly clayish matrix in Geological Horizon 9 and lenticular gypsum. Note that the fine material is not arranged in coatings. XPL, scale at lower right 0.2mm.

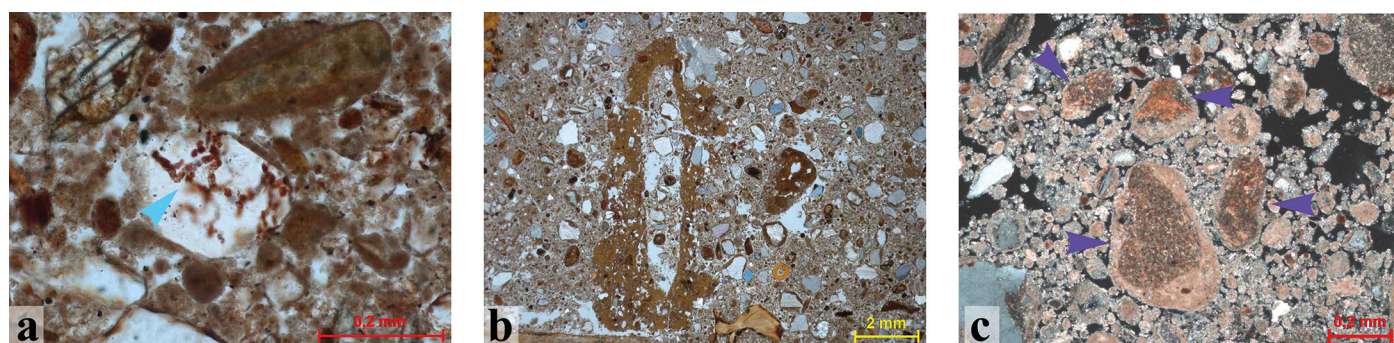


Figure 12. Bioturbation features. (A) Quartz grain with excrement (blue arrow) in Geological Horizon 6 of the Main Area. PPL, scale at lower right 0.2mm (B) Oxide feature in Geological Horizon 6 of the Main Area. Note the abundance of reddened bone (yellow arrows) and the absence of limestone rubble in this horizon. PPL, scale at lower right 2mm. (C) Transported soil aggregates (purple arrows) in Geological Horizon 4 in the Main Area. XPL, scale at lower right 0.2mm.

grains can be produced by colluvial processes (see, e.g., Bertrand and Texier 1999), freeze and thaw (see, e.g., van Vliet-Lanoë 2010), or calcrete formation (see, e.g., Braithwaite 1983; Candy et al. 2003; Wright and Tucker 1991). The round nature of the coating, its composition of several laminae and their position on the slope make a colluvial process combined with rolling on a wet surface the most likely explanation (Bertrand and Texier 1999; Hay and Reeder 1978; Rose et al. 2000). Concerning the calcareous crust, its formation is the result of subsurface redistribution of carbonates in these calcareous rich sediments (see, e.g., Rabenhorst and Wilding 1986). The plant pseudomorphs indicate a biogenic process of carbonate redistribution with plant and soil fauna as the driving factors (Wright and Tucker 1991), while the micritic nature of the calcite indicates rapid evaporation (Braithwaite 1983) as a process. A combination of these processes is not unusual (Wright and Tucker 1991). The calcareous crust incorporates coated grains and granules meaning that the colluvial deposition was followed by bioturbation and crust formation in Geological Horizons 4 and 5, with the latter being a sign of drier conditions as also indicated by minor gypsum formation here. The formation of the crust was then again followed by bioturbation dissecting the crust. The more organic and clay-rich sediment of Geological Horizon 6 indicate moister conditions than in the upper horizons. To summarize, we observe a change from moister conditions during the formation of the site to post-depositional alterations with drier conditions.

Within the shelter, as seen in TP-III, the conditions were generally much drier and more sheltered as the preservation of secondary gypsum and the absence of colluvial coating indicates. Nevertheless, soil aggregates are washed in through the chimney. The increased presence of clay in the protected deposits of the shelter might also indicate better preservation due to more sheltered conditions; clay particles are not washed away here by surface run-off in contrast to the slope deposits. This being said, the cause of the depositional change from a calcareous matrix to an almost carbonate depleted clay-rich matrix from Geological Horizon 6, 7, and 8 to Geological Horizon 9 is still unclear.

Of interest is the connection between the brown silt inside (GH 9) and outside the shelter (GH 6). While both horizons are characterized by a strong presence of burnt sand-sized bones, as is typical for Paleolithic layers (Miller 2015), and by an increased presence of clay compared to the upper horizons, some differences remain. Geological Horizon 6 on the slope has a more colluvial character and shows several bioturbation features whereas inside the shelter the sediments of Geological Horizon 9 do not show a transported character.

#### IMPLICATIONS FOR SITE FORMATION

This geoarchaeological research can inform on the primary or secondary depositional context of the sedimentary and archaeological materials on the slope and in the shelter. The micromorphological analysis reveals different formation processes and conditions on the slope from those inside the shelter, which have different implications for the

archaeological materials (i.e., the larger artifact classes) contained within the sediments. On the slope in the Main Area, sedimentary material exhibits local-scale re-deposition (reworking) and bioturbation. Bioturbation by roots and insects possibly caused post-depositional translocation of quartz grains. The influence of colluvial processes on archaeological materials is demonstrated by the presence of coating of small bone fragments; however, the absence of coating on microdebitage suggests that lithic clasts above sand-size (i.e., the stone artifacts) are generally in primary context. This is consistent with use-wear analysis of tool edges, which suggests most artifacts are well-preserved (see use-wear section below). In sum, the sequence in the Main Area is intact at the level of the geological horizon with evidence for within-horizon reworking of sediments and very fine clasts of archaeological material, but the larger archaeological materials (>3mm) are close to where they were deposited. Based on the sedimentary characteristics, sedimentary material inside the shelter (TP-III) presents mostly a primary context with minor root and insect bioturbation that possibly caused post-depositional translocation of quartz grains. There is no evidence to suggest significant translocation of archaeological materials.

#### CHRONOLOGY

To assess the chronological sequence of the VR003 deposits, we submitted five radiocarbon samples from the LSA deposits and ten optically stimulated luminescence (OSL) samples from the MSA deposits for analysis.

#### RADIOCARBON

Five samples of wood, bone collagen, and charcoal were submitted for AMS radiocarbon dating, and results were calibrated with OxCal 4.2.3 using the SHCal13 curve for the Southern Hemisphere (Bronk-Ramsey 2009; Hogg et al. 2013) (Table 4). The wood sample from the highest dated layer, III-1B/C (UGAMS11684) indicates recent occupation sometime between the mid-seventeenth century and the end of the eighteenth century CE in the uppermost deposits. Although this is the youngest radiocarbon date from the area, Reception Shelter contained historical material indicating contact period deposits (Orton et al. 2011b). However, no such artifacts were found at VR003. The bone collagen sample (UGAMS11685) from TP-III-8 indicates deposition between the mid-seventh and mid-eighth centuries CE. The remaining three dates, despite being from a span of six layers (III-11 to III-16), cluster within the 41 BCE to CE 340 range. Although the stone artifacts as described below might support minor mixing of the III-11 to III-16 deposits, the chronological ordering of these dates suggests that this is likely to be limited and does not significantly impact the overall interpretation. III-16 shows the most evidence for mixing between the LSA and MSA, which is consistent with this level incorporating the contact between the two.

#### OPTICALLY STIMULATED LUMINESCENCE

Ten optically stimulated luminescence (OSL) dating sam-

**TABLE 4. RADIOCARBON DATES FROM TP-III (calibrated with OxCal 4.2.3 using the SHCal13 curve for the Southern Hemisphere [Bronk-Ramsey 2009; Hogg et al. 2013]).**

| Lab. No.     | Archaeological Layer | Sample    | Radiocarbon date ( <sup>14</sup> C years BP) | Material      | Calibrated age (2 sigma) |
|--------------|----------------------|-----------|--|---------------|--------------------------|
| UGAMS11684   | III-1B/C             | VR003-393 | 220±20                                       | Wood          | 1657–1804 CE             |
| UGAMS11685   | III-8                | VR003-592 | 1410±20                                      | Bone collagen | 640–681 CE               |
| D-AMS 004516 | III-11               | VR003-674 | 1829±27                                      | Charcoal      | 136–340 CE               |
| D-AMS 004517 | III-14               | VR003-719 | 1930±28                                      | Charcoal      | 53–209 CE                |
| D-AMS 004518 | III-16               | VR003-818 | 1962±30                                      | Charcoal      | 41 BCE–CE 202            |

ples were collected from the site to provide a preliminary chronology of the deposits. Of these, eight provided age estimates which we interpret as reliable with respect to quality control criteria (Table 5); we discuss the results and this assessment in more detail below. The luminescence behavior and characteristics of the single grain analyses, combined with micromorphological data, suggest that general suitability of the site for OSL dating is limited by inhomogeneity of the sediment mineralogy and grain size, which affects the dose rate at the single grain level.

### OSL Methodology

OSL samples were collected from the northern and southern ends of the Main Area and from TP- III, which is inside the shelter, with the aim to support the field correlation between archaeological layers in addition to providing a chronologic framework (see Table 5). Archaeological layers that were relatively more fine-grained and contained fewer large boulders and exhibited minimal evidence for bioturbation were preferentially selected for sampling in order to reduce potential complications with dose rate calculations and mixed single grain age populations. In the Main Area, three samples were collected from the north end (downslope) from archaeological Layers 05, 06, and 07. Four samples were collected from the south end (upslope) of the Main Area, one each from Layers 03/04, the upper part of 04, and Layers 06 and 07. Three samples were collected from within the shelter—one from the lowermost dark organic layer containing artifacts corresponding to the HP (III-20), one from the overlying MSA-bearing unit (III-17), and one from the silty layer (III-15) that captures the transition between the MSA and LSA materials (see below for artifact descriptions).

OSL samples were collected by driving 4cm diameter, 10cm long stainless steel tubes horizontally into the cleaned, vertical surfaces of the excavation. The sample holes were then widened and deepened to accommodate a portable sodium iodide gamma spectrometer with a three-inch crystal detector. Sediment removed during this process was collected in a sealed plastic bag for moisture content and

laboratory measurements of radionuclide concentrations. Gamma spectra were measured within each hole for 1800 s.

In the laboratory, the OSL sample tubes were opened and the sediments processed under low intensity red light using previously published methods (Fitzsimmons et al. 2014). The 90–212µm quartz size fraction was extracted and used for equivalent dose ( $D_e$ ) measurement due to the relatively low yield of sand-sized material. The clean quartz grains were prepared as single grains (600 grains, 6 discs, per sample).  $D_e$  measurements were undertaken using the single aliquot regenerative dose (SAR) protocol of Murray and Wintle (2000, 2003) on an automated Risø TL-DA-20 reader with a single grain attachment (Botter-Jensen 1997; Botter-Jensen et al. 2000). Preheat and cutheat temperatures of 220°C and 200°C respectively were determined by the results of a preheat plateau test on sample EVA1130 (Figure 13a). All 600 individual grains measured from each sample were assessed for their suitability using a set of systematic selection criteria described in Fitzsimmons et al. (2014), and a dose recovery test (Figures 13b, c, d). In all cases, at least 50 grains were accepted for analysis for each sample, facilitating statistically robust age calculation (Rodnight 2008). The  $D_e$  and overdispersion values for the grains were then assessed using both radial plots (Galbraith 1990) and probability distribution functions (Figures 13e, f, S1). Overdispersion values are relatively large (see Table 5), considering the stratigraphic integrity and depositional processes of the sediments. This is most likely to be due to dose rate heterogeneity, although bioturbation at microscopic scales cannot be entirely precluded (see micromorphology above). For those samples yielding Gaussian  $D_e$  distributions, an overdispersion threshold of 35% was used in order to justify using the Central Age Model (CAM) of Galbraith et al. (1999) to calculate the age. For the remaining samples, the Finite Mixture Model (FMM) was used to isolate populations of grains and their proportion (Galbraith and Green 1990) (see Table 5; Table S2).

The gamma component of the dose rates was calculated using *in situ* gamma spectrometry and high resolution germanium gamma spectrometry (HRGS), measured

**TABLE 5. EQUIVALENT DOSE (D<sub>e</sub>), DOSES RATE DATA AND OSL AGE ESTIMATES FOR ALL TEN OF THE SAMPLES FROM VARSCHHE RIVIER 003\*.**

| Sample        | Archaeological Layer       | Depth (m) | De (Gy)                                       | Overdispersion (%) | Water content (%) | K (%)     | U (ppm)   | Th (ppm)  | Cosmic dose rate (Gy/ka) | Total dose rate (Gy/ka) | Age (ka)                                      |
|---------------|----------------------------|-----------|---|--------------------|-------------------|-----------|-----------|-----------|--------------------------|-------------------------|---|
| OSL1-EVA1129  | Inside the Shelter III-15  | 2.9±0.0   | 6.2±0.6 <sup>a</sup><br>56.4±2.3 <sup>a</sup> | 111                | 8±4               | 1.29±0.07 | 2.11±0.11 | 5.74±0.29 | 0.13±0.01                | 2.39±0.12               | 2.6±0.3 <sup>c</sup><br>23.6±1.6 <sup>c</sup> |
| OSL2-EVA1130  | Inside the Shelter III-17  | 3.1±0.0   | 86.6±2.8 <sup>b</sup>                         | 36                 | 5±4               | 1.03±0.05 | 2.25±0.11 | 5.16±0.26 | 0.13±0.01                | 2.05±0.10               | <b>42.3±2.7</b>                               |
| OSL3-EVA1131  | Inside the Shelter III-20  | 3.2±0.0   | 114±4 <sup>b</sup>                            | 28                 | 9±4               | 1.63±0.08 | 3.20±0.16 | 6.57±0.33 | 0.12±0.01                | 2.73±0.15               | <b>41.7±2.9</b>                               |
| OSL4-EVA1132  | Main Area (south) AL 03/04 | 0.5±0.0   | 85.2±6.8 <sup>a</sup>                         | 56                 | 3±2               | 0.85±0.04 | 1.91±0.10 | 3.95±0.20 | 0.17±0.02                | 1.92±0.09               | 44.5±4.2 <sup>c</sup>                         |
| OSL5-EVA1133  | Main Area (south) AL 04    | 0.6±0.0   | 98.4±3.8 <sup>b</sup>                         | 33                 | 5±4               | 1.00±0.05 | 2.51±0.13 | 4.66±0.23 | 0.17±0.02                | 2.15±0.10               | <b>45.7±2.8</b>                               |
| OSL6-EVA1134  | Main Area (south) AL 06    | 1.0±0.0   | 131±6 <sup>b</sup>                            | 35                 | 6±4               | 1.31±0.07 | 6.70±0.34 | 5.73±0.29 | 0.16±0.01                | 3.24±0.17               | <b>40.4±2.9</b>                               |
| OSL7-EVA1135  | Main Area (south) AL 07    | 1.2±0.0   | 121±9 <sup>a</sup>                            | 52                 | 9±4               | 1.30±0.07 | 4.30±0.22 | 5.75±0.29 | 0.16±0.01                | 2.77±0.14               | 43.7±4.1                                      |
| OSL8-EVA1136  | Main Area (north) AL 05    | 0.6±0.0   | 121±21 <sup>a</sup>                           | 44                 | 8±4               | 1.10±0.06 | 2.01±0.10 | 5.01±0.25 | 0.17±0.02                | 2.21±0.11               | 54.7±9.9                                      |
| OSL9-EVA1137  | Main Area (north) AL 06/07 | 0.7±0.0   | 126±3 <sup>b</sup>                            | 18                 | 10±4              | 1.06±0.05 | 1.95±0.10 | 4.73±0.24 | 0.17±0.02                | 2.10±0.10               | <b>59.9±3.4</b>                               |
| OSL10-EVA1138 | Main Area (north) AL 07    | 0.9±0.0   | 105±6 <sup>b</sup>                            | 24                 | 9±4               | 1.12±0.06 | 2.07±0.10 | 4.87±0.24 | 0.16±0.01                | 2.10±0.11               | <b>61.4±3.8</b>                               |

\*Ages and age ranges considered most reliable are in **bold**; EVA1135 and EVA1136 (in *italics*) are considered less reliable due to overdispersion. EVA1129 and EVA1132 (in plain text) are rejected from the chronology of the site.

<sup>a</sup>Calculated using the finite mixture model of Galbraith and Green (1990).

<sup>b</sup>Calculated using the central age model of Galbraith et al. (1999).

<sup>c</sup>Rejected from the chronology of the site.

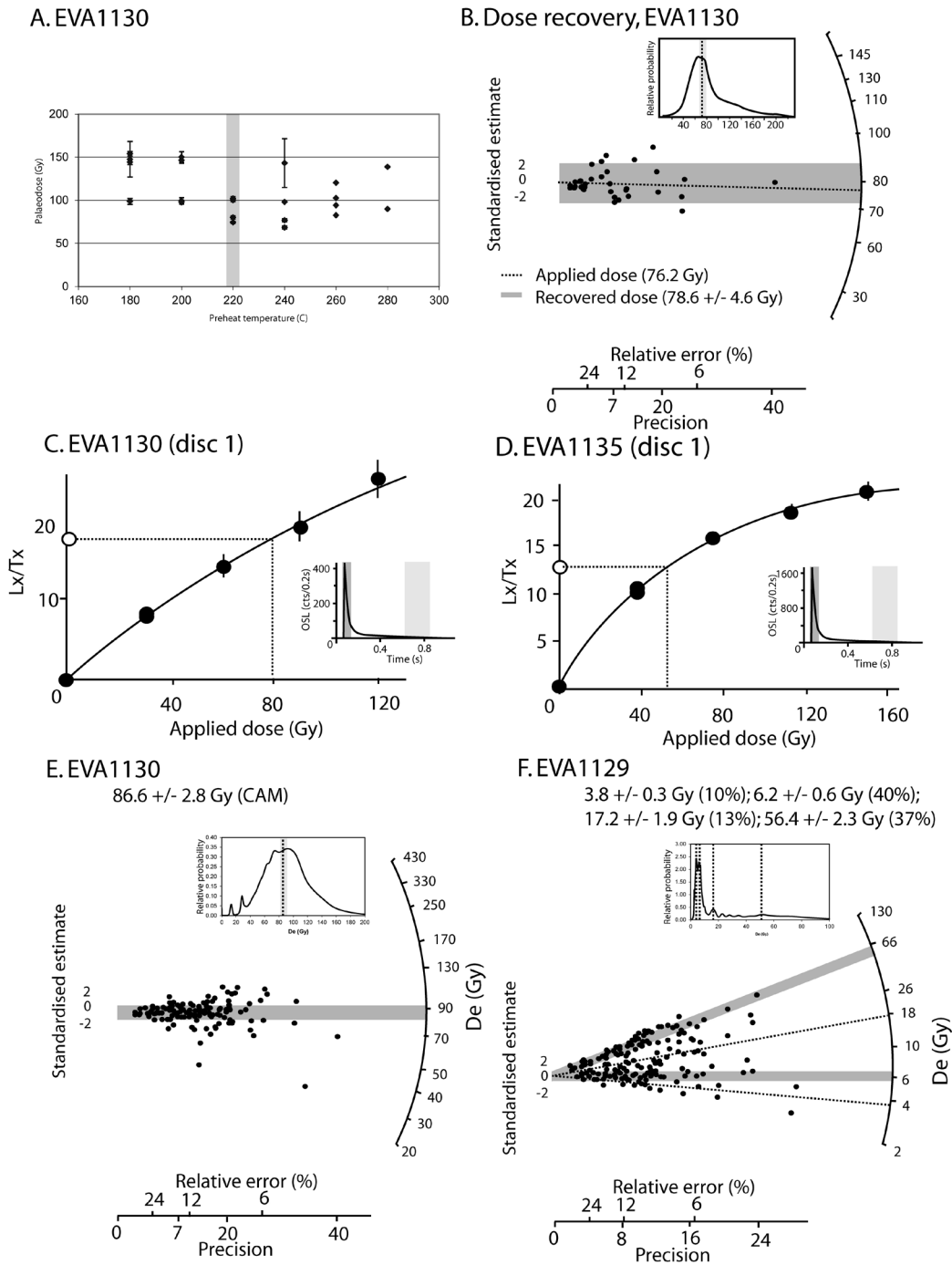


Figure 13. Luminescence characteristics of representative samples investigated in this study. (A) Preheat plateau results for EVA1130. The selected preheat temperature (220°C) is highlighted. (B) Single grain dose recovery test results for EVA1130, showing the applied dose (76.2Gy) as a dotted line, compared with the recovered dose (78.6±4.6Gy) as grey shading, both as a probability density function and radial plot. (C-F) Dose response curves for accepted single grains of (C) EVA1130 (Test Pit III) and (D) EVA1135 (Main Excavation), showing fitting using a single exponential function. Insets illustrate the OSL signal decay for those single grains; the integration ranges for the signal and background are shown in darker and lighter shading respectively. Dose distributions for (E) EVA1130 and (F) EVA1129, as both radial plots (main image) and probability distribution functions (inset). The shaded area in the EVA1130 radial plot and probability distribution function represents the age range within 2σ calculated using the central age model. The shaded areas in the EVA1129 radial plot represent the two largest populations, and the dotted lines represent the two minor populations, calculated using the finite mixture model. The dotted lines in the EVA1129 probability distribution function represents all four populations calculated using the age model. The frequency curve represents the probability distribution of all accepted aliquots from the measurements, and therefore the dose distribution. The dose distributions for all other samples, as radial plots and probability density functions, are given in the Supplementary Information.

at the “Felsenkeller” Laboratory (VKTA) in Dresden, Germany. The beta component was calculated from the HRGS results, converted using published factors (Adamiec and Aitken 1998), and by beta counting. The moisture content of each sample was incorporated into the dose-rate calculations to account for attenuation (Mejdahl 1979). The cosmic ray component of the dose rate was calculated based on equations published in Prescott and Hutton (1994).

### OSL Characteristics and Limitations of the Dating

The fundamental luminescence characteristics of the sand-sized quartz from the VR003 site suggest that the sediments are well suited to OSL dating. Of the 600 grains measured from each sample, at least 8% pass the selection criteria for further analysis, a proportion which appears to be typical (or even at the upper end of the range) for single grains of South African quartz (e.g., Jacobs et al. 2003). These grains exhibit rapid signal decay indicating dominance of the readily and rapidly bleached fast component of the OSL signal which is the target component for analysis (see Figures 13c, d—insets), as well as a generally high sensitivity suggesting efficient transmission of absorbed radiation as luminescence. The accepted grains also exhibit low thermal transfer, recycling within 20% of unity, and dose-response characteristics which can be fitted to simple saturating exponential functions (see Figures 13c, d). The dose recovery test applied to single grains from representative sample EVA1130 yielded a recovery ratio of  $1.03 \pm 0.06$  (see Figure 13b), with an overdispersion value for the dose distribution of 21.1%. The dose recovery ratio lies well within the 10% of unity suggested as acceptable limits (Murray and Wintle 2003). The response of the relatively high proportions of accepted grains to internal checks of the SAR protocol further underscore the general suitability of the VR003 samples for dating based on inherent luminescence characteristics.

However, the dose distributions of those grains accepted for analysis suggest limitations in the suitability of the VR003 sediments for the actual determination of ages. In almost all samples, the dose distributions show a larger scatter in individual grain ages than would generally be expected for well-bleached, rapidly deposited, non-bioturbated sediments (see Figures 13e, f, S1). Overdispersion averages  $43.7 \pm 26.4\%$  across the sample suite. Of the ten samples analysed in this study, seven yielded overdispersion values greater than 30%, and four yielded values over 36% (see Table 5). This scatter, despite largely Gaussian dose distributions in 60% of cases, provides the primary cause for concern in assessing the reliability of the samples for dating.

In OSL dating, the observed spread in grain ages can be attributed to a range of causes. These include incomplete zeroing of the luminescence signal and thermal transfer of charge, instrument consistency and variations in photon counting during measurement, and inhomogeneity in the dose rates. The spread which cannot be directly attributable to any quantifiable cause is known as overdispersion (Thomsen et al. 2005). The very high degree of scatter observed in the VR003 samples is unlikely to have been caused by incomplete bleaching of the signal during deposition,

although post-depositional mixing remains a possibility despite our attempts during sampling to avoid bioturbated sediments. Generally, however, our micromorphological analyses indicate good potential for resetting of the signal and rapid deposition, requiring additional explanations for the scatter in dose distributions to be sought, in particular for those samples inside the shelter. As described above, thermal transfer of charge is not an issue with the accepted grains. Our understanding of site formation processes would therefore appear to justify use of the FMM for age determination in most of the samples (particularly in the potentially bioturbated Main Area), since the FMM aims to extract grain populations of different ages controlled by geological processes (Galbraith and Green 1990). The FMM has also been used to argue for bimodality in the dose rate (Gliganic et al. 2012; Jacobs et al. 2008; 2012), although the latter situation has yet to be demonstrated either in the environment or by simulation (Brennan et al. 1997; Nathan et al. 2003).

One of the most likely explanations for the high overdispersion values in the VR003 samples—at least for the samples inside the shelter, and potentially as an additional explanation for the bioturbated Main Area samples—is heterogeneity of dose rates at the single grain level. This is probably caused by variability in grain size and poor sorting of the sediments, resulting in local radioactive “hotspots” and “coldspots” and referred to as microdosimetry. Micromorphologic analysis of the VR003 sediments support the hypothesis for poorly sorted sediments throughout the stratigraphic sequence. Particle size inhomogeneity is highly likely to cause issues of microdosimetry at the single grain level.

At present, however, issues of dose rate heterogeneity due to particle size distributions cannot be adequately adjusted for in single grain dating calculations. Microdosimetry is beginning to be addressed using techniques such as autoradiography, which screens for sediment inhomogeneity (Rufer and Preusser 2009; Schmidt et al. 2013). Furthermore, mass spectrometry shows that dose rate “hot spots” up to two times the average can occur (Schmidt et al. 2012), and statistical modelling has been used to reconstruct heterogeneous dose rates in three dimensions (Guérin and Mercier 2012; Guérin et al. 2012). At present, our quantitative understanding of the problem remains limited to well sorted sediment matrices. Since the VR003 sediments are relatively poorly sorted, their wide dose distributions, combined with our understanding of site formation processes, support the hypothesis for inhomogeneous dose rates, for which there is as yet no solution for calculating spatial variability at the single grain level. The most parsimonious approach is therefore to use the average dose rate for the bulk sediment in each stratigraphic unit (Guérin et al. 2013), which we have done here. We also urge caution in the interpretation of those ages for which a particularly high degree of overdispersion (>36%) is observed (see Table 5).

In summary, despite the apparent fundamental suitability of luminescence characteristics from sand-sized

quartz from VR003 for OSL dating, the inhomogeneity of the sediments due to grain size and mineralogy, and bioturbation in the Main Area samples, limits their reliability for age determination. The particularly high degree of scatter in samples EVA1129 (see Figure 13f) and EVA1132 (see Figure S1) prevents reliable age calculation, and therefore these two samples have been excluded from the final chronology. Particular caution is urged in including the widely distributed samples EVA1135 and EVA1136 in the final interpretation, although these samples yielded better results than the two rejected samples (lower BIC factors and higher proportions of grains attributed to a single age population).

### OSL Chronology

The dating results suggest surprisingly young ages for the VR003 sequence, extending from  $61.4 \pm 3.8$  kya to  $41.7 \pm 2.9$  kya (see Table 5). Inside the shelter, the combination of the radiocarbon and OSL chronologies highlights likely mixing at the contact between the MSA and LSA in III-15 and III-16. The OSL sample from III-15 yielded multiple grain populations, including one population that was close ( $2.6 \pm 0.3$  kya) to the range of the radiocarbon dates obtained on charcoal above and below the sample in III-14 and III-16. This sample was interpreted as unreliable.

The oldest ages occur in the lowermost levels of the north end of the Main Area; they suggest deposition of Layer 07 around  $61.4 \pm 3.8$  kya and of Layer 06 between  $59.9 \pm 3.4$  kya and  $54.7 \pm 9.9$  kya. However, the two oldest ages from the southern end (up slope), correlated with these units, are substantially younger, yielding  $43.7 \pm 4.1$  kya and  $40.4 \pm 2.9$  kya for Layers 07 and 06 respectively. The discrepancy between these two sets of results presents two possible alternatives. Either the stratigraphic correlation between the two excavation areas is incorrect, or one set of ages is inaccurate. Given the particularly high degree of scatter in the dose distributions from the southern samples compared with those from the north, the older ages are probably the more accurate ones.

Two OSL samples were collected from archaeological layers yielding similar artifacts (see below), from the southern (upslope) end of the Main Area (Layer 04) and TP-III inside the shelter (III-20). These yield ages of  $45.7 \pm 2.8$  kya and  $41.7 \pm 2.9$  kya respectively. An additional, overlying unit, III-17, inside the shelter, containing MSA artifacts, provides an age of  $42.3 \pm 2.7$  kya. All three ages lie within 95% confidence limits of each other ( $2\sigma$  error) and are younger than some of the stratigraphic unit ages from the lowest levels of the Main Area.

The OSL chronology from VR003 therefore suggests deposition of the oldest excavated sediments in the Main Area outside the cave between approximately  $61.4$ – $54.7$  kya (range using  $1\sigma$  uncertainty,  $65.2$ – $44.8$  kya), followed by subsequent (re)occupation around  $45.7$ – $41.7$  kya (range according to  $1\sigma$  uncertainty,  $48.5$ – $38.8$  kya).

### MIDDLE STONE AGE LITHIC ASSEMBLAGES

Excavations at VR003 have thus far produced an MSA assemblage of 83,724 flaked and battered stone artifacts, of

which 80,731 derive from the Main Area excavation, and the remaining 2,993 from TP-III within the shelter (Table 6). These two areas are as yet not stratigraphically linked, and so they are discussed here separately with suggestions for matching provided at the end.

The principal objective of initial analysis of the VR003 artifacts was to assess the site relative to southern Africa's known culture historic units. This is facilitated by the fact that VR003 occurs ~70km from the documented MSA sequences at Klein Kliphuis, Hollow Rock Shelter, Klipfonteinrand, Mertenhof, and Putslaagte 8 and ~100km from Diepkloof and Elands Bay Cave (Högberg and Larsson 2011; Klein et al. 2004; Mackay 2009, 2010; Mackay et al. 2015; Porraz et al. 2013a; 2013b; Will et al. 2015). The pattern at these sites suggests a sequence where the oldest component is generally quartzite-rich, with a heavy emphasis on local rocks, variable but generally infrequent production of blades and flakes with convergent lateral margins, and relatively high proportions of discoidal and Levallois cores. With respect to retouch, morphologically regular implements are rare in these contexts, and denticulates are the most common type when they occur. We follow Mackay et al. (2014a) in referring to these assemblages simply as 'earlier MSA' and avoid sub-divisions on the basis that the general utility of these has not been established, and that there is considerable site-to-site variability in more specific assemblage characteristics (e.g., Wurz 2012). At sites near VR003, such as Diepkloof, Hollow Rock Shelter, and Mertenhof, these earlier MSA assemblages are replaced by bifacial point-bearing (Still Bay, SB) assemblages somewhat richer in silcrete. At Diepkloof the appearance of bifacial points is immediately preceded by the production of small numbers of unifacial points (Porraz et al. 2013b), and unifacial points occur with bifacial points at Hollow Rock Shelter (Evans 1994). These SB-assigned assemblages in turn give way to backed artifact-bearing (Howiesons Poort, HP) layers at Diepkloof and Mertenhof, in which laminar reduction is more common, though at Diepkloof the backed artifacts and bifacial points overlap for several layers. The backed artifact-bearing layers are generally more silcrete-rich than the earlier or later parts of the MSA, though there is considerable variation in silcrete frequency within the HP-assigned layers at several sites both close to VR003 and further afield (e.g., Diepkloof, Klasies River, Klein Kliphuis, and Klipdrift (Henshilwood et al. 2014; Mackay 2010; Porraz et al. 2013b; Schmidt and Mackay 2016; Singer and Wymer 1982). The HP assemblages at these sites are also often extremely dense when compared to overlying and underlying units (Mackay 2010). Backed artifacts later give way to unifacial points and scrapers, and the proportion of silcrete gradually declines as does the prevalence of laminar reduction. Assemblages with these characteristics are often referred to as post-HP (Conard et al. 2012) and where dated usually fall within the range from 60–50 ka (Conard et al. 2012; Guérin et al. 2013; Jacobs et al. 2008; Tribolo et al. 2013). Most sites near VR003 have a major gap in the cultural and chronological sequence after this—a lacuna that appears to span most of MIS 3 (Mackay et al. 2014a).

**TABLE 6. THE MIDDLE STONE AGE LITHIC ASSEMBLAGES:  
MAJOR ARTIFACT CLASSES BY LAYER, 2011 EXCAVATIONS ONLY\*.**

| Layer                             | Flakes |            | Retouched Flakes |            | Cores |            | Flaked Pieces |             | Total |
|-----------------------------------|--------|------------|------------------|------------|-------|------------|---------------|-------------|-------|
|                                   | n      | Adj. res.  | n                | Adj. res.  | n     | Adj. res.  | n             | Adj. res.   |       |
| <i>Main Area</i>                  |        |            |                  |            |       |            |               |             |       |
| 03                                | 800    | -3.3       | 23               | 2.0        | 27    | <b>3.1</b> | 134           | 1.7         | 982   |
| 04                                | 4934   | <b>4.1</b> | 175              | <b>3.9</b> | 114   | <b>3.2</b> | 706           | -7.2        | 5684  |
| 05                                | 2908   | <b>5.7</b> | 62               | 2.1        | 44    | -1.1       | 280           | -6.6        | 3291  |
| 06                                | 3473   | 0.9        | 51               | -0.9       | 71    | 1.1        | 463           | -1.1        | 4058  |
| 07                                | 4412   | -6.8       | 37               | -5.2       | 53    | -3.9       | 857           | <b>10.8</b> | 5359  |
| s1                                | 905    | -2.7       | 10               | -1.4       | 9     | -2.0       | 175           | <b>4.2</b>  | 1099  |
| <i>TP-III: Inside the Shelter</i> |        |            |                  |            |       |            |               |             |       |
| III-16                            | 146    | 0.8        | 5                | -2.0       | 10    | 1.1        | 37            | -0.3        | 198   |
| III-17                            | 168    | -1.0       | 8                | -1.6       | 7     | -0.8       | 60            | 2.4         | 243   |
| III-18                            | 141    | -1.9       | 19               | 2.7        | 9     | 0.4        | 43            | 0.4         | 212   |
| III-19                            | 19     | -0.7       | 3                | 1.2        | 1     | -0.1       | 6             | 0.2         | 29    |
| III-20                            | 178    | 2.4        | 13               | 0.3        | 7     | -0.6       | 31            | -2.6        | 229   |

\*Small classes such as hammerstones and heat shatter are excluded. Chi-square test for the Main Area suggests significant variation in class abundance ( $\chi^2=245.379$ ,  $df=15$ ,  $p<0.001$ ). Positive adjusted residuals greater than 3.078 (statistically significant at  $p<0.002083$  to account for the 4x6 table) in the Main Area sample are shown in bold, reflecting instances of significant over-representation of a given class. No cells in the Test Pit III sample have adjusted residual values exceeding the significance cut-off of 3.0234, though the chi-square test suggests statistically significant variation ( $\chi^2=23.606$ ,  $df=12$ ,  $p=0.023$ ).

The sequences at Diepkloof, Hollow Rock Shelter, Klein Kliphuis, Klipfonteinrand, Putslaagte 8 and Mertenhof are fairly consistent with those across southern Africa more broadly (Henshilwood et al. 2014; Lombard et al. 2012; Minichillo 2005; Singer and Wymer 1982; Soriano et al. 2007; Villa et al. 2010; Vogelsang et al. 2010; Volman 1981; Wurz 2002, 2013), though there are differences. The MIS 3 hiatus is a feature of sites with significant winter rainfall input (Winter and Year-Round Rainfall Zones – W/YRZ), but this does not hold further to the north and east at sites in the summer rainfall zone (SRZ) (Mackay 2010; Mackay et al. 2014a). Moreover, while an abundance of either bifacial points or backed artifacts tends to occur in discrete sets of successive layers in W/YRZ sites, this is not true of SRZ sites such as Sibudu, Rose Cottage Cave, or Umhlatuzana, where bifacial points in particular tend to recur through the sequence (Beaumont 1978; de la Pena et al. 2013; Grün and Beaumont 2001; Kaplan 1990; Wadley 2005c, 2012; Wadley and Harper 1989). The significance of this is worth restating—independent of chronometric age estimations, where sites in the W/YRZ contain both bifacial points and backed artifacts, the former always underlie the latter and neither has been documented to occur again earlier or later in large numbers.

#### MAIN AREA

Our 2009 excavations in the Main Area at VR003 suggested the presence of HP and possibly SB components based on the presence of small numbers of backed artifacts ( $n=11$ )

and bifacial points ( $n=2$ ), the former in 2009 Layer II-04 and the latter in stratigraphically-insecure contexts. Renewed excavation in the Main Area resulted in the recovery of an additional 36 clearly identifiable backed artifacts and 23 new bifacial points. In addition, seven specimens were classified as possibly backed and five as bifacially-worked pieces. Four unifacial points have been identified with one further possible example. The majority of implements in all three of these classes occurs in stratigraphic Unit 04, with small numbers in 03 and 05 and outlying examples in 02 and 06 (Table 7, Figure 14). The partial exception is the unifacial point class, which has slightly more specimens (including ambiguous examples) in 05. In addition to the bifacial points themselves, 13 of the 32 aggregate samples (buckets) from 04 contained probable bifacial thinning flakes; two single examples were also recovered from 05, but none from the other layers. We classified bifacial thinning flakes based on a set of specific characteristics—acute platform angle, diffuse bulb, curved (weakly concave) longitudinal ventral profile, acute lateral margins, and as being generally thin relative to surface area (cf., Andrefsky 2005).

The spatial distribution of key implement types is shown in Figure 15. Only confidently identified examples are included. These artifacts form a single fairly well-defined band within the main excavation, with a few outlying specimens above and below this. The band is approximately ~200mm thick and largely follows the slope of the deposit surface, being flat at the top of the site and sloping down

**TABLE 7. THE MIDDLE STONE AGE LITHIC ASSEMBLAGES:  
RETOUCHED FLAKE TYPES BY LAYER, 2011 EXCAVATIONS ONLY\*.**

| Layer                             | Backed | Bifacial | Unifacial | Scraper | Denticulate | Complex Notch | Pièces Esquillées | Core on Flake | No Type |
|-----------------------------------|--------|----------|-----------|---------|-------------|---------------|-------------------|---------------|---------|
| <i>Main Area</i>                  |        |          |           |         |             |               |                   |               |         |
| 03                                | 2 (1)  | 1        | 0         | 0       | 0           | 1             | 3 (2)             | 1 (1)         | 10      |
| 04                                | 30 (3) | 20 (4)   | 2         | 10      | 5           | 11            | 9 (1)             | 9 (1)         | 55      |
| 05                                | 2 (3)  | 2 (1)    | 2 (1)     | 7       | 7           | 5             | 1                 | 1 (2)         | 28      |
| 06                                | 2      | 0        | 0         | 6       | 5           | 5             | 2 (2)             | 5 (4)         | 20      |
| 07                                | 0      | 0        | 0         | 1       | 5           | 5             | 1 (1)             | 1 (3)         | 20      |
| s1                                | 0      | 0        | 0         | 1       | 3           | 0             | 0                 | 0             | 6       |
| <i>TP-III: Inside the Shelter</i> |        |          |           |         |             |               |                   |               |         |
| III-16                            | 0      | 0        | 0         | 1       | 0           | 0             | 0                 | 0             | 4       |
| III-17                            | 0      | 0        | 0         | 2       | 1           | 1             | 0                 | 1             | 3       |
| III-18                            | 3      | 0        | 0         | 1       | 0           | 1             | 2                 | 1             | 11      |
| III-19                            | 1      | 0        | 0         | 0       | 0           | 0             | 0                 | 0             | 2       |
| III-20                            | 4      | 0        | 0         | 0       | 0           | 3             | 0                 | 0             | 6       |

\*Values in parentheses are additional pieces classified as 'possible', most of which are retouched flake fragments.

to the north. The unifacial and bifacial points both appear to occupy the same band-space and are not obviously spatially distinct from one another, though stratigraphically unifacial points have a stronger association with Layer 05 than do bifacial points. The backed artifacts generally occur slightly higher than the other two implement types though their distributions become notably less distinct immediately upslope of the major boulder, and again in the downslope area.

The presence of backed artifacts and bifacial points is consistent with HP and SB deposits given data from nearby sites. An additional facet of these units in this region is the preferential selection of fine-grained rocks, particularly silcrete in the HP. As in the 2009 sample, quartz dominates the assemblages in all strata, accounting for between 54.5% and 67.4% of artifacts. As noted in Steele et al. (2012) this dominance has the effect of swamping variation in the other material classes. Consequently, all non-quartz rock classes show less than 10% total variation through the sequence. Nevertheless, there is statistically significant variation in raw material proportions through the Main Area sequence ( $\chi^2=563.928$ ,  $df=20$ ,  $sig<0.001$ ; Table 8), with over-representation of silcrete in the uppermost layers, 03 and 04 (based on adjusted residuals, cf. Haberman 1973)<sup>1</sup>, and non-significant over-representation in the lowest Layer s1. Quartz values are elevated in Layers 04 and 05, while quartzite is unusually common in Layers 06 and 07. Hornfels is dispropor-

tionately abundant in 07 only.

Graphical representation of variation in the distribution of silcrete percentage for aggregated samples adds further detail to the stratigraphic pattern (see Figure 15). The greatest concentration of high silcrete percentages occurs in aggregate samples towards the top of the flattest part of the deposit. It can be noted that these elevated values correspond to the distribution of the major implement types. A second observation is that this uppermost concentration of elevated silcrete percentages disappears further downslope where backed artifacts and bifacial points occur closer to the surface. The implication is that these deposits may be, to some extent, missing or mixed in this area, probably as a result of low net sedimentation.

Beyond the main upper concentration, a second band of elevated silcrete percentages occurs at the current lowest excavated level in Layer s1, the deep sounding. This comprises seven aggregate samples with silcrete percentages >19%, which is approximately one third of all the aggregate samples in the layer ( $n=22$ ). Given that the 15 overlying aggregate samples generally have quite low silcrete percentages, these data suggest at least two distinct archaeological strata within the deep sounding, the lower of which is among the most silcrete-rich in the deposit as it has so far been excavated. A final point relating to this set of values is that they also appear to track the slope of the deposit surface quite well, and would underlie the upper excavation



Figure 14. Selected artifacts from the 2011 sample. Scale bars are in 10mm increments; all artifacts to the same scale. Crypto-crystalline silicates = ccs. 1. Backed point, hornfels (04); 2. Backed point, ccs (III-20); 3. Backed point, quartz (04); 4. Backed point, quartz (04); 5. Truncated flake, quartz (III-20); 6. Truncated flake, hornfels (04); 7. Truncated flake, quartz (04); 8. Truncated flake, crystal quartz (III-19); 9. Backed blade fragment, ccs (04); 10. Backed blade fragment, clear quartz (04); 11. Backed blade fragment, quartz (04); 12. Backed blade fragment, ccs (04); 13. Segment, mudstone (02); 14. Segment, quartz (III-15); 15. Segment, quartz (06); 16. Notched flake, silcrete (04); 17. Notched flake, silcrete (04); 18. Notched blade, ccs (06); 19. Notched blade, ccs (05); 20. End scraper, ccs (III-18); 21. End scraper, quartz (04); 22. End scraper, quartz (04); 23. Bifacial point, clear quartz (05); 24. Partly bifacial point with dorsal working to the tip and ventral working to the base, hornfels (04); 25. Partly bifacial point with dorsal working to the tip and ventral working to the base, hornfels (04); 26. Convergent flake with burin spalls from tip (white arrows), hornfels (05); 27. Early stage bifacially-worked piece, silcrete (04); 28. Bifacial point tip, quartz (04); 29. Unifacial point, quartzite (04); 30. Unifacial point, silcrete (04); 31. Unifacial point, quartzite (05); 32. Unworked smokey quartz crystal (III-15); 33. Unworked quartz crystal with red staining (04); 34. Denticulate, ccs (05); 35. Denticulate, quartz (06); 36. Denticulate, quartz (06); 37. Denticulate, quartz (07); 38. Denticulate, quartz (07); 39. Large blade, clear quartz (06); 40. Large blade, hornfels (03); 41. Large discoidal core, silcrete (07); 42. Discoidal core, quartz (04); 43. Platform core, quartzite (04).

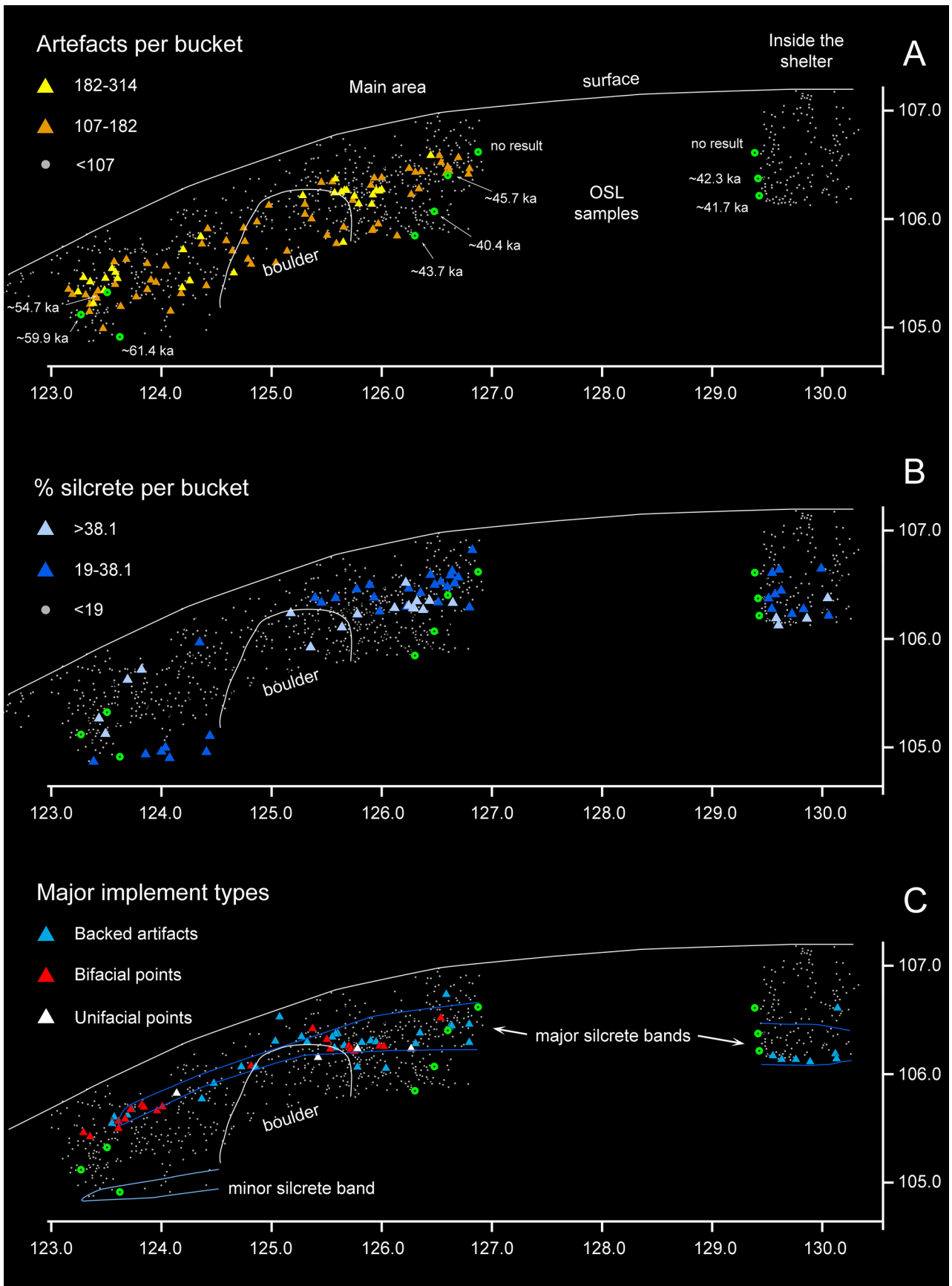


Figure 15. Distribution of key changes through the VR003 sequence: (A) variability in artifact densities for all aggregate contexts (buckets); (B) variability in silcrete percentage for all aggregate contexts; (C) distribution of backed artifacts, bifacial points, and unifacial points.

TABLE 8. THE MIDDLE STONE AGE LITHIC ASSEMBLAGES:  
PERCENTAGE OF RAW MATERIAL TYPES BY LAYER (artifacts >15mm only), 2011 EXCAVATIONS\*.

| Layer                             | Quartz      |            | Quartzite  |             | Silcrete   |            | Hornfels   |            | Other     |            | Total |
|-----------------------------------|-------------|------------|------------|-------------|------------|------------|------------|------------|-----------|------------|-------|
|                                   | n (%)       | Adj. res.  | n (%)      | Adj. res.   | n (%)      | Adj. res.  | n (%)      | Adj. res.  | n (%)     | Adj. res.  |       |
| <i>Main Area</i>                  |             |            |            |             |            |            |            |            |           |            |       |
| 03                                | 581 (59.2)  | -0.6       | 111 (11.3) | -2.1        | 158 (16.1) | <b>5.3</b> | 70 (7.1)   | -4.4       | 62 (6.3)  | <b>3.7</b> | 982   |
| 04                                | 3651 (64.0) | <b>7.2</b> | 446 (7.8)  | -14.8       | 777 (13.6) | <b>7.7</b> | 595 (10.4) | -3.1       | 235 (4.1) | 0.4        | 5704  |
| 05                                | 2154 (65.4) | <b>6.9</b> | 421 (12.8) | -1.3        | 237 (7.2)  | -7.5       | 368 (11.2) | -0.7       | 114 (3.5) | -1.8       | 3294  |
| 06                                | 2366 (58.2) | -2.7       | 704 (17.3) | <b>8.0</b>  | 441 (10.9) | -0.2       | 424 (10.4) | -2.5       | 131 (3.2) | -2.9       | 4066  |
| 07                                | 2910 (54.2) | -10.2      | 944 (17.6) | <b>10.2</b> | 493 (9.2)  | -4.8       | 811 (15.1) | <b>9.5</b> | 215 (4.0) | -0.1       | 5373  |
| s1                                | 652 (59.3)  | -0.5       | 143 (13.0) | -0.5        | 135 (12.3) | 1.5        | 100 (9.1)  | -2.6       | 69 (6.3)  | <b>3.9</b> | 1099  |
| <i>TP-III: Inside the Shelter</i> |             |            |            |             |            |            |            |            |           |            |       |
| III-16                            | 129 (62.9)  | -0.9       | 16 (7.8)   | 1.7         | 33 (16.1)  | 0.8        | 12 (5.9)   | -1.1       | 15 (7.3)  | 0.3        | 205   |
| III-17                            | 171 (66.5)  | 0.3        | 8 (3.1)    | -1.9        | 37 (14.4)  | 0.0        | 21 (8.2)   | 0.3        | 20 (7.8)  | 0.7        | 257   |
| III-18                            | 139 (61.8)  | -1.4       | 11 (4.9)   | -0.4        | 38 (16.9)  | 1.2        | 21 (9.3)   | 1.0        | 16 (7.1)  | 0.2        | 225   |
| III-19                            | 21 (72.4)   | 0.8        | 4 (13.8)   | 2.0         | 0 (0)      | -2.2       | 3 (10.3)   | 0.5        | 1 (3.5)   | -0.7       | 29    |
| III-20                            | 167 (69.9)  | 1.6        | 13 (5.4)   | 0.0         | 29 (12.1)  | -1.1       | 17 (7.1)   | -0.4       | 13 (5.4)  | -1.0       | 239   |

\*Chi-square test for the Main Area suggests significant variation ( $\chi^2=563.928$ ,  $df=20$ ,  $p<0.001$ ). Positive adjusted residuals greater than 3.144 ( $p<0.001667$  to account for the 5x6 table) in the Main Area sample are shown in bold, reflecting instances of significant over-representation of a given raw material. No cells in the Test Pit III sample have adjusted residual values exceeding the significance cut-off of 3.0903, and the chi-square results were not statistically significant ( $\chi^2=20.821$ ,  $df=16$ ,  $p=0.208$ ).

**TABLE 9. THE MIDDLE STONE AGE LITHIC ASSEMBLAGES: THE TOTALED NUMBER OF BUCKETS (12 L) OF SEDIMENTS EXCAVATED AND THE NUMBER OF STONE ARTIFACTS RECORDED WITHIN THE LAYER, WHICH WERE THEN USED TO CALCULATE ARTIFACT DENSITY (total number of artifacts for the layer divided by the total number of 12 L buckets excavated for that layer, rounded to nearest integer). 2011 EXCAVATIONS ONLY.**

| Layer                             | N Buckets | N Artifacts | Artifact Density |
|-----------------------------------|-----------|-------------|------------------|
| <i>Main Area</i>                  |           |             |                  |
| 03                                | 13.5      | 984         | 73               |
| 04                                | 38.25     | 7485        | 196              |
| 05                                | 18.75     | 3273        | 175              |
| 06                                | 34.75     | 4066        | 117              |
| 07                                | 50.5      | 5371        | 106              |
| s1                                | 20.5      | 1099        | 54               |
| <i>Average</i>                    |           |             | <b>120</b>       |
| <i>TP-III: Inside the Shelter</i> |           |             |                  |
| III-16                            | 9         | 206         | 23               |
| III-17                            | 10        | 257         | 36               |
| III-18                            | 6         | 225         | 38               |
| III-19                            | 1         | 29          | 29               |
| III-20                            | 3.25      | 239         | 74               |
| <i>Average</i>                    |           |             | <b>33</b>        |

area if hypothetically extended on that slope.

Artifact density is another potentially important variable in southern African technological sequences, as it may relate to intensity of site use and/or changes in technological organization (Mackay et al. 2014a; Riel-Salvatore and Barton 2004). Artifact densities are highest in Layer 04 (Table 9), which also has elevated values for silcrete and large numbers of backed artifacts and bifacial points. Interestingly the overlying Layer 03, which also has high proportions of silcrete, has very low artifact densities, while the underlying Layer 05 has high densities despite low proportions of silcrete. Figure 15 suggests that the highest densities of artifacts broadly correspond to the distribution of backed artifacts, bifacial points, and unifacial points in the lower half of 04. A second, lower band of high artifact densities corresponds to part, but not all, of Layers 06 and 07. Artifact densities are lower at the uppermost end of those strata. At the lower end the two bands almost coincide, suggesting that the archaeological strata may pinch together downslope somewhat.

The data presented so far allow several conclusions to be drawn with respect to the issues outlined at the start

of this section. Potentially significant markers of the HP and SB—including backed artifacts/bifacial points, high proportions of silcrete, and in the case of the HP, high artifact densities— have been tested with respect to their distribution relative to our archaeological excavation units, and more generally with respect to their spatial occurrence through the deposit. Clearly, these three markers can operate as independent variables in the main area sequence, occurring and reoccurring in spatially-distinct clusters and bands. Only in the lower half of Layer 04, however, do all three correspond. This part of the sequence contains a single coherent band of aggregate samples with high artifact densities, high frequencies of silcrete, and large numbers of backed artifacts and bifacial points. The fact that these three factors occur together only once in the sequence is consistent with evidence from other WRZ sites. Even the occurrence of small numbers of unifacial points amongst and immediately below the bifacial points in the sequence is consistent with evidence from sites such as Hollow Rock Shelter, Apollo 11, and particularly Diepkloof. Overall the VR003 sequence sufficiently mirrors sequences at other well-resolved sites nearby that it seems to us unlikely that

**TABLE 10. THE MIDDLE STONE AGE LITHIC ASSEMBLAGES: PROPORTIONS OF CORE TYPES BY LAYER, 2011 EXCAVATIONS ONLY\*.**

| Layer                             | Bipolar |            | Platform |           | Rotated |           | Discoid |           | Levallois |           | No Type |            | Total |
|-----------------------------------|---------|------------|----------|-----------|---------|-----------|---------|-----------|-----------|-----------|---------|------------|-------|
|                                   | n       | Adj. res.  | n        | Adj. res. | n       | Adj. res. | n       | Adj. res. | n         | Adj. res. | n       | Adj. res.  |       |
| <i>Main Area</i>                  |         |            |          |           |         |           |         |           |           |           |         |            |       |
| 03                                | 10      | <b>3.9</b> | 0        | -1.5      | 3       | 0.2       | 3       | -1.9      | 2         | -1.1      | 9       | 0.6        | 27    |
| 04                                | 6       | -3.0       | 5        | -1.5      | 9       | -0.8      | 30      | -0.2      | 17        | 0.0       | 47      | <b>3.8</b> | 114   |
| 05                                | 5       | -0.3       | 5        | 1.1       | 8       | 2.0       | 8       | -1.4      | 5         | -0.7      | 13      | 0.2        | 44    |
| 06                                | 3       | -2.5       | 6        | 0.4       | 9       | 0.9       | 28      | 2.7       | 11        | 0.2       | 14      | -1.8       | 71    |
| 07                                | 16      | <b>4.1</b> | 6        | 1.3       | 2       | -1.6      | 15      | 0.2       | 11        | 1.3       | 3       | -4.0       | 53    |
| s1                                | 1       | -0.2       | 1        | 0.5       | 0       | -1.0      | 2       | -0.3      | 1         | -0.3      | 4       | 1.1        | 9     |
| <i>TP-III: Inside the Shelter</i> |         |            |          |           |         |           |         |           |           |           |         |            |       |
| III-16                            | 7       |            | 0        |           | 1       |           | 0       |           | 0         |           | 2       |            | 10    |
| III-17                            | 3       |            | 1        |           | 0       |           | 0       |           | 2         |           | 1       |            | 7     |
| III-18                            | 2       |            | 3        |           | 0       |           | 3       |           | 0         |           | 1       |            | 9     |
| III-19                            | 0       |            | 0        |           | 0       |           | 1       |           | 0         |           | 0       |            | 1     |
| III-20                            | 1       |            | 0        |           | 0       |           | 2       |           | 0         |           | 4       |            | 7     |

\*Chi-square test for the Main Area suggests significant variation ( $\chi^2=76.798$ ,  $df=25$ ,  $p<0.001$ ). Positive adjusted residuals greater than 3.197 ( $p<0.001389$  to account for the 6x6 table) in the Main Area sample are shown in bold, reflecting instances of significant over-representation of a given core type. Sample sizes from inside the shelter (TP-III) were too low to run chi-square.

we are considering unrelated phenomena. Therefore, based on data derived from the lithic assemblages, we feel that it is broadly reasonable to label the bifacial point-bearing and backed artifact-bearing components of the VR003 sequence as, respectively, SB and HP.

Having considered the rough culture historic sequence of the Main Area excavation at VR003 relative to other sites in the region, attention is now turned to the more general technological characteristics of the site sequence as reflected in the 2011 assemblage.

### Layer 03

Layer 03 is the uppermost fully analyzed layer in the site. It contains at least three backed artifacts and one bifacial point fragment (see Table 7). Retouch is overall reasonably common in 03—no other layer in the main excavation has a higher ratio of retouched to unretouched flakes; however, typologically regular retouched artifacts are rare (see Table 6). Retouched flakes which conform to no type and which display no regular morphology account for ~43% of the retouched sample (see Table 7). The most common retouched classes are *pièces esquillées* and backed artifacts. Layer 03 lacks unifacial points, scrapers, and denticulates, and contains only one flake with a complex notch. These implement types are comparatively common in lower strata.

As with all Main Area strata, Layer 03 includes discoidal and Levallois cores. However, the dominant core type is bipolar (Table 10), which is disproportionately common in this layer (definitions for bipolar, platform and rotated cores follow Mackay [2006]; discoidal and Levallois are distinguished on the basis of hemisphere volumes following Boëda [1995]). Cores conforming to no type are also reasonably common, but not statistically so. Layer 03 also has the

highest ratio of cores to flakes in the Main Area (see Table 6). Both blades and convergent flakes are relatively uncommon in 03 (Table 11).

Overall, and in spite of the relatively high proportion of silcrete (see Table 8), Layer 03 appears to be characterized by fairly expedient technological systems in which easily acquired materials were reduced through either non-systematic or bipolar core techniques, or opportunistically maintained through flake retouch. The one other element of the layer that stands out is the presence of rare but exceptionally large blades, up to 140mm (see Figure 14-40). Two of these were recovered in the relatively small sample. In total, only 15 aggregate samples contained blades exceeding 70mm, and the majority of these were recovered from quite deep in the deposit.

### Layer 04

Like Layer 03, retouch is particularly well represented in Layer 04—the ratio of 1 retouched flake per 45 unretouched is the second highest in the sequence. Based on the distribution of key implement types (see Table 7; see Figure 15), Layer 04 appears to contain three different technological components; this was also the impression given during excavation. The uppermost part of 04 is generally poor in backed artifacts; the middle to lower part is rich in backed artifacts; and, the lower part contains bifacial points, unifacial points, and a few backed artifacts. The layer also contains *pièces esquillées*, scrapers, and complex notches.

The complex notch category includes notched blades typical of the earlier HP documented in Diepkloof, Klein Kliphuis, and Klipdrift (Henshilwood et al. 2014; Mackay 2010; Porraz et al. 2013b). The scraper category, however, includes several distinct end-scrapers (see Figure 14-21 and

TABLE 11. THE MIDDLE STONE AGE LITHIC ASSEMBLAGES: BLADE, CONVERGENT FLAKES AND OTHER FLAKE FORMS PER LAYER, 2011 EXCAVATIONS ONLY, ALONG WITH RAW MATERIAL COMPOSITION OF BLADES AND CONVERGENT FLAKES\*.

| Layer                             | Blades |           | Convergent flakes |           | Other Flakes |            | Blades         |          |             | Convergent Flakes |          |             |
|-----------------------------------|--------|-----------|-------------------|-----------|--------------|------------|----------------|----------|-------------|-------------------|----------|-------------|
|                                   | n      | Adj. res. | n                 | Adj. res. | n            | Adj. res.  | % fine-grained | % quartz | % quartzite | % fine-grained    | % quartz | % quartzite |
| <i>Main Area</i>                  |        |           |                   |           |              |            |                |          |             |                   |          |             |
| 03                                | 5      | -2.2      | 2                 | -1.1      | 793          | 2.5        | 60.0           | 20.0     | 20.0        | 0                 | 50.0     | 0           |
| 04                                | 79     | 0.1       | 15                | -2.6      | 4840         | 1.2        | 65.8           | 25.3     | 8.9         | 33.3              | 33.3     | 33.3        |
| 05                                | 57     | 1.8       | 14                | -0.4      | 2837         | -1.4       | 38.6           | 43.9     | 17.5        | 50.0              | 21.4     | 28.6        |
| 06                                | 49     | -0.9      | 26                | 2.0       | 3398         | -0.2       | 40.8           | 30.6     | 24.5        | 42.3              | 42.3     | 15.4        |
| 07                                | 82     | 1.7       | 33                | 2.3       | 4297         | -2.6       | 57.3           | 25.6     | 17.1        | 27.3              | 24.2     | 48.5        |
| s1                                | 4      | -2.8      | 2                 | -1.3      | 899          | <b>3.1</b> | 25.0           | 50.0     | 25.0        | 100.0             | 0        | 0.0         |
| <i>TP-III: Inside the Shelter</i> |        |           |                   |           |              |            |                |          |             |                   |          |             |
| III-16                            | 2      |           | 1                 |           | 143          |            |                |          |             |                   |          |             |
| III-17                            | 4      |           | 0                 |           | 164          |            |                |          |             |                   |          |             |
| III-18                            | 5      |           | 0                 |           | 136          |            |                |          |             |                   |          |             |
| III-19                            | 0      |           | 0                 |           | 19           |            |                |          |             |                   |          |             |
| III-20                            | 8      |           | 1                 |           | 169          |            |                |          |             |                   |          |             |

\*The category 'fine-grained' includes siltcrete, hornfels, and crypto-crystalline silicates (ccs). Note that blade raw materials in Layer 06 include two blades classed as 'other,' and so do not total 100%; similarly, convergent flakes in 03 include one 'other.' Chi-square test on abundance of blades, convergent flakes, and other flakes for the Main Area suggests significant variation ( $\chi^2=32.796$ ,  $df=10$ ,  $p<0.001$ ). Positive adjusted residuals greater than 2.991 ( $p<0.002778$ ) in the Main Area sample are shown in bold; 'other flakes' in s1 reach this conservative level of significance. Sample sizes from inside the shelter (TP-III) were too low to run chi-square.

14-22), which also occur in HP contexts at Klasies River and possibly Diepkloof (Porráz et al. 2013b; Singer and Wymer 1982). The backed artifacts in 04 include three distinct morphologies, classified here as 'point,' 'blade,' and 'truncated' (e.g., see Figure 14-1 to 14-12). Backed 'points' are defined here as backed artifacts where the backed margin is set at an angle to the chord and where the intersection of the backed margin and the chord is  $<45^\circ$ . Backed blades are those in which the backed section is parallel to the chord. 'Truncated' backed pieces are those where the backed margin is limited to one or both ends of the artifacts (not all along the margin as with segments) and where the intersection of the backed margin and the chord is  $>45^\circ$ . The 'point' backed morphology noted here seems to be uncommon or absent at HP sites to the south though it may have parallels in Apollo 11 based on images in Vogelsang et al. (2010). The classic segment forms which characterize many HP occurrences are uncommon in Layer 04.

The bifacial points in Layer 04 are dominated by quartz, though there are important exceptions. Two such cases involve a pair of hornfels points with partial bifacial working recovered in close proximity to one another towards the base of the layer. These points are both large, unusually elongate, are heavily worked towards the tip and feature butt thinning but little other working at the proximal end (see Figure 14-24 and 14-25).

Layer 04 also has a significantly high proportion of atypical or expediently worked cores and core fragments (see Table 10), however, in contrast to the overlying layer, Layer 04 exhibits little bipolar reduction. Discoidal and Levallois cores are proportionally quite common.

Blades<sup>2</sup> occur throughout Layer 04, at a ratio of approximately 1.6 per hundred flakes—very slightly above average for the site overall (see Table 11). What is notable about the blades in 04 is that they are dominated by fine-grained rocks such as silcrete, hornfels, and cryptocrystalline silicate (CCS). Quartz and quartzite blades are proportionally less common in this layer than in those underlying it. Thus while the prevalence of blades in 04 might be less than expected for an assemblage including a possible HP component, this needs to be viewed against the overall dominance of quartz in the assemblage and the fact that blades were preferentially made on less common materials in this unit. By contrast, the elevated proportion of blades in 05 and 07 may reflect the fact that knappers at these times were less selective of rock type when making such artifacts.

Overall Layer 04 is quite different from the overlying and underlying units in spite of some elements of continuity. Most obviously, Layer 04 has numerous backed artifacts and bifacial points, while these items are relatively uncommon before and after. Layer 04 is also much richer in silcrete than 05 and has a far higher density of artifacts than 03. Layer 04 also generally lacks bipolar core forms that are common both to 03 and 05. The exceptional density of finds, the high ratio of cores to flakes and retouched to non-retouched flakes, and the abundance of silcrete suggests that VR003 was regularly and/or heavily occupied during the formation of Layer 04. The site was provisioned

with both tools and tool-making potential, and implement manufacture and maintenance occurred on site, as demonstrated by the presence of incomplete bifacial points and thinning flakes.

### Layer 05

Distinguishing Layer 05 from the overlying layers is the relative abundance of quartzite in the assemblage, that rock type being almost twice as common as silcrete. Layer 05 has the second highest density of flaked stone artifacts in the VR003 sequence, and the highest proportion of blades. Unlike in Layer 04, where there was evidence for some preferential selection of fine-grained rock in blade production, in Layer 05 material prevalence among blades is more proportional to material prevalence overall, with quartz and quartzite both well represented. The blades in 05 are generally small. Only one of the large blades  $>70$ mm discussed for Layer 03 was identified in the 05 sample; this artifact was complete and measured  $\sim 100$ mm. Layer 05 also witnesses an increase in the prevalence of convergent flake morphologies. While these are not common in the assemblage generally, they become more frequent in layers below 04 (see Table 11). One large convergent flake shows several distinct burin spalls originating at the tip (see Figure 14-26).

Retouch is relatively common in Layer 05, which includes all of the major retouched implement types; scrapers and denticulates are the most common individual forms (see Table 7). As with 03, however, retouched pieces that conform to no type account for almost half of the retouch total. In a similar vein, all of the major core type classes are quite evenly represented in 05. Platform, rotated and to a lesser extent atypical cores, occur at slightly higher-than-average frequencies (see Table 10).

In summary, Layer 05 records relatively low core discard at the site, though the abundance of artifacts suggests a continuation of on-site knapping and fairly intensive site use. It is conceivable that technological systems at this time involved the transportation and maintenance of cores and flakes, the latter of which were discarded at relatively high rates, while the former were retained for further transport. With respect to flake forms and material selection, 05 is fairly typical of nearby earlier MSA assemblages such as Diepkloof, Elands Bay Cave, Klipfonteinrand, and Puts-laagte 8 (Mackay 2009; Mackay et al. 2015; Volman 1981), with some convergent flakes and blades, numerous denticulates, and a reasonable proportion of quartzite.

### Layer 06

Layer 06 exhibits a number of clear differences from the overlying layer. First, artifact density drops by around 35% (see Table 9). The abundance of retouched flakes also drops, though the characteristic forms remain generally the same, with scrapers, notches, and denticulates being common (see Table 7). Also of interest in this layer are two backed artifacts. While the backed pieces in 05 are part of the general cluster more strongly associated with 04, the two pieces in 06 are vertically quite distinct from those overlying. One of these is a quartz segment (see Figure 14-15), and the

other is a fragment. The occurrence of occasional backed pieces in earlier MSA deposits is not unusual in large samples (Mackay 2016), and it may be that the two pieces in 06 represent a very brief period in which these items were made. The identification in this unit of a CCS debitage flake produced during backing suggests that such artifacts may have been manufactured on site.

The other important component of the retouched flake class is the group of artifacts classified as 'core on flake' (see Table 7). These are large flakes from which flakes have subsequently been removed—and thus by strict materialist definition are retouched flakes (Hiscock 2007)—but of which we infer that the flakes produced were intended for use. If ambiguous examples are included, these are the most common retouched flake type in the layer, and may reflect a different organization of core technology. In that respect it can be noted that discoidal cores are comfortably the dominant form in the layer, and some if not many of these may have started out as large flakes.

Convergent flakes are far more common in 06 and the underlying 07 than in any of the overlying layers. While blades are not particularly common in 06, this is the layer in which large blades occur most frequently. Layer 06 included nine blades exceeding 70mm, with the largest being 110mm.

In general, Layer 06 falls within our broad definition of earlier MSA, with high proportions of quartzite, small proportions of convergent flakes, and rare blades. Large flakes were sometimes used as cores in this unit, often flaked in a centripetal pattern consistent with discoidal reduction. Retouched flakes are rare, with occasional notches, scrapers, and denticulates. Backed artifacts may have been manufactured briefly during this period, but perhaps the most distinctive single element of the unit is the production of unusually large blades. Relative to later units, site use appears to have been considerably reduced in 06, if artifact density is used as a proxy.

### Layer 07

Layer 07 has a relatively low density of artifacts and significantly lower than average proportions of both cores and retouched flakes (see Table 6). Denticulates and complex notches are the most common retouched forms, though retouched pieces conforming to no type dominate, accounting for more than half of the sample (see Table 7). Levallois and discoidal cores are numerically common, though only the frequency of bipolar cores significantly exceeds average values (see Table 10).

Material selection strongly favored quartzite and hornfels over silcrete in Layer 07, and quartz has its lowest prevalence in this layer (see Table 8). That said, the spatial data presented suggests that the layer may contain lenses in which silcrete frequencies briefly increased; there may thus be more than one archaeological layer within 07. It was observed during analysis that the silcreted within this layer seemed to be unusually diverse, though this requires substantiation.

Both blades and convergent flakes occur in above-average

frequencies in 07, and these may have been the focus of provisioning given the poverty of cores and retouched flakes, and the relative abundance of bipolar cores.

In summary, Layer 07 appears to reflect transportation of flakes, convergent flakes, and blades which may have been supplemented by the opportunistic bipolar reduction of available quartz nodules and the occasional transportation of larger discoidal and Levallois cores. It is also possible that the various components of the technological package in 07 are temporally unrelated, a point implied by the spatially-restricted band of elevated silcrete values, and also to some extent by the contrast between the bipolar cores (one of which was reduced to 1.6g) and the large discoidal cores such as that mentioned earlier. It seems safe to ascribe Layer 07 to the earlier MSA in the broadest sense.

### Layer s1

As discussed above, Layer s1 is not an archaeological or geological stratigraphic unit but an aggregate created by the objective of maximizing excavation depth in one area. The unit is thus likely to be quite heterogeneous. These caveats aside, s1 does have a number of consistent characteristics. Foremost among these is the low density of finds (see Table 9). At ~54 artifacts per aggregate sample, s1 has the lowest density of artifacts in the Main Area, and less than one third of peak value in Layer 04. Cores and retouched flakes are also quite poorly represented throughout s1, and the layer has very few blades or convergent flakes, in contrast to Layer 07 (see Table 6; Table 13 [below]). The majority (60%) of the retouched flakes in the sample were of no type, with three denticulates and a scraper the only identifiable types (see Table 7). In a similar vein almost half of the cores in the small sample were of no clear type, with two discoidal cores, and isolated instances of Levallois, platform, and bipolar pieces accounting for the remainder (see Table 10). Indeed, expedient flaking of quartz and some discoidal working of other materials, including silcrete in the lowest aggregate samples, seems best to characterize the unit generally.

### TP-III: INSIDE THE SHELTER

The following analysis is concerned with the technological characteristics of the assemblages from III-16 through III-20 inclusive, while III-15 and above are discussed separately as LSA material. III-16 is included because of the presence of numerous flakes with faceted platforms; however, a piece of charcoal from III-16 provided a late Holocene date (see Table 4). The transition from MSA to LSA materials occurs around the transition from III-15 to III-16, and III-16 appears to have some mixing of elements of both. The III-20 to III-16 sample comprises ~3000 artifacts, of which 991 are >15mm (see Table 6).

No points, either unifacial or bifacial, were identified in the MSA assemblages inside the shelter, nor were any bifacial thinning flakes found (see Table 7). Backed artifacts, including point and truncated morphologies are, however, well represented in Layers III-18 through III-20 (see Figure 14-2, 14-5, and 14-8). Well-defined end scrapers were also

noted in III-17 and III-18 (Figure 14-20), again with morphology comparable to those in 04. Figure 15 shows the distribution of backed artifacts and points in both excavations. This figure helps make clear the cluster of backed pieces at the bottom of TP-III, and it also reveals a significant height difference between the major clusters of backed pieces in TP-III inside the shelter and in the Main Area—on the order of 0.25m over a distance of 2.5m. A single isolated backed piece in III-15 (see Figure 14-14) appears to be a better fit for the main cluster, however, it is likely to be of Holocene age and is in any case an isolated occurrence. This suggestion is reinforced by the distribution of aggregate samples with high proportions of silcrete, which cluster towards the bottom of the TP-III excavation (see Figure 15), and below the height of the upper silcrete band in the Main Area. In general, material selection inside the shelter most closely matches the characteristics of Layers 03 and 04 and is quite different from the lower strata in the Main Area (see Table 8). There is no statistically significant variation in raw material prevalence in the TP-III sample ( $\chi^2=20.281$ ,  $df=16$ ,  $p=0.208$ ), probably reflecting the limited temporal range so far recovered.

Artifact densities inside the shelter are generally much lower than those in the Main Area (see Table 9). The highest density inside the shelter (74, III-20) is only marginally higher than the lowest value in the Main Area (54, layer s1), while the lowest values inside the shelter are less than half those in the Main Area. This may reflect temporal differences or it may reflect differences in discard behavior inside and outside of the shelter. This point is returned to later. Between-trench differences aside, there is minor variation in artifact density through the TP-III sequence, with increasing density towards the bottom of the excavated sequence.

A total of 34 cores was recovered from the MSA layers inside the shelter (see Table 6). Bipolar cores are the most common type followed by discoidal and platform cores. Proportionally, bipolar cores are at their most common in III-16 and III-17, where they account for more than half of the cores in each layer. In the lowest three layers (III-18 through III-20), discoidal and platform cores are the most abundant types.

The value of relative core and retouched flake abundance measures inside the shelter is limited by the small samples on a layer to layer basis; what can be noted is that these values are invariably higher than their counterparts in the Main Area (see Table 6). Considering only the layers with more than 100 flakes (III-16 through III-18 and III-20), the lowest core to flake ratio is 0.039 in III-20. All other values exceed 0.04 with 0.068 (III-16) being the highest. In contrast, the highest value in the Main Area is 0.034 in Layer 03. In a similar vein, retouched to unretouched flake ratios vary from 0.034 (III-16) to 0.158 (III-19) inside the shelter but never exceed 0.029 in the Main Area.

Convergent flakes form a negligible component of the TP-III assemblage ( $n=1$ ), though blades are fairly common (see Table 11), generally increasing relative to other flake forms throughout the sequence (see Table 11). Again there

are contrasts with comparable values in the Main Excavation, blades occur at a rate of 0.03 (blade per 33 flakes) inside the shelter and about half as frequently in the Main Area (0.016, or 1 blade per 62 flakes). The highest proportion of blades in the Main Excavation assemblage is 0.02 in Layer 05, comparable to the lowest proportion among MSA layers inside the shelter (0.016 in III-16). The peak value of 0.047 (III-20) inside the shelter is more than double the peak value in the Main Area.

### Summary of the TP-III MSA Assemblage

Structured change in TP-III inside the shelter is quite weakly expressed in material percentages but is evident in respect to other factors, including implements and core types and blade prevalence. Layers III-18 through III-20 contain backed artifacts, higher proportions of blades, and lower proportions of bipolar cores than the overlying strata. We suggest that these layers are most likely to relate to the HP. The overlying layers, with few backed artifacts, small numbers of blades, and a preponderance of bipolar cores, more closely resemble the MIS 3 MSA at Klein Kliphuis and possibly Apollo 11 (Mackay 2006, 2010; Vogelsang et al. 2010). Of the latter, Vogelsang et al. (2010: 193) state that in the late MSA “[b]acked pieces, which are numerous in the underlying Howieson’s Poort layers, are also represented only by sporadic finds”, while “[b]lades are relatively rare and the proportion of angular debris is high”. Angular debris has previously been argued to be a useful indicator of bipolar working (Eren et al. 2013). Indeed, bipolar reduction of quartz appears to dominate many mid- to late MIS 3 assemblages across southern Africa (Mitchell 1988a, b). Neither the TP-III nor Main Area data provide evidence of a unifacial point-based post-HP assemblage.

### RELATING THE TP-III ASSEMBLAGES TO THE MAIN AREA

With regard to the relationship between the sequences in TP-III and in the Main Area, it seems difficult to reconcile the TP-III assemblage with any component other than Layers 03 and 04. These are the only strata, with the exception of s1, in which silcrete artifacts consistently outnumber quartzite artifacts, and 04 contains backed artifacts and endscrapers similar in abundance and form to those recovered from the lowest layers inside the shelter. If we accept that the silcrete-rich, backed artifact-bearing layers at the bottom of the excavation inside the shelter were laid down at roughly the same time as the middle to lower layers in 04, and that the Layers III-16 and III-17 roughly equate to either 03 or upper 04, a few important implications follow.

First, there is necessarily a considerable slope in the site stratigraphy from the deposits immediately outside the shelter down into the shelter itself (see Figure 15). This slope is in the order of 10%. Given the clear north slope in the talus deposits, the implication is that the sediment body at VR003 is ‘humped’ with its peak around the top of the Main Area excavation.

Second, backed artifacts appear likely to have a different stratigraphic distribution to bifacial points at VR003.

Data from the Main Excavation left open the possibility that the two were not clearly stratigraphically distinct. Layers III-18, III-19, and III-20 all suggest, however, that backed artifacts are present without bifacial points in layers showing little reworking. Further excavation may demonstrate that backed artifacts and bifacial points overlap inside the shelter, or they may be discrete with the latter underlying the former. It is also possible that bifacial points are absent in this part of the site. The occurrence of backed artifacts without bifacial points inside the shelter also implies that their lack of distinction in the downslope deposits is, in part at least, an artifact of lagging associated with erosion of fine sediments on the slope.

Third, discard patterns appear to be different in synchronous assemblages formed inside and outside the shelter. Though the assemblages share crucial characteristics, artifact densities inside the shelter are invariably much lower than those outside, something potentially modulated by differences in sedimentation rate and winnowing of small particles (see *Geoarchaeology* section above). Less affected by variability in sedimentation/erosion, however, are differences in artifact class proportions—cores, retouched flakes, and blades are all proportionally much more common inside the shelter than on the slope. It seems plausible that this reflects preferential manufacture of artifacts outside the shelter and use within, or perhaps principal reduction outside the shelter and later reduction within. Further study is required to clarify these possibilities, though the possibility of contrasting within- and outside-shelter lithic reduction behavior would add novel elements to studies of MSA spatial organization in southern Africa.

#### ANALYSIS OF USE-WEAR ON MSA LITHICS

The purpose of this initial study is to evaluate if the state of preservation of the MSA lithic assemblage from VR003 provides information on site formation processes and if the preservation encourages further and more detailed use-wear analyses. If the surfaces of the stone artifacts are well preserved, then examination of use-wear preserved on edges and surfaces of tools should clarify on what and how stone tools were used. Lithic use-wear studies allow us to directly infer functionality from tools, which provides significant insights into the range of activities performed at the site. These activities can be related to subsistence practices, lithic technology, and economic strategy.

#### MATERIAL AND METHODS

A sample of 45 artifacts made of quartz, quartzite, and silcrete was analyzed (see Table S3). The test included backed blades and bladelets (n=18), notched blades (n=9), end-scrapers (n=5), blades (n=5), blades with scars (n=4), points (n=3), and one scraper, all from MSA layers. Artifacts were first examined under a stereomicroscope (Olympus, magnifications up to 100x) followed by the analysis using a metallurgical incident light microscope equipped with Differential Interference Contrast (DIC) (Olympus, magnification up to 200x), following the standard procedures used in use-wear analysis (Gonzalez-Urquijo and Ibanez-Estevéz

2004; Plisson 1985). We highlight the accuracy of the DIC in the study of tools made of stone materials such the ones that are represented in the lithic assemblage of VR003 (silcrete, quartzite, quartz). Conventional bright-field microscopy, commonly used in use-wear analysis for tools made of flint, proved to be inappropriate for the study of coarse grained and reflective rocks. With the DIC microscopy, slopes, valleys, and other discontinuities on the surface of the specimen create optical path differences, which are transformed by reflected light in DIC microscopy into amplitude or intensity variations that reveal a topographical profile. This technique is preferred over conventional binocular microscopy because it provides a higher resolution and contrasting and three-dimensional views of microtopography (Igreja 2009). Photomicrographs were taken with a digital camera Canon EOS 600D.

We use lithic use-wear analysis pioneered by Semenov (1964) and later developed by Keeley (1980). Contact between a tool and a given worked material mechanically and chemically modifies the tool's edge and surface. These modifications are visible under low magnifications (up to 100x) in the form of scars, fractures, edge rounding, and under the microscope (up to 400x) in the form of polishes, striations, and micro edge rounding. Combined, they are reliable indicators of the material worked and of the gestures performed. Use-wear attributes such as the pattern and distribution on the tool vary with the nature and hardness of the stone materials, the type of motion executed, and the duration that the tool has been used (Keeley 1980).

Functional inferences from stone tools on the basis of tool edge wear can be problematic, because taphonomic processes such as trampling and fluvial transport can mimic edge wear produced by human use, in particular concerning macrowear damage such as scars and fractures. Fortunately, damage due to post-depositional processes such as trampling, compaction, and fluvial transport produce surface and edge wear that is distinguishable from wear traces caused by human use on the basis of various qualitative attributes of the macro and microscopic traces (Bergman and Newcomer 1983; Cattelain 1997; Fischer et al. 1984; Geneste and Plisson 1990; Gonzalez-Urquijo and Ibanez-Estevéz 2004; Kamminga 1982; Odell 1978; Odell and Odell-Vereecken 1980; Tringham et al. 1974). In addition, while post-depositional phenomena tend to produce wear traces randomly distributed all over the tool, edge, and surface, damage as result of human use has a strong preferential distribution (Levi-Sala 1986, 1988, 1993). To consider this, artifacts also are described as having "good preservation" or "weathering," where original edges and surfaces have been modified by post-depositional events that can be mechanical (trampling, transport; visible macroscopically in the form of scars, fractures, edge rounding, and microscopically in the form of random striation and shiny surfaces) and that can also be chemical (water, acidic soils; testified by the presence of patinated or white surfaces).

We therefore underline that it is necessary to incorporate in the analysis as many lines of evidence as possible,

**TABLE 12. THE MIDDLE STONE AGE LITHIC ASSEMBLAGES:  
QUALITY OF PRESERVATION OF LITHIC MATERIAL AS ASSESSED THROUGH THE USE-WEAR STUDY.**

| Layer                              | Good Preservation | Weathered | Total     |
|------------------------------------|-------------------|-----------|-----------|
| 02                                 | 1 (100%)          | 0         | 1         |
| 04                                 | 22 (71%)          | 9         | 31        |
| 05                                 | 1 (50%)           | 1         | 2         |
| III-15                             | 0 (0%)            | 1         | 1         |
| III-18                             | 4 (80%)           | 1         | 5         |
| III-19                             | 1 (100%)          | 0         | 1         |
| III-20                             | 2 (50%)           | 2         | 4         |
| <b>Total</b>                       | <b>31 (69%)</b>   | <b>14</b> | <b>45</b> |
|                                    |                   |           |           |
| <b>Sector</b>                      |                   |           |           |
| <i>I – Main Area downslope</i>     | 17 (63%)          | 10        | 27        |
| <i>II – Main Area top of slope</i> | 7 (100%)          | 0         | 7         |
| <i>III – Inside the shelter</i>    | 7 (64%)           | 4         | 11        |
| <b>Total</b>                       | <b>31 (69%)</b>   | <b>14</b> | <b>45</b> |

by combining systematically the observation of macroscopic edge damage features (scarring, edge rounding, and fractures) with the analysis of microscopic use-wear traces (polishes, striae, and micro edge rounding) for successful behavioral interpretations. Interpretations on the functionality of VR003 stone tools were based on a large experimental reference collection of use-wear traces on a wide range of rocks that has been developed in the scope of the analysis of stone artifacts from other MSA contexts in the Western Cape of South Africa (Igreja 2010; Igreja and Porraz 2013; Porraz et al. 2015).

## RESULTS

### State of Preservation

Generally, the edges and surfaces of artifacts are sufficiently well preserved to allow the use-wear analysis in reliable analytical conditions (Table 12). From the 45 artifacts analyzed, 31 are well-preserved, showing no signs of natural weathering. Interestingly, the preservation is consistent across the Main Area and in TP-III, where 71% (n= 24 of 34) and 64% (n=7 of 11) of the artifacts have “good” preservation—those in geomorphically-stable contexts are no better preserved than those on the slope ( $\chi^2=0.187$ ,  $df=1$ ,  $p=0.665$ ). Nevertheless, some pieces (n=14) do exhibit edges and surfaces moderately damaged by post-depositional phenomena, presumably linked with a mechanical origin because tool surfaces are marked by striae and flat bright polishes. The latter can be distinguished from those resulting from use by their texture and random distribution on the artifacts affecting the whole microtopography of the tool surface (Figure 16). No evidence of use-wear was recognized on these artifacts.

### Tool Use: Worked Materials and Motions

Thirteen artifacts show recognizable use-wear traces (Table 13; Figures 17–19). The traces indicate the processing of organic materials such as animal soft materials (n=3), wood (n=6), and bone (n=2). Two additional artifacts indicate use related with hard materials in the scope of a cutting motion, but the exact nature of the contact material remains uncertain (see Figure 19).

Wood processing dominates the range of the contact materials identified (see Figures 17 and 18). Notched blades (n=4) in particular seem to be a specialized tool for wood scraping. The morphological attributes of the notches themselves and the location of the polish on the ventral surface of the scar suggest that they were probably voluntarily created, prior to use, and therefore are not use scars. In addition to notched artifacts, one scraper and one endscraper also were used to scrape wood.

One blade (see Figure 19b), one backed blade, and one backed bladelet indicate the cutting of animal soft materials, likely corresponding to butchering. In addition to the polish, use-wear also includes parallel microstriation, whose orientation and length provide an indicator of the type of motion—in this case, typical of cutting. The morphology of the scars and their distribution on both sides of the used edge support this conclusion. Given the size of the bladelet we could presume that it was used as an insert element of a composite tool, but no sign of use-wear from hafting was detected.

Surprisingly, we observe use-wear related with bone processing while no evidence of bone technology has been identified within the archaeological collection. The artifacts showing contact with bone, an endscraper used to scrape (see Figure 18a and 18b) and a medial fragment of blade (see Figure 19a) bearing evidence of a longitudinal motion

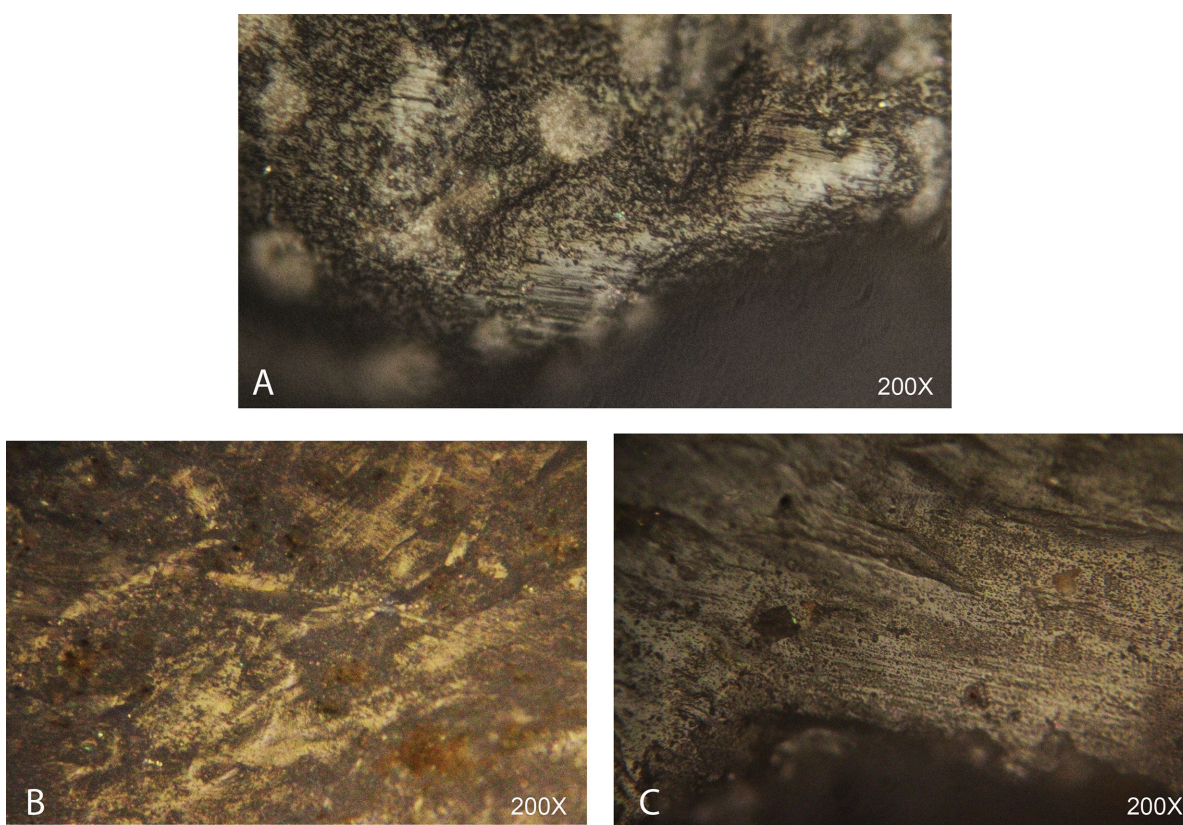


Figure 16. Examples of microscopic wear observed on artifacts from VR003 to illustrate the difference between (A) polish resulting from use, which shows striae preferentially distributed along the edge and well orientated, and (B, C) striation caused by natural phenomena, which show flat bright polish with random development on the surface of the artifact.

(e.g., cutting), present a typical polish characterized by its brightness and compact matrix close to the tools' edge (Gonzalez-Urquijo and Ibanez-Estevéz 2004; Plisson 1985).

## CONCLUSION

Results from the present study, aimed to test the potential of the MSA lithic assemblage for use-wear analysis, are extremely positive and encourage the further pursuit of the analysis in a more extensive way. The sample ranges between being well preserved (69%) to edges and surfaces with moderate impact from post-depositional phenomena, most probably mechanical. This preservation compares to

Diepkloof, where 55% (n=75 of 136) of the assemblage studied for use-wear exhibited "good" preservation (Igreja and Porraz 2013). Commonly, Paleolithic assemblages often show internal variation in their preservation. In VR003, the variation is within each layer and region of the site; there is no statistical relationship between weathering and location relative to the slope (see above), which confirms geoarchaeological suggestions of minimal movement of clasts above the size of sand grains. We can conclude that the majority of artifacts is well preserved and allow for the observation of use-wear in reliable analytical conditions. The artifacts that were successfully studied show recognizable use-wear fea-

**TABLE 13. THE MIDDLE STONE AGE LITHIC ASSEMBLAGES: THIRTEEN STONE ARTIFACTS HAVE RECOGNIZABLE PATTERNS OF USE-WEAR (motion and type of material are indicated for each artifact type).**

| Tool Type                                       | Cut | Scrape | Soft | Hard |
|---|-----|--------|------|------|
| Backed (III-18, III-20)                         | 2   | -      | 1    | 1    |
| Blade (two from Layer 04)                       | 2   | -      | 1    | 1    |
| Flake (Layer 04)                                | 1   | -      | -    | 1    |
| Blade with notch (Layer 04, 05, III-18, III-20) | -   | 4      | -    | 4    |
| Scraper (Layer 04)                              | -   | 1      | -    | 1    |
| Endscraper (Layer 04, two from III-18)          | -   | 3      | -    | 3    |

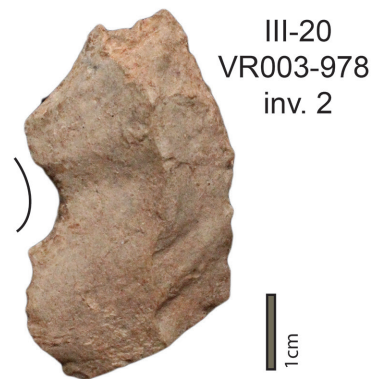
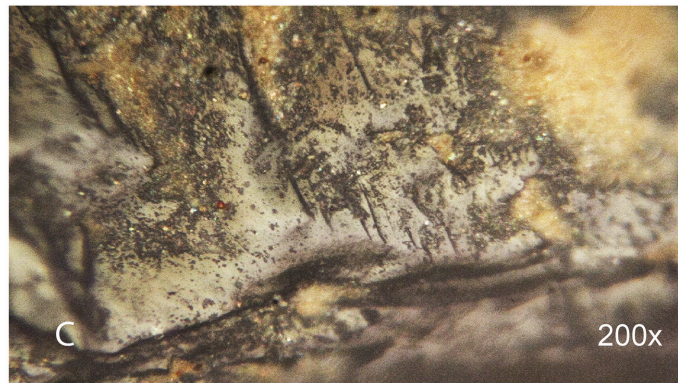
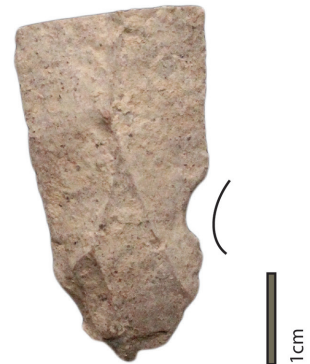
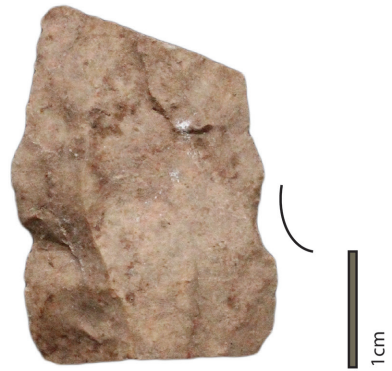


Figure 17. Use-wear observed on VR003 blades with notches related with wood scraping (A-D). The size and morphology of the notches and the location of use-wear inside the notch suggest that these were intentionally produced to be used to process a specific amount of contact material.

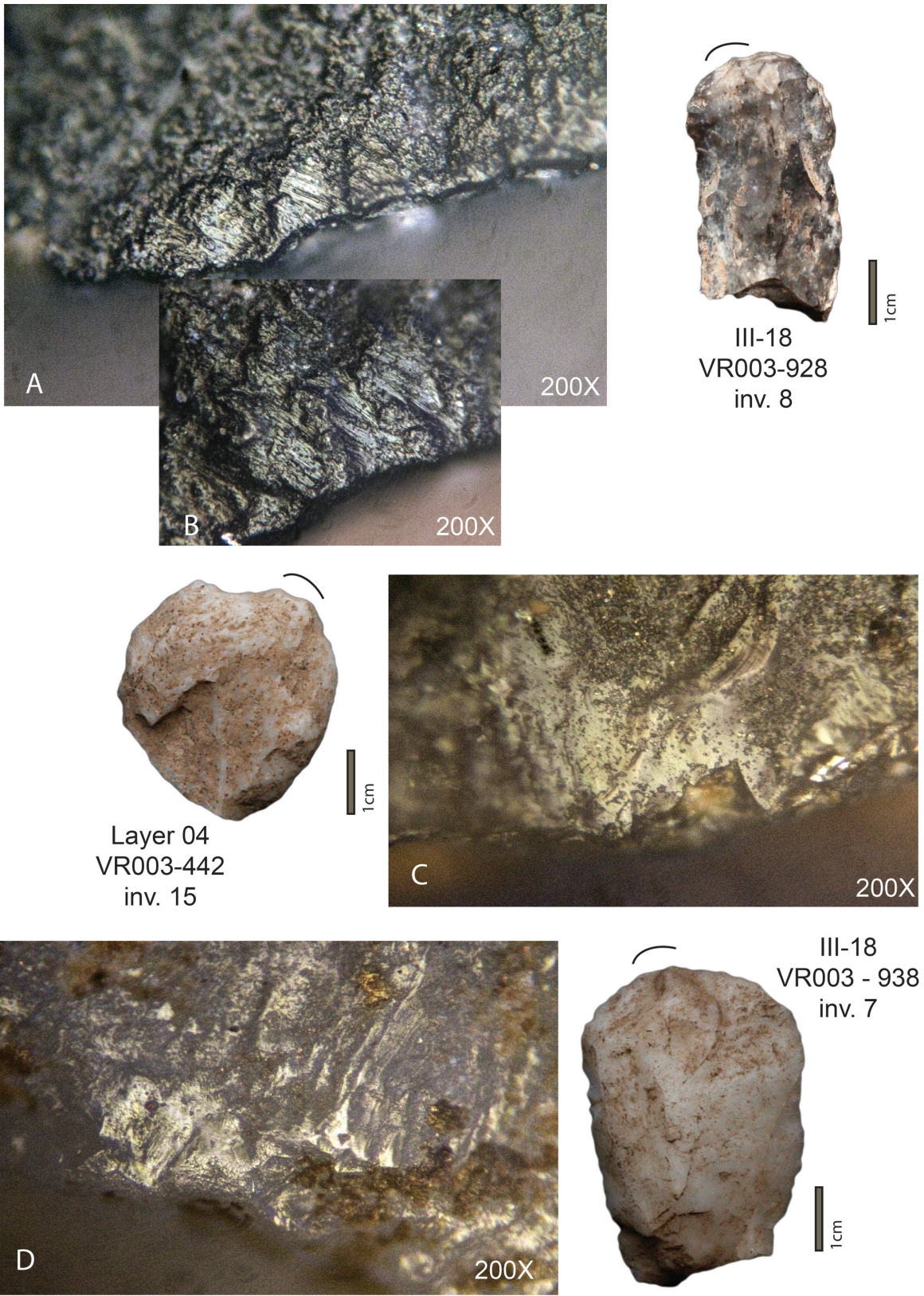


Figure 18. Artifacts from VR003 with use-wear: (A, B) endscraper used to scrape bone; (C) endscraper with polish from wood scraping; and, (D) endscraper used to scrape wood.

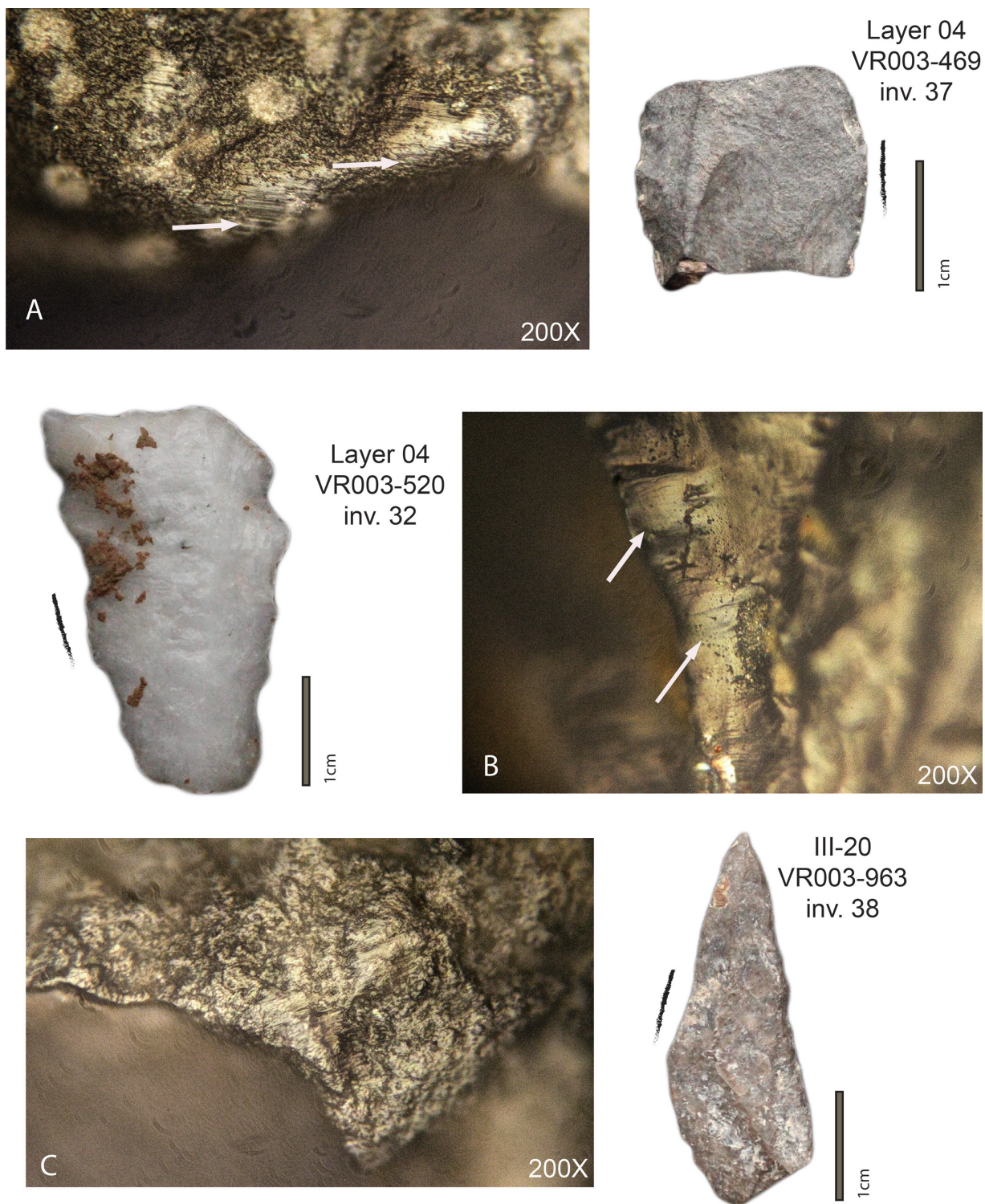


Figure 19. Examples of artifacts from VR003 with evidence of use-wear: (A) fragment of blade used to cut bone; the white arrow indicates the parallel orientation of striae typical of cutting motion; (B) blade used to cut animal soft material; the white arrow shows parallel microstriae; and, (C) backed bladelet testifying of hard material cutting.

tures related with different gestures and contact materials.

Results testify to the processing of organic materials that are not preserved in the site. Evidence of wood-working mainly was found inside the notches of artifacts. The technical features of notches and the use-wear characteristics are convergent with recent work on this type of tool that demonstrates that notches are voluntarily shaped and used in the scope of the preparation of small wooden surfaces, such as peeling and smoothing sticks, for example (Gassin et al. 2012). This is also observed on MSA pieces from Diepkloof where notches also are first intentionally produced and then used to scrape wood (M. Igreja, unpublished data).

Another interesting feature provided by this study is the evidence of bone work while there are no artifacts made of bone in the archaeological material. The polished areas on the endscraper and on the fragment of blade are restricted (affect small and specific portions of tool edge) and therefore could imply that the tools were used in the final stages of bone tool manufacture, such as “finishing” operations, as described by Averbough (2000); however, additional data are necessary to test this hypothesis.

In sum, we believe that this first analysis provides interesting results and some functional hypothesis that have to be, along with the future extension of use-wear analysis to more artifacts, explored and tested.

#### LATER STONE AGE LITHIC AND POTTERY ASSEMBLAGES

A few typical LSA artifacts (including pottery and one fragment of engraved OES) were recovered in isolation from the surface and immediate sub-surface layers of the Main Area excavation during our 2009 season. However, when we excavated inside the shelter in 2011, it became clear that VR003 preserves a substantial, although fairly low density, LSA component. Layers III-15 to III-1 are clearly LSA in character (Tables 14 and S4), while Layer III-16 contains elements of both MSA and LSA industries. OSL results for III-15 support minor mixing surrounding the contact of the MSA and LSA deposits, and a radiocarbon date on charcoal from III-16 supports a late Holocene component (see Tables 4 and 5). Although there must have been a lengthy occupational hiatus, this zone representing the contact between the MSA and LSA showed no clear distinction (sedimentary non-conformity) during excavation. Here we present a summary of the small sample of LSA materials from the 2011 excavation. The sample will increase as we expand excavations in this part of the site, and therefore a more substantial report will be provided in the future when more meaningful interpretation becomes possible.

The flaked artifact assemblage is strongly dominated by quartz with frequencies varying between 74% and 93% (Table 15 and see Table S4)—higher than any MSA component of the site. Silcrete, the next most frequent material, never exceeds 13%. Quartz domination is typical for equivalent-aged LSA assemblages in western South Africa (Dewar 2008; Orton 2006, 2012). The clear quartz backed tools suggest that Layers III-1 to III-15 are late Holocene

deposits (<2100 years old), consistent with the radiometric chronology. Although backed bladelets and points in clear quartz could occur earlier, it has been shown at the regional level that they are most common in assemblages dating within the last 2100 years, particularly in the absence or near-absence of scrapers and retouched artifacts in other materials (Orton 2012). These types of assemblages have been dubbed ‘Group 3’ and on open, single occupation sites they contrast strongly with assemblages rich in retouched artefacts on materials other than quartz (Group 1) and those that lack retouch and are based on milky quartz (Group 2; Orton 2012). Rock shelter deposits will always provide a less clear signature because of the minor ‘mixing’ of deposits that occurs every time the site is occupied and the surface scuffed. This restricts interpretation of the larger assemblage to a degree, especially when it is small, as is the case here.

When compared to collections recovered elsewhere in Namaqualand (Dewar 2008; Orton 2012), the VR003 LSA assemblage is broadly consistent with the late Holocene age implied by the radiocarbon dates. However, we cannot yet completely exclude the possibility that some very limited use of the shelter occurred during earlier millennia. A backed scraper made on fine-grained black rock from III-10 could have been made more than 2000 or even 2500 years ago (Orton 2012). Although rare backed scrapers do occur in clear quartz on some late Holocene sites, Namaqualand examples in other materials invariably come from older occupations and we do have mid- to late mid-Holocene occupation confirmed at nearby VR005 (Orton 2012). A broken large endscraper in quartzite occurs in the very small assemblage from III-12. This type of artifact is more commonly reported from terminal Pleistocene / early Holocene non-microlithic assemblages, although isolated examples can be found in younger ones. Material of this age is almost entirely absent from Namaqualand, with only one possible case on record—Webley (2002) noted large quartz scrapers at the base of her Spoeg River Cave excavation, a signal that in Elands Bay Cave (EBC) would have indicated early Holocene deposits (Orton 2006). In neither of these instances can a single artifact demonstrate anything conclusive and it is hoped that larger assemblages from future excavations will assist in this regard.

Possible MSA elements, although not isolated in the tables do occur in the LSA assemblages, but these could easily have been collected and introduced from the extensive surrounding surface exposures where MSA artifacts are abundant (Orton et al. 2011a; Schwartz et al. 2012).

Pottery is very limited with two sherds of approximately 4.7mm and 5.5mm thicknesses having been found in III-4A inside the shelter and one more of 5.9mm thickness in Layer 02 of the Main Area excavation; their presence is consistent with a late Holocene antiquity for the majority of the LSA deposits. The Main Area piece, although out of context in near-surface material, is important because it shows clear evidence of fibre temper, a trait generally recorded only in the central parts of South Africa (Bollong et al. 1993; 1997; Rudner 1979). The only other exception is a

**TABLE 14. THE LATER STONE AGE LITHIC ASSEMBLAGES BY ARTIFACT TYPE, ALL FROM TP-III (see Table S4 for artifact types by material).**

| Artifact Type                  | Layer      |           |           |            |           |           |           |           |            |            |            |           |           |            |            | Total       |
|--------------------------------|------------|-----------|-----------|------------|-----------|-----------|-----------|-----------|------------|------------|------------|-----------|-----------|------------|------------|-------------|
|                                | 1          | 2         | 3         | 4          | 5         | 6         | 7         | 8         | 9          | 10         | 11         | 12        | 13        | 14         | 15         |             |
| bipolar core                   | 4          | 1         | -         | 5          | -         | -         | -         | 3         | 3          | 3          | -          | -         | -         | 4          | 7          | 30          |
| bipolar bladelet core          | -          | -         | -         | -          | -         | -         | -         | -         | -          | -          | -          | -         | -         | -          | 1          | 1           |
| single platform core           | -          | 1         | -         | -          | -         | 1         | -         | -         | 1          | 2          | 1          | -         | -         | -          | -          | 6           |
| single platform bladelet core  | -          | -         | -         | -          | -         | -         | -         | -         | -          | -          | -          | -         | -         | -          | 1          | 1           |
| irregular core                 | 3          | -         | -         | 1          | -         | -         | -         | 1         | -          | -          | 1          | 1         | -         | -          | 1          | 8           |
| blade                          | 7          | 4         | -         | 1          | -         | 1         | -         | -         | 2          | -          | 6          | -         | -         | 1          | 2          | 24          |
| bladelet                       | 11         | 1         | 4         | 5          | 1         | 2         | 2         | 2         | 3          | 8          | 9          | 1         | 3         | 4          | 25         | 81          |
| edge-damaged flake             | 3          | -         | 2         | 1          | -         | 1         | 1         | -         | 1          | -          | 7          | 1         | -         | 1          | 10         | 28          |
| flake                          | 202        | 17        | 45        | 45         | 5         | 40        | 35        | 36        | 52         | 53         | 135        | 13        | 27        | 53         | 209        | 967         |
| chunk                          | 70         | 11        | 6         | 12         | 1         | 16        | 8         | 9         | 15         | 19         | 42         | 1         | 7         | 11         | 79         | 307         |
| chip                           | 175        | 28        | 41        | 60         | 7         | 27        | 38        | 17        | 70         | 41         | 146        | 9         | 40        | 99         | 339        | 1137        |
| triangle                       | 1          | -         | -         | -          | -         | -         | -         | -         | -          | -          | -          | -         | -         | -          | -          | 1           |
| segment                        | -          | -         | -         | -          | -         | -         | -         | -         | -          | -          | -          | -         | -         | -          | 1          | 1           |
| backed bladelet                | 2          | -         | -         | 1          | -         | -         | -         | -         | -          | -          | -          | -         | -         | 1          | 1          | 5           |
| backed bladelet fragment       | -          | -         | -         | 1          | -         | -         | -         | -         | -          | -          | -          | -         | -         | -          | -          | 1           |
| backed point                   | -          | -         | -         | -          | -         | -         | -         | -         | -          | 1          | -          | -         | -         | -          | -          | 1           |
| backed point fragment          | -          | -         | -         | -          | -         | -         | -         | 1         | -          | -          | -          | -         | -         | -          | -          | 1           |
| curve-backed bladelet          | 1          | -         | -         | -          | -         | -         | -         | -         | -          | -          | -          | -         | -         | -          | -          | 1           |
| curve-backed bladelet fragment | -          | -         | -         | -          | -         | -         | -         | -         | -          | 1          | -          | -         | -         | -          | -          | 1           |
| miscellaneous backed piece     | -          | -         | -         | -          | -         | -         | -         | -         | -          | -          | 1          | -         | -         | -          | -          | 1           |
| backed scraper                 | -          | -         | -         | -          | -         | -         | -         | -         | -          | 1          | -          | -         | -         | -          | -          | 1           |
| sidescraper                    | -          | -         | -         | -          | -         | -         | -         | -         | -          | -          | -          | -         | -         | -          | 1          | 1           |
| large endscraper               | -          | -         | -         | -          | -         | -         | -         | -         | -          | -          | -          | 1         | -         | -          | -          | 1           |
| notched piece                  | 2          | -         | -         | -          | -         | 1         | -         | -         | -          | -          | -          | -         | 1         | -          | -          | 4           |
| edge-damaged chunk             | -          | -         | -         | -          | -         | -         | -         | -         | -          | -          | 1          | -         | -         | -          | -          | 1           |
| scraper fragment               | 1          | -         | -         | -          | -         | -         | -         | -         | -          | -          | -          | -         | -         | -          | -          | 1           |
| denticulate                    | -          | -         | -         | 1          | -         | -         | -         | -         | -          | -          | -          | -         | -         | -          | -          | 1           |
| adze                           | -          | -         | -         | -          | -         | -         | -         | -         | -          | 1          | -          | -         | -         | -          | -          | 1           |
| miscellaneous retouched piece  | 1          | -         | -         | -          | -         | 1         | -         | -         | 1          | -          | -          | -         | -         | 1          | -          | 3           |
| upper grindstone fragment      | -          | -         | -         | -          | -         | -         | -         | -         | -          | -          | 1          | -         | -         | -          | 1          | 2           |
| <b>Total</b>                   | <b>483</b> | <b>63</b> | <b>98</b> | <b>133</b> | <b>14</b> | <b>90</b> | <b>84</b> | <b>69</b> | <b>148</b> | <b>130</b> | <b>350</b> | <b>27</b> | <b>78</b> | <b>175</b> | <b>678</b> | <b>2620</b> |

single sherd from Wilton Large Rock Shelter near the south coast (Deacon 1972).

### PIGMENTS

We found pigments in all stratigraphic layers in the Main Area sequence and in TP-III within the shelter. These include pieces of soft iron-rich rock that can be classified as ocher, and pebbles of manganese-rich rock that streak purple when tested on unglazed ceramic. Though both may have functioned as a colorant, they appear to have been modified differently—the ocher was sometimes ground but rarely flaked, and the manganese-rich pebbles were sometimes flaked but never ground. It is thus possible that the

manganese-rich pebbles served principally or even exclusively as tool-stone rather than pigment. We cannot presently resolve these two possibilities and so focus hereafter solely on those pieces that we have classified as ‘ocher.’

Ocher is common in Middle Stone Age sites in South Africa and is thought to have been used either as a pigment (Henshilwood et al. 2011; Marean et al. 2007; Watts 2002), as an art object itself with some specimens demonstrating engravings (Henshilwood et al. 2009; Mackay and Welz 2008), or as an ingredient for binding composite tools (Wadley 2005a 2005b). While we have an approximation of the timing and functions of ocher in MSA sites, we have only a limited understanding of how ocher specimens from

TABLE 15. THE LATER STONE AGE LITHIC ASSEMBLAGES BY MATERIAL, ALL FROM TP-III\*.

| Material     | Layer         |              |              |               |              |              |              |              |               |              |               |              |              |               |               | Total          |
|--------------|---------------|--------------|--------------|---------------|--------------|--------------|--------------|--------------|---------------|--------------|---------------|--------------|--------------|---------------|---------------|----------------|
|              | 1             | 2            | 3            | 4             | 5            | 6            | 7            | 8            | 9             | 10           | 11            | 12           | 13           | 14            | 15            |                |
| Quartz       | 407<br>(84.3) | 47<br>(74.6) | 82<br>(83.7) | 108<br>(81.2) | 13<br>(92.9) | 67<br>(74.4) | 64<br>(76.2) | 62<br>(89.9) | 131<br>(88.5) | 97<br>(74.6) | 299<br>(85.4) | 20<br>(74.1) | 61<br>(78.2) | 156<br>(89.1) | 593<br>(87.5) | 2207<br>(84.2) |
| Silcrete     | 27<br>(5.6)   | 6<br>(9.5)   | 6<br>(6.1)   | 4<br>(3.0)    | 0<br>(10.0)  | 9<br>(10.0)  | 10<br>(11.9) | 2<br>(2.9)   | 5<br>(3.4)    | 10<br>(7.7)  | 28<br>(8.0)   | 1<br>(3.7)   | 10<br>(12.8) | 2<br>(2.2)    | 45<br>(6.6)   | 165<br>(6.3)   |
| CCS          | 9<br>(1.9)    | 1<br>(1.6)   | 3<br>(3.1)   | 3<br>(2.3)    | 0<br>(3.3)   | 3<br>(3.3)   | 2<br>(2.4)   | 1<br>(1.4)   | 4<br>(2.7)    | 9<br>(6.9)   | 3<br>(0.9)    | 0<br>(0.9)   | 0<br>(2.9)   | 5<br>(2.9)    | 7<br>(1.0)    | 50<br>(1.9)    |
| Quartzite    | 21<br>(4.3)   | 6<br>(9.5)   | 3<br>(3.1)   | 6<br>(4.5)    | 0<br>(2.2)   | 2<br>(2.2)   | 3<br>(3.6)   | 3<br>(4.3)   | 3<br>(2.0)    | 3<br>(2.3)   | 10<br>(2.9)   | 2<br>(7.4)   | 2<br>(2.6)   | 4<br>(2.3)    | 20<br>(2.9)   | 88<br>(3.4)    |
| FGBR         | 1<br>(2.7)    | 2<br>(3.2)   | 3<br>(3.1)   | 7<br>(5.3)    | 1<br>(7.1)   | 7<br>(7.8)   | 3<br>(3.6)   | 0<br>(3.6)   | 5<br>(3.4)    | 6<br>(4.6)   | 7<br>(2.0)    | 3<br>(11.1)  | 5<br>(6.4)   | 7<br>(4.0)    | 12<br>(1.8)   | 81<br>(3.1)    |
| Other        | 6<br>(1.2)    | 1<br>(1.6)   | 1<br>(1.0)   | 5<br>(3.8)    | 0<br>(2.2)   | 2<br>(2.2)   | 2<br>(2.4)   | 1<br>(1.4)   | 0<br>(3.8)    | 5<br>(3.8)   | 3<br>(0.9)    | 1<br>(3.7)   | 0<br>(0.6)   | 1<br>(0.6)    | 1<br>(0.1)    | 29<br>(1.1)    |
| <b>Total</b> | <b>483</b>    | <b>63</b>    | <b>98</b>    | <b>133</b>    | <b>14</b>    | <b>90</b>    | <b>84</b>    | <b>69</b>    | <b>148</b>    | <b>130</b>   | <b>350</b>    | <b>27</b>    | <b>78</b>    | <b>175</b>    | <b>678</b>    | <b>2620</b>    |

\*The first value is the count, and the value in parentheses is the percentage in that layer. See Table S4 for artifact types by material. CCS=crypto-crystalline silicates and FGBR=fine-grained black rock (e.g., hornfels).

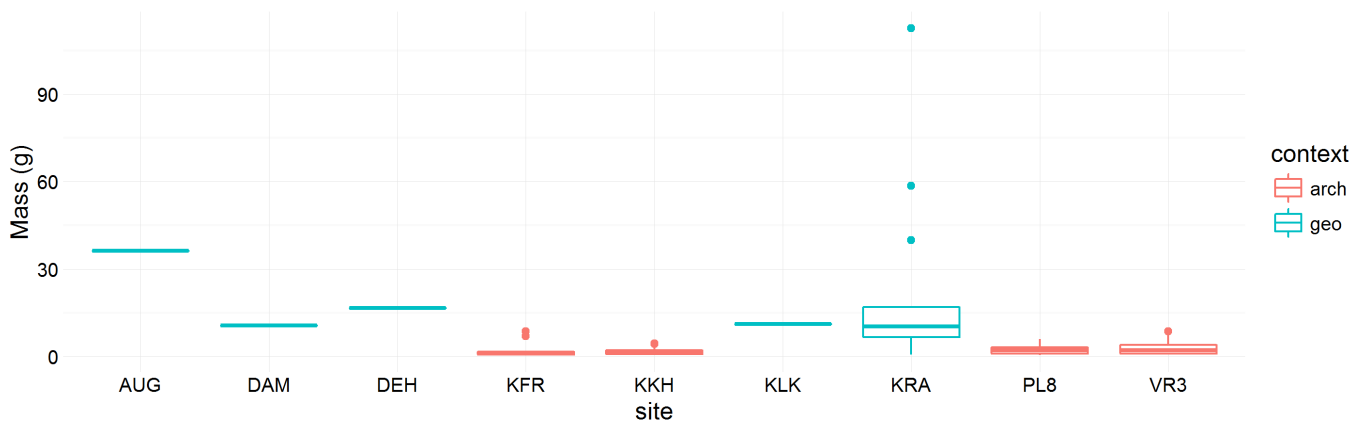


Figure 20. Distributions of mass (grams) of pigment specimens by sample location; see also Figure S2. Figure 1 and Table S5 provide keys to the abbreviations.

different sites relate to each other (Dayet et al. 2015). As a preliminary investigation of the regional context of the ochre from VR003, we sampled ochre from VR003's HP or marginal HP contexts III-17, III-16, III-20; we combined these with 60 samples of ochre from excavations at the three other archaeological sites and geological samples of ochre from four surface outcrops on the landscape surrounding those sites (Table S5). The other three sites are Klipfonteinrand (Mackay 2012), Klein Kliphuis (Mackay 2011; Mackay and Welz 2008; Orton and Mackay 2008), and Putslaagte 8 (Mackay et al. 2015). We included samples from these sites because they are close to VR003, approximately 100km to the south, and like VR003, they contain large Late Pleistocene assemblages in well-stratified sequences.

Our sampling strategy focused on ochers with physically diverse characteristics, with the objective of maximizing the range of ochers examined from each site. We used a set of non-destructive methods to record the metric dimensions, Munsell color, and basic visible attributes. Additional preliminary compositional characterization was undertaken by magnetic susceptibility analysis and X-ray fluorescence analysis.

The mass of the ochre pieces ranges from 112.6g to 0.3g, with the specimens from geological sources significantly larger than the archaeological pieces (Figures 20 and S2, 95% HDI for difference in means = -17.22, -4.53; HDI is 'Highest Density Interval', if this interval excludes zero then the means are credibly different, see Kruschke [2013] for details). Exterior color ranges widely in hue (including red, brown, orange, pink, purple) and value (light, dark). Surface textures of specimens similarly vary with most pieces having an irregular surface (50%) and smaller proportions with angular (sharp edges and flat faces) and rounded surfaces (smooth edges and convex faces). Some pieces are extremely soft and stain on contact with skin, while others have a hardness more typical of shale. These ranges of size, color, surface texture, and durability suggest a diversity of sources and transport mechanisms for ochre on this landscape.

To explore the diversity of sources we investigated the mineralogy of the specimens with two basic non-destructive methods. Non-destructive methods were preferred to minimize damage of the ground facets on some of the specimens. The first method was magnetic susceptibility, with each specimen measured 20 times each at high and low frequency with a Bartington MS2 and MS2K surface sensor. This technique is useful for identifying different proportions of antiferromagnetic magnetic minerals such as hematite (red ochers) and goethite (yellow ochers) and ferrimagnetic minerals such as magnetite or maghemite (Mooney et al. 2003).

Specimens from Klipfonteinrand and Klein Kliphuis stand out with high magnetic susceptibility values, suggesting relatively higher proportions of magnetite and maghemite than hematite and goethite (Figure 21a). The correlation of frequency dependency and low frequency mass susceptibility is low (Figure 21b, 95% HDI of correlation = -0.17, 0.3), indicating high variation in magnetic grain sizes across the specimens. Frequency dependency values vary widely across specimens from a single location, with no sign of location-based clustering. High frequency dependency values indicate the presence of very fine-grained metastable magnetic grains. Such fine sizes are often indicative of authigenic magnetic minerals, suggesting differential mineral transformations at each location. The magnetic susceptibility data are consistent with the basic physical attributes in demonstrating a high degree of variation in the ochre assemblage.

The second non-destructive method we used to characterize compositional variation of the ochre was elemental analysis using X-ray fluorescence (XRF). The elemental composition of each sample was determined using a portable XRF instrument (pXRF, Bruker Tracer III-V Light Element Analyzer) at 40keV, 15uA, using a 0.076mm copper filter and 0.0305mm aluminum filter in the X-ray path for a 300 s live-time count per spot, over ten spot locations on each piece of ochre. Iron oxides are usually the dominant component of ochers, with additions of clays, aluminosili-

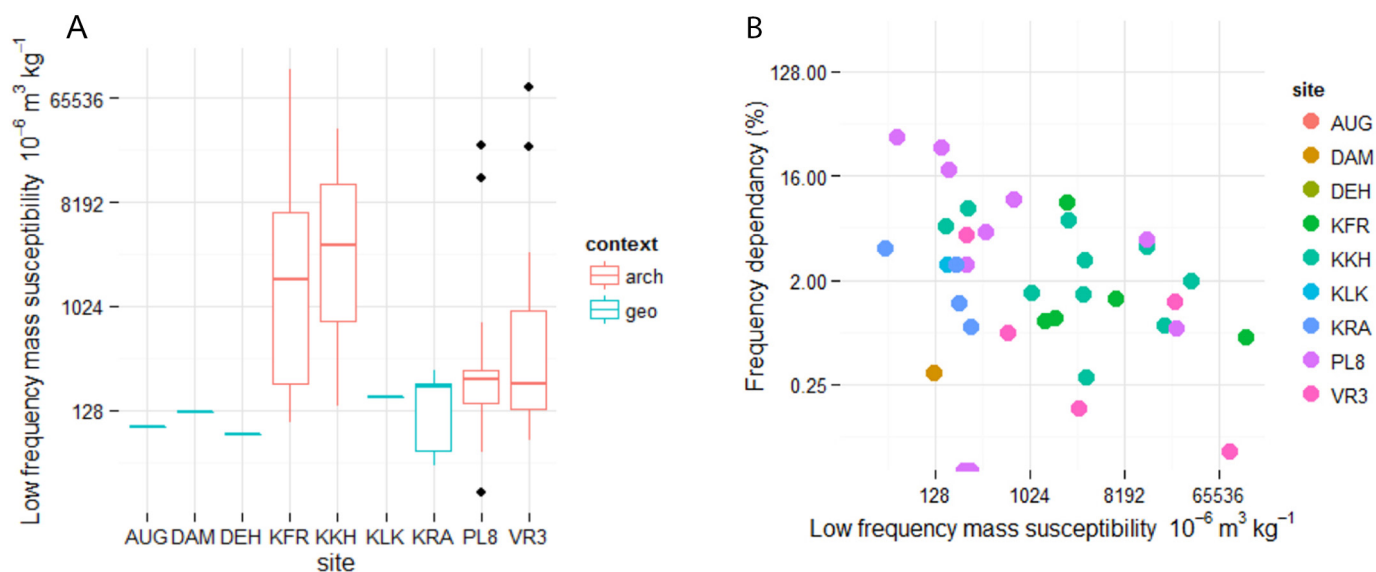


Figure 21. Magnetic susceptibility distributions and relationships for the pigment specimens. (A) Low frequency mass susceptibility distributions by sample location; (B) Relationship of frequency dependency and low frequency mass susceptibility.

cates, and other minerals. During visual inspection of the samples we found the surfaces of the ocher pieces to be quite heterogeneous, so we took a subset of the five locations on each piece of ocher that had the lowest relative standard error in the amount of iron (as the most abundant element) to characterize the bulk composition of the specimen. To analyze the data we used R (R Development Core Team [2014]) and followed the procedures of Popelka-Filcoff et al. (2007; 2008). All of the raw data and code to reproduce this analysis are online at <http://dx.doi.org/10.5281/zenodo.31903>.

Only elements that could be reliably measured in a majority of the samples (i.e., not below detection limits) were used for the analysis. A Pearson's correlation was used to determine which elements were associated with iron, and only those elements that were positively correlated (within the 90% confidence interval) with iron were retained for further analysis. To compensate for the variable levels of non-iron minerals in the ocher specimens (generally low in this sample at 1–11% mass), data analysis was performed on log-10 values of the ratio between the element and Fe in the sample. Taking the iron ratio treats variation in iron concentration as a dilution factor by other components, and the log-10 transformation minimizes the effect of the non-normal distributions of the individual elements (Popelka-Filcoff et al. 2007; 2008). The calibration standards used in the XRF measurements were NIST SRM 97b (Flint Clay), NIST SRM 679 (Brick clay) and NIST SRM 98b (Plastic clay).

The overall low concentrations of iron in these specimens is problematic for pXRF analysis because the diagnostic transition metals and rare earth elements, that are often signatures of sources, are only present in very small quantities that are at or below the sensitivity of the pXRF. Following the correlation analysis and ratio to iron transformations, cobalt and titanium remained as elements with useful measurements. Cornell and Schwertmann (2006)

have suggested that transition metals such as these occur within iron oxides as iron substitutes, so variation in their abundance may be characteristic of different sources, independent of environmental effects such as weathering. Figure 22a shows the output of a principal components analysis with ellipses showing the 68% probability regions for each group. The groups all overlap substantially, indicating that the pXRF data do not indicate groups of distinct sources for the specimens. Looking at the dendrogram in Figure 22b, we see that clustering occurs at low levels, with poor differentiation. One of the most striking patterns is that the geological specimens from Kransvlei form two clear groups; however, these groups do not include all specimens from that outcrop, indicating high within-outcrop variability. Elsewhere on the dendrogram, we see pairs and triplets of archaeological specimens from similar stratigraphic contexts, such as KFR.09 and KFR.10, KFR.04, KFR.05, KFR.06, as well as VR003.05, VR003.06, and VR003.07.

These low-level, small-scale groupings suggest a number of possibilities. First, they may indicate expedient exploitation of numerous sources rather than a systematic and long-term focus on a small number of sources. This might reflect a high level of mobility of site occupants. Second, they may indicate a high rate of circulation of ocher between sites on the landscape, such that each site is supplied by several sources. This would instead be related to a high level of exchange activity, rather than group or individual mobility. However, with the low concentrations of iron in the specimens, and the limitations of our pXRF in measuring only two elements robustly, it is difficult to be certain of the most probable interpretation. Future work with more destructive methods, including removing the surface of the specimens to analyze the core minerals using Instrumental Neutron Activation Analysis (INAA), electron microprobe, or Laser Ablation Inductively Coupled Plasma Mass Spectrometry (LA-ICP-MS) may reveal more detailed patterns

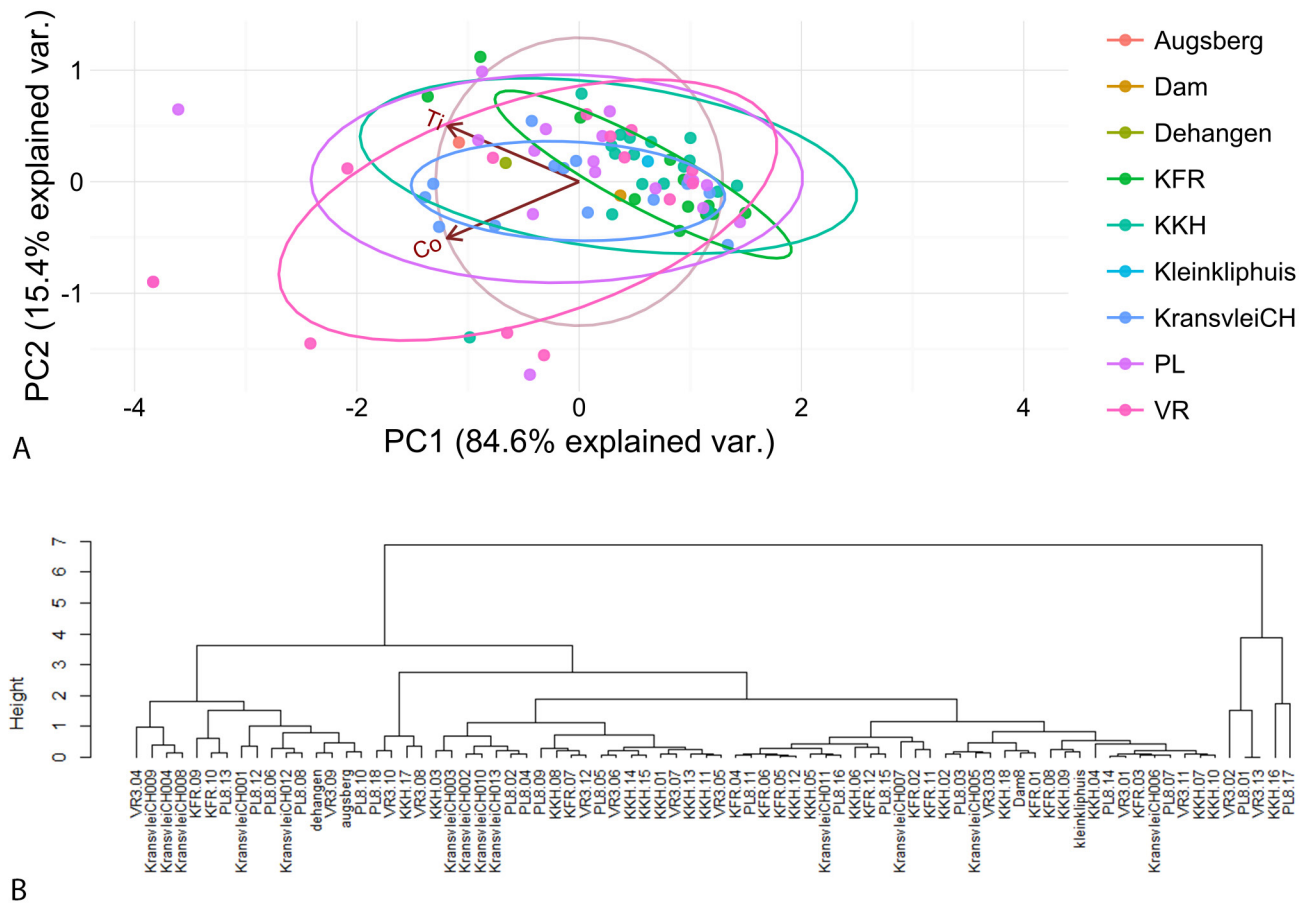


Figure 22. (A) Principal Components Analysis biplot showing substantial overlap of specimens. (B) Plot of hierarchical cluster analysis of elemental data.

because of the higher dynamic ranges of measurement and the wider range of elements that can be detected.

### FAUNAL REMAINS

Faunal remains are preserved throughout VR003, both in the Main Area (Table 16) and inside the shelter (Table 17; scientific binomials are only provided below if they do not appear in Table 16 or 17). The complete 2009 and 2011 samples have been studied (NISP=3,045), and the site has yielded many mammal bones, along with occasional fish and bird bones, a large number of tortoise and snake remains, abundant OES, land snails, and surprisingly, a few marine mollusks (the coast is currently ~45km away). Smaller animals such as tortoises, snakes, and hares are particularly abundant in the assemblage. While preliminary work has been done, a detailed taphonomic analysis of the entire faunal assemblage is planned to further understand their pre- and post-depositional history of the assemblages, especially the small vertebrates. This detailed work is necessary because the severity of post-depositional fragmentation (breakage once the bone was dry) and of surface coatings varies through the sequence, and both limit the visibility of surface modifications. The coatings that were identified in the geological thin sections are also apparent on the larger fau-

nal remains, especially in the Main Area. More systematic recording of both these characters will provide valuable about depositional history and site formation processes.

### MAMMALS

The mammalian fauna from the Main Area contains a mix of both larger and smaller taxa (see Table 16), which allows for the reconstruction of ancient environments. However, small sample sizes limit our ability to reliably reconstruct changes through the sequence. Layer 07 preserves a large number of identifiable specimens and also the highest proportion of macromammals, indicating that the quality of bone preservation improves with depth. The MSA faunal assemblage from inside the shelter is much smaller than the Main Area and contains mostly a subset of the species seen in the Main Area (see Table 17). The mammalian assemblage contains taxa that indicate a grassier and wetter environment during the Late Pleistocene than the present, consistent with other lines of evidence (Chase and Meadows 2007). The presence of a hippopotamus in Layer 03 also indicates the presence of grasses, as well as nearly perennial, reasonably deep standing water, such as a shallow lake or river, which cannot not be found in the area today. Even though their numbers are small in the assemblage,

TABLE 16. THE FAUNAL ASSEMBLAGES FROM THE MAIN EXCAVATION AREA: THE NUMBER OF IDENTIFIED SPECIMENS (NISP) OF FAUNAL REMAINS FOLLOWED BY THE MINIMUM NUMBER OF INDIVIDUALS (MNI) REPRESENTED BY THE FAUNAL REMAINS (NISP/MNI) BY ARCHAEOLOGICAL LEVEL (the 2009 and 2011 samples are combined)\*.

| Linnaean Names                           | Common Names             | Layer |     |     |      |     |     |      |     |
|--|--------------------------|-------|-----|-----|------|-----|-----|------|-----|
|  |                          | 01    | 02  | 03  | 04   | 05  | 06  | 07   | s1  |
| <i>Orycteropus afer</i>                  | aardvark                 | -     | -   | -   | -    | 1/1 | -   | -    | -   |
| <i>Procapra capensis</i>                 | rock hyrax               | -     | 2/1 | -   | 1/1  | -   | -   | 6/2  | -   |
| Leporidae                                | hare(s)                  | 1/1   | -   | 8/1 | 13/2 | -   | -   | 25/3 | 1/1 |
| <i>Hystrix africaeaustralis</i>          | porcupine                | -     | -   | -   | -    | -   | -   | 1/1  | -   |
| <i>Bathergus suillus</i>                 | Cape dune mole-rat       | 1/1   | -   | -   | 1/1  | -   | -   | 3/1  | -   |
| <i>Cryptomys hottentotus</i>             | Hottentot mole-rat       | -     | -   | 1/1 | 1/1  | -   | -   | -    | -   |
| Hyaenidae                                | hyena                    | -     | -   | -   | -    | -   | -   | 3/1  | -   |
| <i>Panthera pardus</i>                   | leopard                  | -     | -   | -   | -    | -   | -   | 1/1  | -   |
| <i>Felis silvestris libyca</i>           | wildcat                  | -     | 1/1 | 2/1 | 4/1  | 1/1 | 2/1 | 3/1  | 1/1 |
| Rhinocerotidae                           | rhinoceros               | -     | -   | -   | -    | -   | -   | 2/1  | -   |
| <i>Equus capensis</i>                    | Cape zebra               | -     | 1/1 | -   | -    | 1/1 | -   | -    | 1/1 |
| <i>Equus cf. quagga</i>                  | quagga                   | -     | -   | -   | -    | -   | 1/1 | -    | -   |
| <i>Equus</i> sp.                         | indet. equid             | -     | -   | -   | -    | 1/1 | 1/1 | -    | -   |
| <i>Hippopotamus amphibius</i>            | hippopotamus             | -     | -   | 1/1 | -    | -   | -   | -    | -   |
| <i>Taurotragus oryx</i>                  | eland                    | -     | -   | -   | -    | -   | 1/1 | 6/1  | 4/2 |
| <i>Connochaetes gnou</i>                 | black wildebeest         | -     | -   | -   | -    | -   | -   | 1/1  | -   |
| <i>Connochaetes</i> or <i>Alcelaphus</i> | wildebeest or hartebeest | -     | -   | -   | -    | -   | 1/1 | 1/1  | -   |
| <i>Hippotragus leucophaeus</i>           | blue antelope            | -     | -   | -   | 1/1  | 1/1 | 2/1 | 2/2  | -   |
| <i>Antidorcas marsupialis</i>            | common springbok         | -     | -   | -   | -    | -   | 2/1 | -    | -   |
| <i>Raphicerus</i> sp.(p.)                | grysbok/steenbok         | -     | -   | -   | -    | -   | 1/1 | -    | 1/1 |

TABLE 16. THE FAUNAL ASSEMBLAGES FROM THE MAIN EXCAVATION AREA: THE NUMBER OF IDENTIFIED SPECIMENS (NISP) OF FAUNAL REMAINS FOLLOWED BY THE MINIMUM NUMBER OF INDIVIDUALS (MNI) REPRESENTED BY THE FAUNAL REMAINS (NISP/MNI) BY ARCHAEOLOGICAL LEVEL (the 2009 and 2011 samples are combined) (continued)\*.

| Linnaean Names               | Common Names             | Layer    |              |           |            |           |           |            |           |   |   |   |   |
|------------------------------|--------------------------|----------|--------------|-----------|------------|-----------|-----------|------------|-----------|---|---|---|---|
|                              |                          | 01       | 02           | 03        | 04         | 05        | 06        | 07         | s1        |   |   |   |   |
| <i>Oreotragus oreotragus</i> | klipspringer             | -        | 1/1          | -         | -          | -         | -         | -          | -         | - | - | - | - |
|                              | small bovid(s)           | -        | 4/1          | 4/1       | 17/2       | 8/1       | 7/1       | 22/2       | -         | - | - | - | - |
|                              | small-medium bovid(s)    | -        | -            | 2/1       | 1/1        | 3/1       | 4/1       | 6/2        | -         | - | - | - | - |
|                              | large-medium bovid(s)    | -        | -            | 3/1       | 4/1        | 5/1       | 4/1       | 15/1       | 6/1       | - | - | - | - |
|                              | large bovid(s)           | -        | 1/1          | -         | 1/1        | 1/1       | 3/1       | 17/2       | 3/1       | - | - | - | - |
|                              | birds                    | -        | 2/1          | 1/1       | -          | -         | -         | 2/1        | -         | - | - | - | - |
|                              | fish                     | -        | 1/1          | -         | 2/1        | -         | -         | -          | -         | - | - | - | - |
|                              | snakes                   | 1/1      | 13/1         | 11/1      | 20/1       | 3/1       | 4/1       | 2/1        | -         | - | - | - | - |
| <i>Chersina angulata</i>     | angulate tortoise humeri | -        | 27/14        | 24/12     | 81/41      | 28/14     | 16/8      | 23/12      | 11/6      | - | - | - | - |
| <i>Pelomedusa</i>            | helmeted turtle          | -        | -            | 2/1       | 2/1        | -         | -         | 2/1        | -         | - | - | - | - |
|                              | <b>TOTAL NISP</b>        | <b>3</b> | <b>53</b>    | <b>59</b> | <b>148</b> | <b>53</b> | <b>49</b> | <b>143</b> | <b>28</b> |   |   |   |   |
|                              | marine mollusk           | 3        | 1            | 2         | 2          | -         | 1         | 1          | 1         |   |   |   |   |
|                              | Land snail (g/MNI)       | 226/20   | 14,364/2,102 | 435/78    | 96/38      | 19/5      | 15/3      | 15/9       | 3/1       |   |   |   |   |
|                              | OES (g/MNI)              | 215/1    | 6,171/26     | 3,014/13  | 22,555/95  | 4,540/20  | 3,476/15  | 4,487/19   | 1,612/7   |   |   |   |   |

\*For land snail, the first values are the grams collected, cleaned as well as possible, and the second values are the counts of apices, which provide the MNI. For ostrich eggshell (OES), the first values are the grams collected, and the second values are that total weight divided by 238g, the average weight of an empty ostrich eggshell, which provides the minimum number of ostrich eggshells represented by the sample (Kandel 2004; see also Keffen and Jarvis 1984; Humphreys 1975; Orton 2008b). Additional data on land snails and ostrich eggshells are provided in Table 18.

**TABLE 17. THE FAUNAL ASSEMBLAGES FROM TP-III: THE NUMBER OF IDENTIFIED SPECIMENS (NISP) OF FAUNAL REMAINS FOLLOWED BY THE MINIMUM NUMBER OF INDIVIDUALS (MNI) REPRESENTED BY THE FAUNAL REMAINS (NISP/MNI) BY ARCHAEOLOGICAL LEVEL (this is the complete 2011 sample; this part of the site had not been started in 2009)\*.**

| Linnaean Names                           | Common Names             | Layer       |           |            |           |            |           |            |           |           |           |           |  |
|--|--------------------------|-------------|-----------|------------|-----------|------------|-----------|------------|-----------|-----------|-----------|-----------|--|
|  |                          | 1           | 2         | 3          | 4         | 4A         | 5         | 6          | 7         | 8         | 9         | 10        |  |
| <i>Procavia capensis</i>                 | rock hyrax               | 17/2        | 1/1       | 2/1        | -         | -          | -         | 9/2        | -         | 2/1       | 1/1       | 2/1       |  |
| Leporidae                                | hare(s)                  | 29/2        | 2/1       | 5/1        | 1/1       | 2/1        | 1/1       | 1/1        | 1/1       | 4/1       | 2/1       | 4/1       |  |
| <i>Bathyergus suillus</i>                | Cape dune mole rat       | 14/3        | 2/1       | 3/1        | -         | 2/1        | 1/1       | 1/1        | -         | 2/1       | 2/1       | -         |  |
| <i>Felis silvestris libyca</i>           | wildcat                  | 1/1         | -         | 1/1        | -         | -          | -         | -          | -         | -         | -         | -         |  |
| <i>Caracal caracal</i>                   | caracal                  | -           | -         | -          | -         | -          | -         | 1/1        | -         | -         | -         | -         |  |
| <i>Canis</i> sp.                         | dog or jackal            | 4/1         | -         | -          | -         | -          | -         | 3/1        | -         | 1/1       | -         | -         |  |
| <i>Mellivora capensis</i>                | honey badger             | 1/1         | -         | 1/1        | -         | -          | -         | -          | -         | -         | -         | -         |  |
| <i>Equus</i> sp.                         | indet. equid             | -           | -         | -          | -         | 1/1        | -         | -          | -         | -         | -         | -         |  |
| Bovini                                   | large bovine             | 1/1         | -         | -          | -         | -          | -         | -          | -         | -         | -         | -         |  |
| <i>Taurotragus oryx</i>                  | eland                    | -           | -         | -          | -         | -          | -         | -          | -         | -         | -         | -         |  |
| <i>Connochaetes</i> or <i>Alcelaphus</i> | wildebeest or hartebeest | -           | -         | -          | -         | -          | -         | -          | -         | -         | -         | -         |  |
| <i>Raphicerus</i> sp.(p.)                | grysbok/steenbok         | 3/1         | 1/1       | -          | -         | -          | -         | 1/1        | 1/1       | -         | -         | 1/1       |  |
|  | small bovid(s)           | 19/1        | 4/1       | 5/1        | 1/1       | 7/1        | -         | 8/1        | 5/1       | 6/1       | 1/1       | -         |  |
|  | small-medium bovid(s)    | 3/1         | -         | -          | -         | 3/1        | -         | -          | -         | -         | 1/1       | -         |  |
|  | large-medium bovid(s)    | -           | -         | -          | 1/1       | -          | -         | -          | -         | -         | -         | -         |  |
|  | large bovid(s)           | -           | -         | 1/1        | 1/1       | -          | -         | -          | -         | -         | -         | -         |  |
|  | birds                    | 7/1         | -         | -          | -         | 1/1        | 1/1       | 2/1        | 1/1       | -         | -         | -         |  |
|  | snakes                   | 1473/?      | 55/1      | 191/1      | 47/1      | 103/1      | 54/1      | 89/1       | 3/1       | 47/1      | 5/1       | 13/1      |  |
| <i>Chersina angulata</i>                 | angulate tortoise humeri | 10/5        | 1/1       | 4/2        | -         | 2/1        | 1/1       | 5/3        | 1/1       | -         | 1/1       | 5/3       |  |
| <i>Psammobates tentorius</i>             | tent tortoise            | 1/1         | -         | -          | -         | -          | -         | -          | -         | -         | -         | -         |  |
|  | tortoise                 | -           | -         | -          | -         | -          | -         | -          | -         | -         | -         | -         |  |
| <i>Pelomedusa</i>                        | helmeted turtle          | 2/1         | -         | -          | -         | -          | -         | 1/1        | -         | -         | -         | -         |  |
|  | <b>TOTAL NISP</b>        | <b>1585</b> | <b>66</b> | <b>213</b> | <b>51</b> | <b>121</b> | <b>58</b> | <b>121</b> | <b>12</b> | <b>62</b> | <b>13</b> | <b>25</b> |  |
|  | marine mollusk           | -           | -         | -          | -         | -          | -         | -          | -         | 1/1       | -         | -         |  |
|  | Land snail (g/MNI)       | 77.5/61     | 8.9/16    | 23.3/9     | 2.8/2     | 15.0/5     | 3.3/4     | 33.6/26    | 25.0/10   | 10.8/5    | 32.7/14   | 133.0/24  |  |
|  | OES (g/MNI)              | 699.6/3     | 64.5/1    | 156.8/1    | 30.2/1    | 380.4/2    | 25.1/1    | 339.8/2    | 167.3/1   | 189.4/1   | 149.1/1   | 369.4/2   |  |

\*For land snail, the first values are the grams collected, cleaned as well as possible, and the second values are the counts of apices, which provide the MNI. For ostrich eggshell (OES), the first values are the grams collected, and the second values are that total weight divided by 238 g, the average weight of an empty ostrich eggshell, which provides the minimum number of ostrich eggshells represented by the sample (Kandel 2004, see also Keffen & Jarvis 1984, Humphreys 1975, Orton 2008b). Additional data on land snails and ostrich eggshells are provided in Table 18.

zebra and wildebeest and their relatives (Alcelaphini) depend on grass, and the presence of these taxa indicates grass in the region. Eland are not unexpected in the assemblage, given their diverse habitat tolerances and preference for more open habitats. They and blue antelope are common in Late Pleistocene assemblages of the Western Cape. The carnivores are typical of the region, and aardvarks active on the river floodplain even today. Hyraxes are to be expected in this rocky location, and they are also still active around the site today. Hares are quite common in both the Main Area and the TP-III assemblages, and a detailed taphonomic analysis will help distinguish their accumulator.

The LSA assemblage is more strongly dominated by small taxa, with hyrax, hares, mole rats, and snakes being particularly common in the surface material inside the shelter (see Table 17). The surface material also preserved one large bovine deciduous premolar; while a positive identification should be made using ancient DNA techniques (Orton et al. 2013), it is possible that this tooth is from a domesticated calf (*Bos taurus*). Domestic cattle were present in northern Namaqualand by 421–559 CE (Orton et al. 2013), and are currently farmed on the VR property. Therefore, if the tooth was further identified as cattle, its presence in the surface material would not be surprising. Small-medium

**TABLE 17. THE FAUNAL ASSEMBLAGES FROM TP-III: THE NUMBER OF IDENTIFIED SPECIMENS (NISP) OF FAUNAL REMAINS FOLLOWED BY THE MINIMUM NUMBER OF INDIVIDUALS (MNI) REPRESENTED BY THE FAUNAL REMAINS (NISP/MNI) BY ARCHAEOLOGICAL LEVEL (this is the complete 2011 sample; this part of the site had not been started in 2009) (continued)\*.**

| Linnaean Names                           | Common Names             | Layer     |          |          |          |           |           |           |           |          |          |
|--|--------------------------|-----------|----------|----------|----------|-----------|-----------|-----------|-----------|----------|----------|
|  |                          | 11        | 12       | 13       | 14       | 15        | 16        | 17        | 18        | 19       | 20       |
| <i>Procavia capensis</i>                 | rock hyrax               | 1/1       | -        | -        | -        | 2/1       | 1/1       | 1/1       | -         | -        | -        |
| Leporidae                                | hare(s)                  | 6/2       | -        | -        | 1/1      | 4/1       | 6/1       | 7/2       | 1/1       | -        | 1/1      |
| <i>Bathyergus suillus</i>                | Cape dune mole rat       | -         | -        | -        | -        | 3/1       | -         | 1/1       | -         | -        | 1/1      |
| <i>Felis silvestris libyca</i>           | wildcat                  | -         | -        | -        | -        | -         | 1/1       | 2/1       | -         | -        | -        |
| <i>Caracal caracal</i>                   | caracal                  | -         | -        | -        | -        | -         | -         | -         | -         | 1/1      | -        |
| <i>Canis</i> sp.                         | dog or jackal            | -         | -        | -        | -        | -         | -         | -         | -         | -        | -        |
| <i>Mellivora capensis</i>                | honey badger             | -         | -        | -        | -        | -         | -         | -         | -         | -        | -        |
| <i>Equus</i> sp.                         | indet. equid             | -         | -        | -        | -        | -         | -         | -         | -         | -        | -        |
| Bovini                                   | large bovine             | -         | -        | -        | -        | -         | -         | -         | -         | -        | -        |
| <i>Taurotragus oryx</i>                  | eland                    | -         | -        | -        | -        | -         | -         | -         | -         | 1/1      | -        |
| <i>Connochaetes</i> or <i>Alcelaphus</i> | wildebeest or hartebeest | 1/1       | -        | -        | -        | -         | -         | -         | -         | -        | -        |
| <i>Raphicerus</i> sp(p.)                 | grysbok/steenbok         | -         | -        | -        | 1/1      | -         | -         | 2/1       | -         | -        | -        |
|  | small bovid(s)           | 1/1       | 1/1      | -        | 2/1      | 1/1       | 1/1       | 4/1       | 1/1       | -        | 1/1      |
|  | small-medium bovid(s)    | -         | -        | -        | -        | 1/1       | -         | 1/1       | -         | -        | -        |
|  | large-medium bovid(s)    | -         | -        | -        | -        | -         | 1/1       | -         | 2/1       | -        | -        |
|  | large bovid(s)           | -         | 1/1      | -        | -        | -         | -         | -         | -         | -        | -        |
|  | birds                    | -         | -        | -        | -        | 1/1       | 4/1       | -         | -         | -        | -        |
|  | snakes                   | 13/1      | 2/1      | 4/1      | 3/1      | 9/1       | 13/1      | 12/1      | 5/1       | -        | 1/1      |
| <i>Chersina angulata</i>                 | angulate tortoise humeri | 1/1       | -        | -        | -        | 3/2       | 4/2       | 7/4       | 3/2       | -        | 1/1      |
| <i>Psammobates tentorius</i>             | tent tortoise            | -         | -        | -        | -        | -         | -         | -         | -         | -        | -        |
|  | tortoise                 | 1/1       | -        | 1/1      | -        | -         | -         | -         | -         | -        | -        |
| <i>Pelomedusa</i>                        | helmeted turtle          | -         | -        | -        | -        | -         | 1/1       | -         | -         | -        | -        |
|  | <b>TOTAL NISP</b>        | <b>24</b> | <b>4</b> | <b>5</b> | <b>7</b> | <b>24</b> | <b>32</b> | <b>37</b> | <b>12</b> | <b>2</b> | <b>5</b> |
|  | marine mollusk           | -         | -        | -        | -        | -         | -         | -         | -         | -        | -        |
|  | Land snail (g/MNI)       | 48.4/12   | 7.4/4    | 364.7/52 | 49.3/13  | 11.2/1    | 12.4/33   | 0.7/7     | 5.4/25    | 0.0/0    | 0.4/1    |
|  | OES (g/MNI)              | 275.0/2   | 32.2/1   | 113.0/1  | 75.5/1   | 449.2/2   | 483.7/2   | 709.8/3   | 365.8/2   | 19.6/1   | 129.1/1  |

\*For land snail, the first values are the grams collected, cleaned as well as possible, and the second values are the counts of apices, which provide the MNI. For ostrich eggshell (OES), the first values are the grams collected, and the second values are that total weight divided by 238 g, the average weight of an empty ostrich eggshell, which provides the minimum number of ostrich eggshells represented by the sample (Kandel 2004, see also Keffen & Jarvis 1984, Humphreys 1975, Orton 2008b). Additional data on land snails and ostrich eggshells are provided in Table 18.

bovid bones attributed to a modern sheep or goat (*Capri- ni*) were on the site's surface before we started excavation, and sheep (*Ovis aries*) are currently farmed on neighboring ranches. Small-medium bovids were also identified in the excavated assemblage; however, of these, none were indicative of sheep or goat and a few that were indicative of taxa were most likely bush duiker (*Sylvoicapra grimmia*). Medium-sized canids are also present in the late Holocene assemblage, and again, ancient DNA would be needed to determine if they represent dogs or jackals (Horsburg 2008; Mitchell 2014). One zebra and one alcelaphine suggest the presence of some grasses, but otherwise the LSA fauna

lacks larger bovids, larger carnivores, rhinoceros, and hippopotamus.

A few burnt bones are found through the assemblages (n=30), and of these, 14 of them come from Layer 07. We have seen no clear burnt or ashy patches in this area, but one was documented deeper in Layer s1 as s1f1 (see Figure 6 and Table 1). Only two carnivore-chewed and two small rodent-gnawed bones were found, and these were all from the surface inside the shelter. Two cut-marks were identified, one on a bone from III-02 and another from III-20. Green breaks were common throughout the assemblages, and percussion-notched bones were found in Layers 05, III-

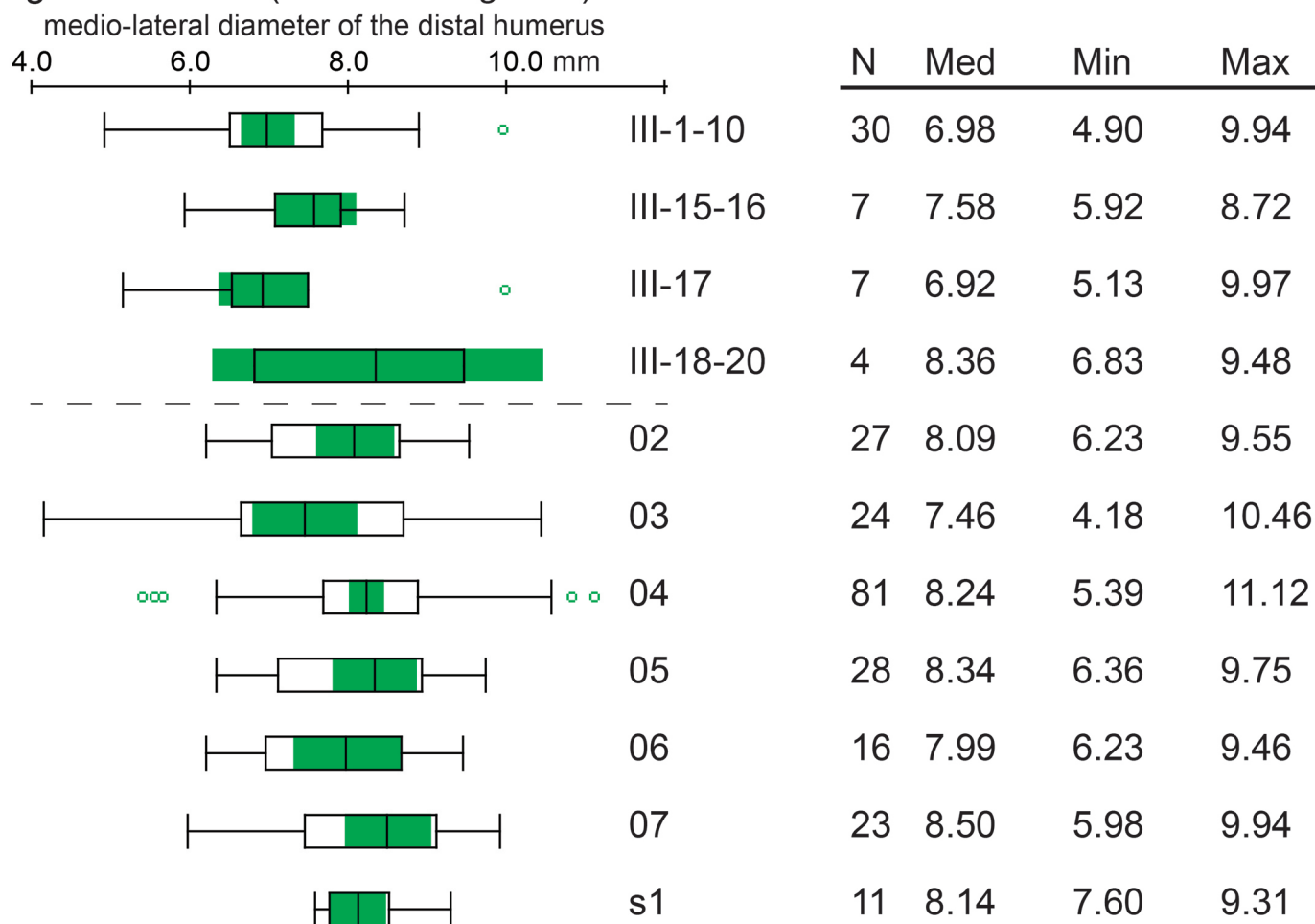
Angulate tortoise (*Chersina angulata*) size

Figure 23. Variation in the size of angulate tortoises, as estimated from measurements of their distal humerus, through the VR003 sequence. The boxplots compare medians of the samples, because we do not expect tortoise size to be normally distributed. The median is shown as the vertical black line, and the 95% confidence interval around that median is shaded green. If two green zones do not overlap, then the samples can be considered significantly different. The open rectangles enclose the middle-half of the data, the data between the 25th and 75th percentiles. The horizontal line bisecting each plot shows the range of continuous data, while open circles mark the outliers.

01, and two in III-08.

## REPTILES

Tortoise elements are extremely common in the assemblages; tortoises comprise about half of the identifiable faunal remains from the Main Excavation area. Overwhelmingly, the tortoise remains were derived from angulate tortoises, the most common species on the Western Cape landscape and in these faunal assemblages. In a few instances, tent tortoises are clearly identifiable because of their distinct carapaces. Helmeted turtles also are present, indicating some persistence of moisture in the area, likely the muddy areas of the Varsche River. Snake vertebrae are common in the sequence, especially in the surface material inside the shelter; however, we have been unable to further identify these to species. A detailed taphonomic study of the entire reptile assemblage to assess how they were processed is planned (e.g., Thompson and Henshilwood 2014).

In other Western Cape assemblages, angulate tortoises from LSA sites are smaller than their MSA counterparts, potentially because they were more heavily preyed upon by humans (Klein and Cruz-Urbe 1983; Steele and Klein 2005/06). The patterning in the VR003 tortoise sample is less clear (Figure 23). While the tortoises from the LSA deposits tend to be smaller, the variation is not significant; the specimens from III-17, the late MSA, are comparably small. Within the MSA of the Main Area, the confidence limits around the medians also overlap, indicating no significant change through the sequence.

## BIRDS (INCLUDING OSTRICH EGGSHELL)

Bird bones are rare in the sequence and are mostly from the late Holocene layers. Two fragments from Layer 07 of the distal tarsometatarsus of an ostrich (*Struthio camelus*) are exceptional. While ostrich eggshells (OES) are common in many regional faunal assemblages, bones of ostriches are

**TABLE 18. OSTRICH EGGSHELL (OES) AND LAND SNAIL DENSITY BY LAYER**  
(the 2009 and 2011 samples are combined; the density values are per liter [L]).

| Layer                             | Ostrich Eggshell (OES) |          |          |      |     | Land Snails |          |     |      |
|-----------------------------------|------------------------|----------|----------|------|-----|-------------|----------|-----|------|
|                                   | n Liters               | n Pieces | Grams    | n/L  | g/L | n Apices    | Grams    | n/L | g/L  |
| <i>Main Area</i>                  |                        |          |          |      |     |             |          |     |      |
| 01                                | 57                     | 729      | 215.3    | 12.8 | 0.8 | 20          | 226.4    | 0.4 | 4.0  |
| 02                                | 1063                   | 10,256   | 6,170.9  | 9.7  | 0.1 | 2,102       | 14,364.0 | 2.0 | 13.5 |
| 03                                | 359                    | 4,825    | 3,013.8  | 13.4 | 0.2 | 78          | 435.0    | 0.2 | 1.2  |
| 04                                | 691                    | 30,824   | 22,554.6 | 44.6 | 0.5 | 38          | 96.1     | 0.1 | 0.1  |
| 05                                | 324                    | 5,606    | 4,539.8  | 17.3 | 0.5 | 5           | 18.7     | 0.0 | 0.1  |
| 06                                | 547                    | 3,909    | 3,475.7  | 7.1  | 0.1 | 3           | 15.2     | 0.0 | <0.1 |
| 07                                | 669                    | 5,859    | 4,486.9  | 8.8  | 0.1 | 9           | 14.7     | 0.0 | <0.1 |
| s1                                | 282                    | 2,128    | 1,611.8  | 7.5  | 0.2 | 1           | 3.3      | 0.0 | <0.1 |
| <i>TP-III: Inside the Shelter</i> |                        |          |          |      |     |             |          |     |      |
| III-01                            | 198                    | 1,032    | 699.6    | 5.2  | 0.2 | 61          | 77.5     | 0.3 | 0.4  |
| III-02                            | 24                     | 110      | 64.5     | 4.6  | 1.3 | 16          | 8.9      | 0.7 | 0.4  |
| III-03                            | 42                     | 262      | 156.8    | 6.2  | 1.1 | 9           | 23.3     | 0.2 | 0.6  |
| III-04                            | 9                      | 31       | 30.2     | 3.4  | 4.5 | 2           | 2.8      | 0.2 | 0.3  |
| III-04A                           | 27                     | 471      | 380.4    | 17.4 | 6.3 | 5           | 15.0     | 0.2 | 0.6  |
| III-05                            | 9                      | 27       | 25.1     | 3.0  | 3.7 | 4           | 3.3      | 0.4 | 0.4  |
| III-06                            | 60                     | 347      | 339.8    | 5.8  | 1.1 | 26          | 33.6     | 0.4 | 0.6  |
| III-07                            | 36                     | 166      | 167.3    | 4.6  | 1.5 | 10          | 25.0     | 0.3 | 0.7  |
| III-08                            | 24                     | 245      | 189.4    | 10.2 | 3.9 | 5           | 10.8     | 0.2 | 0.5  |
| III-09                            | 45                     | 169      | 149.1    | 3.8  | 0.9 | 14          | 32.7     | 0.3 | 0.7  |
| III-10                            | 48                     | 435      | 369.4    | 9.1  | 1.9 | 24          | 133.0    | 0.5 | 2.8  |
| III-11                            | 66                     | 323      | 275.0    | 4.9  | 0.8 | 12          | 48.4     | 0.2 | 0.7  |
| III-12                            | 9                      | 42       | 32.2     | 4.7  | 4.8 | 4           | 7.4      | 0.4 | 0.8  |
| III-13                            | 18                     | 108      | 113.0    | 6.0  | 4.2 | 52          | 364.7    | 2.9 | 20.3 |
| III-14                            | 24                     | 113      | 75.5     | 4.7  | 1.6 | 13          | 49.3     | 0.5 | 2.1  |
| III-15                            | 81                     | 654      | 449.2    | 8.1  | 0.8 | 1           | 11.2     | 0.0 | 0.1  |
| III-16                            | 108                    | 640      | 483.7    | 5.9  | 0.5 | 33          | 12.4     | 0.3 | 0.1  |
| III-17                            | 120                    | 900      | 709.8    | 7.5  | 0.6 | 7           | 0.7      | 0.1 | 0.0  |
| III-18                            | 72                     | 492      | 365.8    | 6.8  | 0.8 | 25          | 5.4      | 0.3 | 0.1  |
| III-19                            | 12                     | 38       | 19.6     | 3.2  | 1.6 | 0           | 0.0      | 0.0 | 0.0  |
| III-20                            | 39                     | 171      | 129.1    | 4.4  | 1.0 | 1           | 0.4      | 0.0 | 0.0  |

rare. Like other regional sites, such as Ysterfontein 1, Spitzkloof, Diepkloof, and Apollo 11 (e.g., Avery et al. 2008; Dewar and Stewart 2012; Texier et al. 2013; Vogelsand et al. 2010), fragments of OES are abundant throughout the VR003 sequence. Ostriches are common on the landscape today, and fragments of their eggshells provide evidence of their persistence throughout the Late Pleistocene. OES peaks in density in Layer 04 in the Main Area (Table 18). If the average weight of modern, empty eggshells is taken from Kandel (2004) as 238g (see also Humphrey 1975; Keffen and Jarvi

1984; Orton 2008b), then at least 95 ostrich eggs are represented in the present Layer 04 sample. Relatively speaking, OES is less abundant inside the shelter; here, density peaks in III-4A. When quantifying the assemblage, we also examined the fragments for unusual taphonomic histories, such as engraving, canteen mouths, or hyena breakage (Kande 2004; Texier et al. 2010). Only one fragment of engraved ostrich eggshell was found, from Layer 02 in the Main Area, in a context that has a few isolated LSA pieces, including pottery; it had parallel-incised lines on it (Steele et al. 2012).

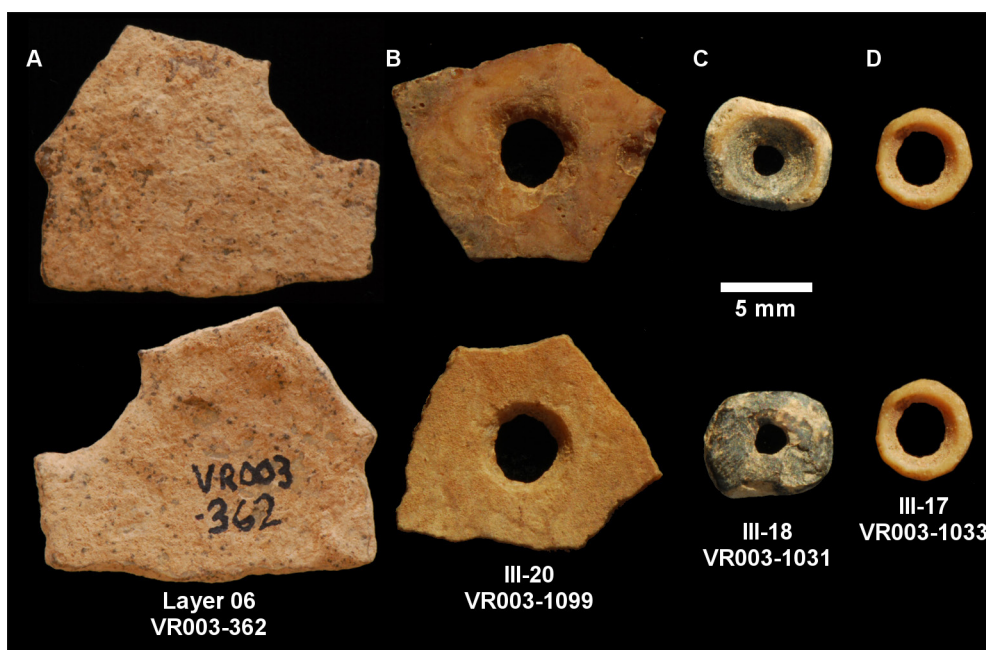


Figure 24. (A) Example of a “notched” piece of OES (VR003-362); (B) OES bead preform (Stage IIIa from Orton 2008b: Table 1) (VR003-1099) found in III-20, an HP layer; (C) bone bead (VR003-1031) found in III-18, an HP layer; and, (D) OES bead found in III-17 (VR003-1033), a late MSA layer.

Other pieces had smooth notches or chipped edges, but they formed a continuous range of variation within the assemblage, and their significance is currently unclear (Figure 24) (see also photos in Steele et al. 2012).

### MARINE MOLLUSKS

One of the most surprising aspects of the VR003 faunal assemblage is the presence of a few marine mollusks, despite the sea currently being ~45km to the west ( $n=12$ , see Tables 16 and 17). During the Late Pleistocene, when sea levels were lower, the sea would have been even further away. The VR003 MSA shells are mainly limpets, and when the species can be identified, granular (*Scutellastra granularis*) and Argenville’s (*Scutellastra argenvillei*) limpets. These taxa are well-known from other West Coast MSA mollusk-bearing sites, such as Boegoeberg 2, Hoedjiespunt 1 and 3, Sea Harvest, and Ysterfontein 1 (Avery et al. 2008; Kyriacou et al. 2015; Parkington 2003; Volman 1978), where the limpets appear in abundance and almost certainly were a source of food for the humans. At VR003, the meaning of the long-distance transport of a small sample of these taxa (normally considered food refuse) is less clear. Numerous examples exist in LSA assemblages where marine shells (of taxa normally considered food refuse) have been transported for >45km distance, including the LSA deposits of VR003, VR001, and VR005 (this study; Orton et al. 2011b). During the MSA, the only greater transport distances for taxa normally considered food refuse are known from Apollo 11 and Pockenbank Rock Shelter, which are ~140km and ~120km respectively from the present coast in southern Namibia (Schmidt et al. 2016; Thackeray 1979; Vogelsang 1998; Vogelsang et al. 2010); Apollo 11 preserves a few

isolated fragments of granite limpet, (*Cymbula granatina* [Vogelsang 1998]) and Pockenbank has provided granite limpet and black mussel (*Choromytilus meridionalis*) fragments [T. Steele, personal observation]. Depending on the reconstructed ages of deposition, the marine mollusks in Unit M1 of Blombos Cave may have been transported up to ~40km, but this is not supported by all of the available data, and maximum distances of around 10km or less were much more likely (Dusseldorp and Langejans 2013; Fisher et al. 2010). The MSA deposits of Diepkloof Rock Shelter and Sibudu Cave preserve some marine mollusks; these sites are 14–15km from the current coasts, but would have been further during the Late Pleistocene. The Diepkloof sample of limpets and mussels is large enough to suggest that these shells primarily reflect subsistence; the flat margin of the local vlei may have minimized transport costs (Steele and Klein 2013). The Sibudu marine mollusk sample is small and composed almost exclusively of brown mussels (*Perna perna*) (Plug 2006). Mussels are bivalves, and as such, fresh mussels retain moisture, making them last longer and allowing them to be transported over longer distances. However, it still may be possible that the transport of mussels to Sibudu reflects something other than subsistence (Plug 2006). In addition, six African periwinkle (*Afrolittorina africana*) also are found in MSA contexts there (d’Errico et al. 2008). Examples from the MSA exist of the use of larger marine mollusks (e.g., abalone, *Haliotis midae*; helmet or lipped cask shell, *Phalium labiatum*) for non-food purposes, but in each case, the shells were transported for minimal distances, at least in terms of their final resting place (Henshilwood et al. 2011; Jerardino and Marean 2010). In MSA contexts, the only mollusks that appear to have been

TABLE 19. OSTRICH EGGSHELL (OES) BEADS FROM THE 2009 AND 2011 SAMPLES\*.

| Layer                        | n         | External Diameter (mm)  |
|------------------------------|-----------|---|
| Main Area Layer 01 (Surface) | 1         | Pathway 1: Stage IIIb   |
| Main Area Layer 02           | 7         | 4.83, 4.84, 3.70, 5.02, 4.83, Pathway 1: Stage IIb, Pathway 1: Stage IIIa |
| III-01                       | 5         | 5.39, 5.69, 10.00, 5.08, 4.93   |
| III-02                       | 1         | 8.33  |
| III-03                       | 1         | 5.21  |
| III-04A                      | 1         | 4.55  |
| III-06                       | 1         | 5.47  |
| III-07                       | 1         | 5.22  |
| III-08                       | 2         | 5.23, 5.15  |
| III-09                       | 1         | 8.83  |
| III-10                       | 3         | 6.11, 5.00, 6.50  |
| III-11                       | 1         | 5.03  |
| III-12                       | 1         | 5.92  |
| III-17                       | 1         | 5.68  |
| III-20                       | 1         | Pathway 1: Stage IIIa   |
| <b>Total</b>                 | <b>28</b> |   |

\**Italicized* measurements are estimates of partially broken pieces. Beads in earlier stages of manufacture were not measured. Bead manufacturing stages follow Orton (2008b: Table 1), where Pathway 1 Stage II describes the central hole as partially drilled and Stage III as completely drilled and 'a' indicates a complete bead while 'b' a broken one.

transported for long distances are small shells that would have had little utility as a food resource but may have been used as ornaments. Swollen nassa (*Nassarius gibbosulus*; ~14–17mm) was transported at least 50km to Rhafas Cave, Morocco, and 200km to Oued Djebbana, Bir-et-Ater, Algeria (Bouzouggar et al. 2007; d'Errico et al. 2009; Vanhaeren et al. 2006). In southern Africa, tick (*Nassarius kraussianus*; ~7–11mm) shells have a very similar size and morphology. Generally, they have been found in assemblages close to the coast (d'Errico et al. 2005; Henshilwood et al. 2004; Vanhaeren et al. 2013), but one was transported >95km to Putslaagte 8 possibly during the late MSA 45–33 kya (Mackay et al. 2015). The significance of the marine mollusks in the MSA deposits at VR003 requires further investigation to examine if they could have been used as tools (Szabó and Koppel 2015), containers (Henshilwood et al. 2011), or other purposes (Jerardino and Marean 2010).

#### LAND SNAILS

Land snails (terrestrial gastropods) are preserved throughout the sequence, and for the most part, the sample is well preserved. While a more detailed study is necessary, they appear to overwhelmingly belong to *Trigonephrus* sp. In the Main Area and in TP-III inside the shelter, they present with clear peaks and valleys of density (see Table 18). In the Main Area, Layer 02 was particularly rich in land snails, and inside the shelter, a thick band of land snails was used to demarcate Layer III-13 in the northern part of the square (see Figure 8). These peaks of land snails occur at similar elevations in the site, and so our future excavations at the site will attempt to directly link these two occurrences and

investigate if they represent a stratigraphic phenomenon or a post-depositional one that cross-cuts stratigraphic layers. In contrast, land snails are notably absent in the deepest levels (Layers 05 and lower), and are particularly sparse in the deepest layer, s1, where faunal preservation is good and eland and zebra bones have been identified. Land snails may accumulate in archaeological sites for a number of reasons, and their taphonomic history must be considered carefully before their data yields interpretations. In VR003, the reasons for concentrations of land snails are currently unclear. There is no evidence of burning (see Kinahan and Kinahan 2003) or other human-induced damage, such as repetitive breakage patterns for extraction by humans (as is seen in some Moroccan assemblages: Hutterer et al. 2014). If the land snails can be associated with the archaeological materials, the snails may provide information about subsistence or local environment (see also Langejans et al. 2012). A framework for investigating land snails is better established in northern Africa (Hutterer et al. 2014; Lubell 2004; Lubell et al. 1976; Taylor et al. 2011) and more recently in Europe (Girod 2011; Pablo et al. 2014) than in southern Africa, where comparable assemblages and investigations of this type are rare.

#### BEADS

Twenty-eight OES beads, bead fragments, and bead pre-forms have been found within the VR003 deposits (Table 19). Eight of these were from the surface and near-surface material in the Main Area and are considered to be from the LSA; pieces of pottery and one piece of engraved OES were also found in these deposits. Three of these eight

were unfinished (manufacturing stages following Orton [2008b])—the central perforation was only partially drilled on one broken bead from Layer 02 (Stage IIb, ‘b’ for broken) and two beads, one from Layer 01 and one from Layer 02 were completely drilled through but not yet shaped and smoothed around the edges (Stage III, broken ‘b’ and complete ‘a,’ respectively). Of the five finished beads from the Main Area, one was broken and four were split laterally (planed), likely as a result of post-depositional circumstances (similar flaking of OES surfaces was noticed on non-worked OES from this context, too). In TP-III, eighteen out of twenty OES beads were located in Layers III-1 to III-12 and are considered to be from the LSA. In the complete LSA assemblage, there is little clear patterning in the external diameters of whole beads. However, one intriguing pattern does emerge—all the large and very large beads (>80mm) are broken (see Table 19). This unusual pattern has been recorded at one other Namaqualand site, KK002, 61km northwest of VR003; there the possibility of ritual was considered with large beads having been deliberately broken (Orton 2012). At VR003 the small sample makes interpretation more problematic.

Notably, three beads, two made from OES and one from bone, are derived from MSA contexts. The two OES beads came from III-17 and III-20, late MSA and HP respectively (see Figure 24). The complete bead from III-17 is small, and its surfaces are not flat like typical OES beads from the younger contexts. The bead from III-20 was unfinished; it is a complete pre-form with its central perforation completely drilled (Stage IIIa following Orton 2008b: Table 1). Quite notably, in III-18 there was a single flat bone bead (see Figure 24). It is rectangular rather than round with its diameter being 7.46mm in one direction and 5.86mm in the other. It has an aperture of 1.58mm and a thickness of 1.92mm. The piece is unique because bone beads are very unusual with very few having been found in Namaqualand and because this bead was found in an MSA, particularly an HP, context. In Namaqualand, two broken bone beads were found at KN2001/008C in a mid-Holocene context and two whole beads came from Jakkalsberg N and could be either mid- or late Holocene in age (Dewar 2008; Orton and Halkett 2010). Further north, one small circular bone bead was found at Spitzkloof in an MSA context (Dewar and Stewart 2012). So, along with Spitzkloof, VR003 provides a rare example of a bone bead found in an MSA context. OES beads have been identified from a few other MSA contexts (Miller and Willoughby 2014); however, their antiquity has not always been assured. Direct dating has provided more secure ages for the oldest OES beads, two examples dated to >50,100 and 49,355–46,368 years ago, which were found in MSA contexts in East Africa (Miller and Willoughby 2014). As noted above, numerous shell beads or ornaments have previously been described from MSA contexts at Blombos Cave (d’Errico et al. 2005; Henshilwood et al. 2004; Vanhaeren et al. 2013), and so it may be expected that other materials would also be used as ornaments during the MSA. However, we are concerned that small items are easily displaced post-depositionally in archaeological con-

texts, a problem well noted from other sites (Wendorf et al. 1979; 1984), despite good preservation conditions inside the shelter. To help confirm the association of these items with MSA contexts and their consistent presence in the MSA, we hope that direct dating will confirm their provenience and that further excavation will increase our sample size of OES and bone beads, from which we can draw more clear patterns for interpretation.

## DISCUSSION AND CONCLUSIONS

The sequence at Varsche Rivier (VR) 003 preserves large assemblages of stone artifacts, along with vertebrate fauna, OES, land snails, pigments, a few marine mollusks, OES beads, and one bone bead. We have established two zones of excavation, a Main Area on the terrace and slope of the site, and a small excavation inside the shelter at the top of the site (TP-III). Macro- and micromorphological analysis of the sedimentary sequence reveals different site formation processes and conditions on the slope (colluvial processes, bioturbation, moist conditions) from those inside the shelter (few post-depositional alterations, dry conditions). Inside the shelter, the sedimentary material, and the archaeological material contained within, is in primary context, while on the slope, the disturbances are more variable. In the Main Area, the deepest materials appear to be pre-SB, followed by unifacial points, bifacial points, and backed artifacts, the last overlapping with but also stratigraphically above the former two. Inside the shelter, we have uncovered HP material at the base of the excavated unit, with late MSA above, and capped by late Holocene LSA materials. Certain isolated stone artifacts suggest that the site may have seen occasional use earlier in the Holocene. This sequence makes VR003 one of only a few examples of sites to preserve both SB and HP industries, especially in the context of a more complete MSA sequence.

In addition, the entire sequence preserves faunal remains, which, with larger sample sizes, will provide data on changing habitats, subsistence, and technology. The current MSA faunal sample contains numerous taxa that indicate a much grassier and wetter environment during the Late Pleistocene than during the Holocene, consistent with other environmental reconstructions for the region. Notable finds within the MSA fauna are marine mollusks, which were transported at least 45km, clearly indicating connections with the coast, either through movements or exchange. We know of no other examples of such long distance transport of larger mollusks during the MSA.

Inside the shelter, we found one OES bead, one OES bead preform, and one rectangular bone bead in MSA contexts. A circular bone bead is known from an MSA context at Spitzkloof, but its morphology is quite different (Dewar and Stewart 2012). While small items such as beads can be displaced in bioturbated deposits, we note that the examples from VR003 derive from the relatively undisturbed contexts inside the shelter. The presence of OES beads has often been considered one of the defining characteristics of the LSA. Beyond VR003 and Spitzkloof, OES and bone beads are virtually unknown from MSA sites in southern

Africa. However, in eastern Africa, direct dating of OES beads indicates that they reliably appear in earlier contexts there (Miller and Willoughby 2014). While our sample remains small it is premature to speculate about the significance of these pieces, but if verified with direct dating and a larger sample, they would increase the known spatial and temporal variability of ornamental expression in the MSA and alter our understanding of some aspects of the beginnings of the LSA.

The stone artifact data recovered suggest considerable changes in site use through the sequence and between different areas of the site. Artifact densities are highest during the putative HP and SB, suggesting greater on-site knapping, more frequent visits, lower sedimentation rates, or potentially different combinations of these factors. During the earlier MSA, on-site knapping appears to have been restricted, based on the relatively low frequency of cores and the lower density of artifacts. Notable raw material changes in the deepest excavated areas hint at further well-structured technological shifts but our sample sizes in the lower deposits are relatively small at this time. Fortunately, faunal preservation is good in these deeper deposits and shows the exploitation of large game, such as eland, alcelaphines, and blue antelope. It is worth restating that we have not reached the base of the site with our excavations.

Results from sediment samples submitted for single-grain OSL analysis provide a chronology for the MSA deposits. The sediments surrounding the HP assemblages each provided one sample (one in the Main Area and one in TP-III inside the shelter), which were bracketed by other samples. These samples suggest that the HP industries were deposited 45.7–41.7 kya and that the SB is bracketed between <59.9–45.7 kya. While our results are stratigraphically consistent, they are substantially younger than any previously published SB or HP chronologies (Jacobs et al. 2008; Tribolo et al. 2013). Not a single grain from any of our samples yielded ages comparable with previously published results. Even taking into account evidence for bioturbation in the Main Area, it is unlikely that all grains would be bleached and reworked during this process; at least several grains from the original depositional event would remain visible in the dose distribution.

The timing of HP and SB stone tool production in southern Africa has been a topic of substantial debate in recent years (Feathers 2015; Galbraith 2015; Guérin et al. 2013; Jacobs and Roberts 2015; Jacobs et al. 2008; 2013; Tribolo et al. 2009; 2013). Based on the sequence of fauna, isotopes, and sediments from Klasies River, Deacon argued that the dating of the HP centered on 70 kya (Deacon 1995). Other studies suggested that the HP technocomplex spanned 65–55 kya (Feathers 2002; Grün et al. 1990b; Miller et al. 1999; Valladas et al. 2005; Vogel 2000), with older ages extending to ca. 76 kya at Border Cave (Grün and Beaumont 2001; Grün et al. 1990a). More recently, Jacobs et al. (2008) used single grain OSL age estimates and statistical methods to constrain the timing of HP production to 64.8–59.5 kya. This chronology has since been disputed on the basis of thermoluminescence and OSL ages arising from Diepkloof

Rock Shelter, the subject of a number of studies yielding conflicting results (Feathers 2015; Jacobs and Roberts 2015; Jacobs et al. 2008; Tribolo et al. 2009; 2013). At present, the chronology of the HP, especially at Diepkloof, remains the subject of a range of methodological debates—the precision of the Jacobs et al. (2008) chronology has been called into question on the basis of flawed assumptions regarding dose rate distributions (Guérin et al. 2013), although the mathematical basis for this claim is unsupported (Galbraith 2015). Nevertheless, the problem of beta dose rate heterogeneity is also discussed as a limitation for the VR003 sediments in this paper.

The ages for HP production range from an old chronology of substantial duration extending from early oxygen isotope stage (MIS) 5 through to early MIS 3 (52±5 kya) (Tribolo et al. 2013), to three short-duration revisions of Jacobs et al. (2008) by the same research group (65±3 kya, 69.8±3.0 kya and 62.6±2.7 kya; Jacobs and Roberts 2015), to a chronology of intermediate age ranging from c. 80–63 kya (Feathers 2015). While we do not comment on the accuracy or precision of previously published ages for the HP, the chronology from Tribolo et al. (2013) argues for a longer duration of HP production than suggested by Jacobs et al. (2008), one extending into MIS 3. This argument could be supported by the VR003 chronology, however, the substantially younger ages for the HP at VR003 are distinct from any of these existing chronologies.

There appear to be three obvious possibilities for explaining the technological/temporal patterns observed at VR003 and their similarities/dissimilarities with other sites:

1. Neither the putative SB or HP from VR003 are in fact SB or HP as traditionally defined, but instead belong to some previously unidentified younger industries containing bifacial points and backed artifacts;
2. The VR003 SB and HP are as claimed, but they are significantly younger than the occurrence of these industries at nearby sites such as Diepkloof and Klein Kliphuis, as well as elsewhere across southern Africa; and,
3. The VR003 SB and HP are as claimed, and the age discrepancies between VR003, Diepkloof, southern coastal sites such as Klasies River, Blombos and Pinnacle Point, and Sibudu reflect broad problems in the luminescence-based chronology.

The viability of the first of these possibilities is reinforced by the poorly resolved chrono-cultural sequence in the WRZ in MIS 3 (Avery et al. 2008; Faith 2013; Mackay et al. 2014b). At present, the technological characteristics of the region from 50–25 kya are not well known and it is not implausible that subsequent MSA industries with characteristics superficially similar to the SB and HP recur in the area at earlier and later times. The limited data that are available, however, are not supportive of this proposition. For example, the MSA assemblage antedating 60 kya from the open-air site of Putslaagte 1, located 70km southeast of VR003, entirely lacks bifacial points and backed artifacts (Mackay et al. 2014b). Similarly, the deep sequence of the

Putslaagte 8 rock shelter records a late MSA dating around 40 kya and lacks either of these markers (Mackay et al. 2015). At Boomplaas, though details on the assemblage remain scant, there is no discussion of a recurrence of HP-like technology in the MIS 3 layers and no mention of SB-like assemblages (Deacon 1979).

The VR003 samples also retain similarities with other HP assemblages beyond backed artifacts. Like many other HP assemblages, the HP at VR003 is enriched with silcrete compared to the older and younger material in the site. In addition, notched artifacts with similar forms to those discussed here have been reported as time-restricted components of HP assemblages in sites to the south of VR003 (Brown et al. 2012; Henshilwood et al. 2014; Mackay 2010; Porraz et al. 2013b). However, the backed artifact morphologies from VR003 do lack the classic HP forms, specifically segments; morphological studies of regional bifacial points are required to interrogate such relationships in the SB. More detailed studies of the flaking systems at VR003 may help clarify the relationship of these assemblages with other SB and HP samples or they may not; the SB at Apollo 11, for example, has several quite different characteristics from the SB in sites further south, something that might be explained by its relative isolation (Mackay et al. 2014a). This does not preclude classification of the Apollo 11 assemblage as SB, but rather suggests that it was weakly connected with sites to the south. Given that the ecological setting at VR003 is unlike other documented SB or HP sites and more similar to Apollo 11, the possibility of stronger connections with Apollo 11 further to the north than with Diepkloof closer to the south cannot be precluded. To that end we note that the morphologies of the VR003 backed artifacts potentially have resonance in forms recovered from Apollo 11 (Vogelsang 1998).

The second possibility is that while the SB and HP at VR003 may be classified as such, they occur considerably more recently than like-named units at most other sites, including those within 70km (e.g., Mackay 2010; Mackay et al. 2015; Tribolo et al. 2013). Setting aside issues of systematics<sup>3</sup>, similar issues have been discussed in the context of the relationship between the Aterian and the Maghrebien Mousterian/MSA of northern Africa (e.g., Dibble et al. 2013; Linstädter et al. 2012; Richter et al. 2010; Scerri 2013) and especially with the temporal and stratigraphic succession of (and definition of) the Bordian facies of the Mousterian in southwestern France (e.g., Guibert et al. 2008; Jaubert 2010; Monnier and Missal 2014; Richter et al. 2013). At issue is the extent to which the variants are contemporaneous or reflect consistent cultural change through time (or are poorly defined). The stratigraphic succession of later MSA industries in southern Africa so far has been repetitive and consistent. While for some comparisons sample sizes remain small, where they occur together, earlier MSA assemblages with little retouch and dominated by large, robust, local rocks (usually quartzite or dolerite) never overlie SB assemblages; no SB assemblage has yet been recovered overlying HP; HP assemblages always underlie unifacial point-bearing post-

HP assemblages (when they occur). Together, the diversity of environments (particularly comparing VR003 with Diepkloof and Sibudu—three modern excavations in three divergent environmental settings) at the sites involved and the current differences in available ages could indicate that these successions are unrelated by adaptive or cultural processes. If the ages are all correct, then consistency of the cultural succession in the southern African MSA—and particularly the area of the modern WRZ—effectively becomes an expression of chance.

The final possibility—that the SB and HP at VR003 are culturally and temporally connected to the same industries elsewhere in southern Africa is inconsistent with the available ages. Discussions about the modeling ages produced using OSL and how to handle challenging samples and sites is on-going, and further refinements to the sampling at VR003 and to the method should contribute to resolving the cultural chronology in the region.

Fortunately, our continuing work at VR003 and on the surrounding landscape will provide data with which we can further explore the relationships between chronology, technology, and ecology during the MSA. Our results from the marginal and understudied environment of southern Namaqualand will increase our understanding of behavioral variability in the MSA when compared to the better-studied coastal caves and Cederberg areas because of the contrasting availability of resources.

#### ACKNOWLEDGEMENTS

We thank Petro and Louis Visser for allowing us to work on their land and for facilitating access during our 2009 and 2011 field seasons; their enthusiasm for our research is much appreciated. The excavations were conducted under Heritage Western Cape Permit No. 2009-04-001 to Orton. Our 2011 field season was funded by the Leakey Foundation, the University of California, Davis, the Australian Research Council, and the Australian National University. ACO Associates cc (formerly the University of Cape Town Archaeology Contracts Office) and the Iziko South African Museum (SAM) provided additional support. The Athene Programme of the University of Tübingen provided M. Stahlschmidt with research support. Ntandazo Mjikeliso, Mpakamo Sasa, Peter Stamos, Tim Weaver, and Aara Welz provided invaluable contributions in the field and in the laboratory afterwards. Michael Williams further assisted in the laboratory. Richard Klein participated with faunal identifications. Graham Avery, Sven Ouzman, and Wilhelmina Seconna provided access and assistance at Iziko SAM. Wesley Flear helped with OSL sample collection, and Steffi Hesse (MPI-EVA) provided assistance with OSL sample preparation. Cuan Hahndiek generously provided geological ocher samples from Augsberg, De Hangen, and Kransvlei for our comparative analysis, and Mariya Jenskibayeva and Amor Silva assisted with the pXRF analysis of the ocher. Thoughtful and detailed comments from the journal editor and three reviewers greatly improved the manuscript. Thank you to all.

## ENDNOTES

1. We used a conservation significance cut-off to account for the possibility of Type I errors given the large number of cells ( $n=30$ ) in the contingency table (e.g.,  $p=(0.05/n\text{ cells})=0.001667$ , corresponding to a z-score cut-off of  $\pm 3.144$ ). The same protocol is used when calculating significant departure from expectations in all other tables.
2. Defined here as non-cortical flakes with parallel sides and at least one dorsal ridge which is parallel to the lateral margins over  $>50\%$  of the extant length of the flake. We used this somewhat cumbersome and problematic definition because: a) we did not undertake a metric analysis, precluding use of the typical elongation definition (e.g., length : width  $\geq 2$ ); and, b) because we applied this classification to all flaking products, complete and broken. To expand that second point, broken flakes whether produced by laminar or other means rarely have elongation values exceeding 2:1 in their remnant portion, and thus strict adherence to elongation as the defining attribute of blades would have meant excluding incomplete flaking products from our classification. An elongation-based definition and the concept of 'blade fragment' are hard to reconcile. We will pursue a better definition situated in assessment of reduction systems during future work.
3. If two HP assemblages do not overlap in time, should they both be called HP? And if so, what does the industry mean if its components share no linkages in time, space, or cultural knowledge?

## REFERENCES

- Adamiec, G. and Aitken, M. 1998. Dose-rate conversion factors: update. *Ancient TL* 16, 37–50.
- Andrefsky, W.A.J. 2005. *Lithics: Macroscopic Approaches to Analysis*, 2nd ed. Cambridge University Press, Cambridge.
- Averbough, A. 2000. *Technologie de la matière osseuse travaillée et implications paleoethnologiques: exemples des chaînes d'exploitation du bois de cervidé chez les magdaléniens des Pyrénées*, Paris, Université de Paris I, Thèse de 3ème cycle, 2 vol.
- Avery, G., Halkett, D., Orton, J., Steele, T.E., Tusenius, M., and Klein, R.G. 2008. The Ysterfontein 1 Middle Stone Age Rock Shelter and the evolution of coastal foraging. *South African Archaeological Society Goodwin Series* 10, 66–89.
- Beaumont, P.B. 1978. *Border Cave*, Department of Archaeology. University of Cape Town.
- Bergman, C. and Newcomer, M. 1983. Flint arrowhead breakage: examples from Ksar Akil, Lebanon. *Journal of Field Archaeology* 10, 921–947.
- Bertrand, P. and Texier, J.-P. 1999. Facies and microfacies of slope deposits. *Catena* 35, 99–121.
- Boëda, E. 1995. Levallois: A volumetric construction, methods, a technique. In: Dibble, H.L. and Bar-Yosef, O. (eds.), *The Definition and Interpretation of Levallois Technology*. Prehistory Press, Madison, WI., pp. 41–68.
- Bollong, C.A., Sampson, C.G., and Smith, A.B. 1997. Khoikhoi and Bushman pottery in the Cape Colony: ethnohistory and Later Stone Age ceramics of the South African interior. *Journal of Anthropological Archaeology* 16, 269–229.
- Bollong, C.A., Vogel, J.C., Jacobson, L., Van der Westhuizen, W., and Sampson, C.G. 1993. Direct dating and identity of fibre temper in pre-Contact Bushman (Basarwa) pottery. *Journal of Archaeological Science* 19, 41–55.
- Botter-Jensen, L. 1997. Luminescence techniques: instrumentation and methods. *Radiation Measurements* 27, 749–768.
- Botter-Jensen, L., Bulur, E., Duller, G.A.T., and Murray, A.S. 2000. Advances in luminescence instrument systems. *Radiation Measurements* 32, 523–528.
- Bouzouggar, A., Barton, R.N.E., Vanhaeren, M., d'Errico, F., Collcutt, S.N., Higham, T.F.G., Hodge, E., Parfitt, S.A., Rhodes, E., Schwenninger, J.-L., Stringer, C., Turner, E., Ward, S., Moutmir, A., and Stambouli, A. 2007. 82,000-year-old shell beads from North Africa and implications for the origins of modern human behavior. *Proceedings of the National Academy of Sciences USA* 104, 9964–9969.
- Braithwaite, C.J.R. 1983. Calcrete and other soils in Quaternary limestones: structures, processes and applications. *Journal of the Geological Society London* 140, 351–363.
- Brennan, B.J., Schwarcz, H.P., and Rink, W.J. 1997. Simulation of the gamma radiation field in lumpy environments. *Radiation Measurements* 27, 299–305.
- Bronk-Ramsey, C. 2009. Bayesian analysis of radiocarbon dates. *Radiocarbon* 51, 337–360.
- Brown, K.S., Marean, C.W., Jacobs, Z., Schoville, B.J., Oestmo, S., Fisher, E.C., Bernatchez, J., Karkanas, P., and Matthews, T. 2012. An early and enduring advanced technology originating 71,000 years ago in South Africa. *Nature* 491, 590–593.
- Candy, I., Black, S., Sellwood, B.W., and Rowan, J.S. 2003. Calcrete profile development in quaternary alluvial sequences, southeast Spain. *Earth Surface Processes and Landforms* 28, 169–185.
- Cattelain, P. 1997. Hunting during the Upper Paleolithic: bow, spearthrower, or both. In: Knecht, H. (ed.), *Projectile Technology*. Plenum Press, New York and London, pp. 213–240.
- Chase, B.M. 2010. South African palaeoenvironments during marine oxygen isotope stage 4: a context for the Howiesons Poort and Still Bay industries. *Journal of Archaeological Science* 37, 1359–1366.
- Chase, B.M. and Meadows, M.E. 2007. Late Quaternary dynamics of southern Africa's winter rainfall zone. *Earth-Science Reviews* 84, 103–138.
- Conard, N.J., Porraz, G., and Wadley, L. 2012. What's in a name? Characterising the 'post-Howiesons Poort' at Sibudu. *South African Archaeological Bulletin* 67, 180–199.
- Cornell, R.M. and Schwertmann, U. 2006. *The Iron Oxides: Structure, Properties, Reactions, Occurrences and Uses*. John Wiley & Sons.
- Courty, M.A., Goldberg, P., and Macphail, R. 1989. *Soils and Micromorphology in Archaeology*. Cambridge University Press, Cambridge.
- Cowling, R. and Pierce, S. 1999. *Namaqualand: A Succulent Desert*. Fernwood Press, Vlaeberg, South Africa.
- d'Errico, F., Henshilwood, C.S., Vanhaeren, M., and van Niekerk, K. 2005. *Nassarius kraussianus* shell beads from Blombos Cave: evidence for symbolic behaviour in the Middle Stone Age. *Journal of Human Evolution* 48, 3–24.
- d'Errico, F., Vanhaeren, M., Barton, N., Bouzouggar, A., Mienis, H., Richter, D., Hublin, J.-J., McPherron, S., and

- Lozouet, P. 2009. Additional evidence on the use of personal ornaments in the Middle Paleolithic of North Africa. *Proceedings of the National Academy of Sciences USA* 106, 16051–16056.
- d’Errico, F., Vanhaeren, M., and Wadley, L. 2008. Possible shell beads from the Middle Stone Age layers of Sibudu Cave, South Africa. *Journal of Archaeological Science* 35, 2675–2685.
- Dayet, L., Le Bourdonnec, F.X., Daniel, F., Porraz, G., and Texier, P.J. 2015. Ochre provenance and procurement strategies during the Middle Stone Age at Diepkloof Rock Shelter, South Africa. *Archaeometry*, 58(5), 807–829.
- de la Pena, P., Wadley, L., and Lombard, M. 2013. Quartz bifacial points in the Howiesons Poort of Sibudu. *South African Archaeological Bulletin* 69, 119–136.
- Deacon, H.J. 1979. Excavations at Boomplaas Cave - A Sequence through the Upper Pleistocene and Holocene in South Africa. *World Archaeology* 10, 241–257.
- Deacon, H.J. 1995. Two late Pleistocene-Holocene archaeological depositories from the southern Cape, South Africa. *South African Archaeological Bulletin* 50, 121–131.
- Deacon, J. 1972. Wilton: an assessment after fifty years. *South African Archaeological Bulletin* 27, 10–48.
- Desmet, P.G. 2007. Namaqualand — A brief overview of the physical and floristic environment. *Journal of Arid Environments* 70, 570–587.
- Dewar, G. 2008. *The Archaeology of the Coastal Desert of Namaqualand, South Africa: A Regional Synthesis*. British Archaeological Reports International Series 1761, Oxford.
- Dewar, G. and Stewart, B.A. 2012. Preliminary results of excavations at Spitzkloof Rockshelter, Richtersveld, South Africa. *Quaternary International* 270, 30–39.
- Dibble, H., Marean, C.W., and McPherron, S. 2007. The use of barcodes in excavation projects. *The SAA Archaeological Record* 7, 33–38.
- Dibble, H.L., Aldeias, V., Jacobs, Z., Olszewski, D.I., Rezek, Z., Lin, S.C., Alvarez-Fernández, E., Barshay-Szmidt, C., Hallett-Desguez, E., Reed, D., Reed, K., Richter, D., Steele, T.E., Skinner, A., Blackwell, B., Doronicheva, E., and El-Hajraoui, M. 2013. On the Industrial Attributions of the Aterian and Mousterian of the Maghreb. *Journal of Human Evolution* 64, 194–210.
- Dibble, H.L. and McPherron, S.P. 1995. *Combe-Capelle on CD-ROM*. University of Pennsylvania Museum of Archaeology and Anthropology Press, Philadelphia.
- Dusseldorp, G.L. and Langejans, G.H.J. 2013. Carry that weight: coastal foraging and transport of marine resources during the South African Middle Stone Age. *Southern African Humanities* 25, 105–135.
- Eren, M.I., Diez-Martin, F., and Dominguez-Rodrigo, M. 2013. An empirical test of the relative frequency of bipolar reduction in Beds VI, V, and III at Mumba Rockshelter, Tanzania: implications for the East African Middle to Late Stone Age transition. *Journal of Archaeological Science* 40, 248–256.
- Evans, U. 1994. Hollow Rock Shelter, a Middle Stone Age site in the Cederberg. *Southern African Field Archaeology* 3, 63–73.
- Faith, J.T. 2013. Taphonomic and paleoecological change in the large mammal sequence from Boomplaas Cave, western Cape, South Africa. *Journal of Human Evolution* 65, 715–730.
- Feathers, J. 2015. Luminescence dating at Diepkloof Rock Shelter – new dates from single-grain quartz. *Journal of Archaeological Science* 63, 164–74.
- Feathers, J.K. 2002. Luminescence dating in less than ideal conditions: case studies from Klasies River main site and Duinefontein, South Africa. *Journal of Archaeological Science* 29, 177–194.
- Fischer, A., Vemming Hansen, P., and Rassmussen, P. 1984. Macro and Micro wear traces on lithic projectile points: experimental results and prehistoric examples. *Journal of Danish Archaeology* 3, 19–46.
- Fisher, E.C., Bar-Matthews, M., Jerardino, A., and Marean, C.W. 2010. Middle and Late Pleistocene paleoscape modeling along the southern coast of South Africa. *Quaternary Science Reviews* 29, 1382–1398.
- Fitzsimmons, K., Stern, N., and Murray-Wallace, C. 2014. Depositional history and archaeology of the central Lake Mungo lunette, Willandra Lakes, southeast Australia. *Journal of Archaeological Science* 41, 349–364.
- Galbraith, R.F. 1990. The radial plot: graphical assessment of spread in ages. *International Journal of Radiation Applications and Instrumentation. Part D. Nuclear Tracks and Radiation Measurements* 17, 207–214.
- Galbraith, R.F. 2015. On the mis-use of mathematics: A comment on “How confident are we about the chronology of the transition between Howieson’s Poort and Still Bay?” by Guérin et al. (2013). *Journal of Human Evolution* 80, 184–186.
- Galbraith, R.F. and Green, P.F. 1990. Estimating the component ages in a finite mixture. *Nuclear Tracks and Radiation Measurements* 17, 197–206.
- Galbraith, R.F., Roberts, R.G., Laslett, G.M., Yoshida, H., and Olley, J.M. 1999. Optical dating of single and multiple grains of quartz from Jinnium rock shelter, northern Australia. Part 1, Experimental design and statistical models. *Archaeometry* 41, 339–364.
- Gassin, B., Gibaja, G., Allard, P., Boucherat, T., Claud, E., Clemente, I., Gueret, C., Jacquier, J., Khedayer, R., Marchand, G., Mazzucco, N., Palomo, A., Perales, U., Perrin, T., Philibert, S., Rodriguez, A., and Torchy, L. 2012. Late Mesolithic notched blades From Western Europe and North Africa: technological and functional variability. In: Marreiros, J. and Bicho, N. (eds.), *International Conference in Use-Wear Analysis: Use-Wear*, Cambridge Scholars Publishing, New Castle, pp. 225–231.
- Geneste, J.-M. and Plisson, H. 1990. Technologie fonctionnelle des pointes a cran solutréennes: l’apport des nouvelles données de la Grotte de Combe Sauniere (Dordogne). In: Kozłowski, J. (ed.), *Feuilles de pierre: les industries a` pointes foliacées du Paleolithique supérieur européen*. Actes du Colloque de Cracovie 1989, Université de Liege (ERAUL 42), Liege, pp. 293–320.
- Girod, A. 2011. Land snails from Late Glacial and Early

- Holocene Italian sites. *Quaternary International* 244, 105–116.
- Gliganic, L.A., Jacobs, Z., Roberts, R.G., Domínguez-Rodrigo, M., and Mabulla, A.Z.P. 2012. New ages for Middle and Later Stone Age deposits at Mumba rockshelter, Tanzania: optically stimulated luminescence dating of quartz and feldspar grains. *Journal of Human Evolution* 62, 533–547.
- Gonzalez-Urquijo, J.E. and Ibanez-Estevez, J.J. 2004. *Metodología de análisis funcional de instrumentos tallados en sílex*. Universidad de Deusto, Bilbao.
- Grün, R. and Beaumont, P.B. 2001. Border cave revisited: a revised ESR chronology. *Journal of Human Evolution* 40, 467–482.
- Grün, R., Beaumont, P.B., and Stringer, C.B. 1990a. ESR dating evidence for early modern humans at Border Cave in South Africa. *Nature* 344, 537–540.
- Grün, R., Shackleton, N.J., and Deacon, H.J. 1990b. Electron-spin-resonance dating of tooth enamel from Klasies River Mouth Cave. *Current Anthropology* 31, 427–432.
- Guérin, G. and Mercier, N. 2012. Field gamma spectrometry, Monte Carlo simulations and potential of non-invasive measurements. *Geochronometria* 39, 40–47.
- Guérin, G., Mercier, N., Nathan, R., Adamiec, G., and Lefrais, Y. 2012. On the use of the infinite matrix assumption and associated concepts: a critical review. *Radiation Measurements* 47, 778–785.
- Guérin, G., Murray, A.S., Jain, M., Thomsen, K., and Mercier, N. 2013. How confident are we in the chronology of the transition between Howieson's Poort and Still Bay? *Journal of Human Evolution* 64, 314–317.
- Guibert, P., Bechtel, F., Bourguignon, L., Brenet, M., Couchoud, I., Delagnes, A., Delpech, F., Detrain, L., Duttine, M., Folgado, M., Jaubert, J., Lahaye, C., Lenoir, M., Maureille, B., Texier, J.-P., Turq, A., Vieilleveigne, E., and Villeneuve, G. 2008. Une base de données pour la chronologie du Paléolithique moyen dans le Sud-Ouest de la France. In: Jaubert, J., Bordes, J.-G., and Ortega, I. (eds.), *Les sociétés du Paléolithique dans us Grand Sud-Ouest : nouveaux gisements, nouveaux résultats, nouvelles méthodes*. *Bulletin de la Société Préhistorique Française* 47, pp. 19–40.
- Haberman, S.J. 1973. The analysis of residuals in cross-classified tables. *Biometrics* 29, 205–220.
- Hay, R.L. and Reeder, R.J. 1978. Calcretes of Olduvai Gorge and the Ndolanya Beds of northern Tanzania. *Sedimentology* 25, 649–673.
- Henshilwood, C.S. 2012. Late Pleistocene techno-traditions in Southern Africa: a review of the Still Bay and Howieson's Poort, c. 75–59 ka. *Journal of World Prehistory* 25, 205–237.
- Henshilwood, C.S., d'Errico, F., Marean, C.W., Milo, R.G., and Yates, R. 2001. An early bone tool industry from the Middle Stone Age at Blombos Cave, South Africa: implications for the origins of modern human behavior, symbolism and language. *Journal of Human Evolution* 41, 631–678.
- Henshilwood, C.S., d'Errico, F., van Niekerk, K.L., Coqui-  
not, Y., Jacobs, Z., Lauritzen, S.-E., Menu, M., and García-Moreno, R. 2011. A 100,000-year-old ochre-processing workshop at Blombos Cave, South Africa. *Science* 334, 219–222.
- Henshilwood, C.S., d'Errico, F., Vanhaeren, M., van Niekerk, K.L., and Jacobs, Z. 2004. Middle Stone Age shell beads from South Africa. *Science* 304, 404.
- Henshilwood, C.S., d'Errico, F., and Watts, I. 2009. Engraved ochres from the Middle Stone Age levels at Blombos Cave, South Africa. *Journal of Human Evolution* 57, 27–47.
- Henshilwood, C.S., d'Errico, F., Yates, R., Jacobs, Z., Tribololo, C., Duller, G.A.T., Mercier, N., Sealy, J., Valladas, H., Watts, I., and Wintle, A.G. 2002. Emergence of modern human behavior: Middle Stone Age engravings from South Africa. *Science* 295, 1278–1280.
- Henshilwood, C.S., van Niekerk, K.L., Wurz, S., Delagnes, A., Armitage, S.J., Rifkin, R.F., Douze, K., Keene, P., Haaland, M.M., Reynard, J., Discamps, E., and Mienies, S.S. 2014. Klipdrift Shelter, southern Cape, South Africa: preliminary report on the Howieson's Poort layers. *Journal of Archaeological Science* 45, 284–303.
- Hiscock, P. 2007. Looking the other way. A materialist/technological approach to classifying tools and implements, cores and retouched flakes. In: McPherron, S.P. (ed.), *Tools versus Cores? Alternative Approaches to Stone Tool Analysis*. Cambridge Scholars Publishing, Cambridge, pp. 198–222.
- Hoffman, M.T. and Rohde, R.F. 2007. From pastoralism to tourism: the historical impact of changing land use practices in Namaqualand. *Journal of Arid Environments* 70, 641–658.
- Högberg, A. 2014. Chronology, stratigraphy and spatial distribution of artefacts at Hollow Rock Shelter, Cape Province, South Africa. *South African Archaeological Bulletin* 69, 142–151.
- Högberg, A. and Larsson, L. 2011. Lithic technology and behavioural modernity: new results from the Still Bay site, Hollow Rock Shelter, Western Cape Province, South Africa. *Journal of Human Evolution* 61, 133–155.
- Hogg, A.G., Hua, Q., Blackwell, P.G., Niu, M., Buck, C.E., Guilderson, T.P., Heaton, T.J., Palmer, J.G., Reimer, P.J., Reimer, R.W., Turney, C.S.M., and Zimmerman, S.R.H. 2013. SHCAL13 southern hemisphere calibration, 0–50,000 yearscal BP. *Radiocarbon* 55, 1889–1903.
- Horsburg, K.A. 2008. Wild or domesticated? An ancient DNA approach to canid species identification in South Africa's Western Cape Province. *Journal of Archaeological Science* 35, 1474–1480.
- Humphreys, A.J.B. 1975. Burchell's Rockshelter: The history and archaeology of a Northern Cape rock shelter. *South African Archaeological Bulletin* 30, 3–18.
- Hutterer, R., Linstädter, J., Eiwanger, J., and Mikdad, A. 2014. Human manipulation of terrestrial gastropods in Neolithic culture groups of NE Morocco. *Quaternary International* 320, 83–91.
- Igreja, M. 2009. Use-wear analysis of non-flint stone tools using DIC microscopy and resin casts: a simple and ef-

- fective technique. *Recent functional studies on non flint stone tools: methodological improvements and archaeological inferences*, 23–25 May 2008. Proceedings of the workshop [CD-ROM]. ISBN978-989-20-1803-4, Lisboa (Pa-drão dos Descobrimentos).
- Igreja, M. 2010. *Tracéologie lithique d'un grand habitat gravetien en France: Les unités OP10 et KL19 de la Vigne Brun (Loire)*. Éditions Universitaires Européennes, Sarrebruck, Germany.
- Igreja, M. and Porraz, G. 2013. Functional insights into the innovative Early Howiesons Poort technology at Diepkloof Rock Shelter (Middle Stone Age, South Africa). *Journal of Archaeological Science* 40, 3475–3491.
- Jacobs, Z., Duller, G.A.T., and Wintle, A.G. 2003. Optical dating of dune sand from Blombos Cave, South Africa: II—single grain data. *Journal of Human Evolution* 44, 613–625.
- Jacobs, Z., Hayes, E.H., Roberts, R.G., Galbraith, R.F., and Henshilwood, C.S. 2013. An improved OSL chronology for the Still Bay layers at Blombos Cave, South Africa: further tests of single-grain dating procedures and a re-evaluation of the timing of the Still Bay industry across southern Africa. *Journal of Archaeological Science* 40, 579–594.
- Jacobs, Z. and Roberts, R.G. 2015. An improved single grain OSL chronology for the sedimentary deposits from Diepkloof Rockshelter, Western Cape, South Africa. *Journal of Archaeological Science* 63, 175–192.
- Jacobs, Z., Roberts, R.G., Galbraith, R.F., Deacon, H.J., Grün, R., Mackay, A., Mitchell, P., Vogelsang, R., and Wadley, L. 2008. Ages for the Middle Stone Age of southern Africa: implications for human behavior and dispersal. *Science* 322, 733–735.
- Jacobs, Z., Roberts, R.G., Nespoulet, R., El Hajraoui, M.A., and Debénath, A. 2012. Single-grain OSL chronologies for Middle Palaeolithic deposits at El Mnasra and El Harhoura 2, Morocco: implications for Late Pleistocene human–environment interactions along the Atlantic coast of northwest Africa. *Journal of Human Evolution* 62, 377–394.
- Jarvis, A., Reuter, H.I., Nelson, A., and Guevara, E. 2008. Hole-filled SRTM for the globe Version 4, available from the CGIAR-CSI SRTM 90m Database (<http://srtm.csi.cgiar.org>).
- Jaubert, J. 2010. Les archéoséquences du Paléolithique moyen en Poitou-Charentes. In: Buisson-Catil, J. and Primault, J. (eds.), *Préhistoire entre Vienne et Charente: hommes et sociétés du Paléolithique*. Association des Publications Chauvinoises, Chauvigny, France, pp. 51–55.
- Jerardino, A. and Marean, C.W. 2010. Shellfish gathering, marine paleoecology and modern human behavior: perspectives from cave PP13B, Pinnacle Point, South Africa. *Journal of Human Evolution* 59, 412–424.
- Kamminga, J. 1982. *Over the Edge: Functional Analysis of Australian Stone Tools*. University of Queensland: Occasional Papers in Anthropology 12.
- Kandel, A.W. 2004. Modification of ostrich eggs by carnivores and its bearing on the interpretation of archaeological and paleontological finds. *Journal of Archaeological Science* 31, 377–391.
- Kaplan, J. 1990. The Umhlatuzana Rock Shelter sequence: 100 000 years of Stone Age history. *Natal Museum Journal of Humanities* 2, 1–94.
- Keeley, L.H. 1980. *Experimental Determination of Stone Tool Uses: A Microwear Analysis*. University of Chicago Press, Chicago.
- Keffen, R.H. and Jarvis, M.J.F. 1984. Some measurements relating to ostrich eggs. *Ostrich: Journal of African Ornithology* 55, 182–187.
- Kinahan, J. and Kinahan, J. 2003. Excavation of a late Holocene cave deposit in the southern Namib Desert, Namibia. *Cimbebasia* 18, 1–10.
- Klein, R.G., Avery, G., Cruz-Urbe, K., Halkett, D., Parkington, J.E., Steele, T., Volman, T.P., and Yates, R. 2004. The Ysterfontein 1 Middle Stone Age site, South Africa, and early human exploitation of coastal resources. *Proceedings of the National Academy of Sciences of the United States of America* 101, 5708–5715.
- Klein, R.G. and Cruz-Urbe, K. 1983. Stone Age population numbers and average tortoise size at Byneskranskop Cave 1 and Die Kelders Cave 1, southern Cape Province, South Africa. *South African Archaeological Bulletin* 38, 26–30.
- Kruschke, J.K. 2013. Bayesian estimation supersedes the t test. *Journal of Experimental Psychology-Human Learning and Memory* 142, 573–603.
- Kyriacou, K., Parkington, J.E., Will, M., Kandel, A.W., and Conard, N.J. 2015. Middle and Later Stone Age shellfish exploitation strategies and coastal foraging at Hoedjiespunt and Lynch Point, Saldanha Bay, South Africa. *Journal of Archaeological Science* 57, 197–206.
- Langejans, G.H.J., Dusseldorp, G.L., and Henshilwood, C.S. 2012. Terrestrial gastropods from Blombos Cave, South Africa: research potential. *South African Archaeological Bulletin* 67, 120–123.
- Levi-Sala, I. 1986. A word of caution: use wear and post-depositional surface modification. *Journal of Archaeological Science* 13, 229–244.
- Levi-Sala, I. 1988. Processes of polish formation on flint tool surfaces. In: Beyries, S. (ed.), *Industries lithiques: tracéologie et technologie*. British Archaeological Reports International Series, 411, Oxford, pp. 83–98.
- Levi-Sala, I. 1993. Use-wear traces: processes of development and post-depositional alterations. In: Anderson, P., Beyries, S., Otte, M., and Plisson, H. (eds.), *Traces et fonction: les gestes retrouvés*, 8–10 Dec 1990. Actes du Colloque International de Liège (ERAUL), Liège, pp. 401–416.
- Linstädter, J.R., Eiwanger, J., Mikdad, A., and Weniger, G.-C. 2012. Human occupation of Northwest Africa: a review of Middle Palaeolithic to Epipalaeolithic sites in Morocco. *Quaternary International* 274, 158–174.
- Lombard, M., Wadley, L., Deacon, J., Wurz, S., Parsons, I., Mohapi, M., Swart, J., and Mitchell, P. 2012. South African and Lesotho Stone Age sequence updated. *South African Archaeological Bulletin* 67, 120–144.

- Lubell, D. 2004. Prehistoric edible land snails in the circum-Mediterranean: the archaeological evidence. In: Brugal, J.-P. and Desse, J. (eds.), *Petits animaux sociétés humaines: du complément alimentaire aux ressources utilitaires*. Éditions APDCA, Antibes, pp. 77–98.
- Lubell, D., Hassan, F.A., Gautier, A., and Ballais, J.-L. 1976. The Caspian escargotiers. *Science* 191, 910–920.
- Mackay, A. 2006. A characterisation of the MSA stone artefact assemblage from the 1984 excavation at Klein Kliphuis, Western Cape. *South African Archaeological Bulletin* 61, 181–189.
- Mackay, A. 2009. *History and Selection in the Late Pleistocene Archaeology of the Western Cape, South Africa*, School of Archaeology and Anthropology. Australian National University, Canberra.
- Mackay, A. 2010. The Late Pleistocene archaeology of Klein Kliphuis rockshelter, Western Cape, South Africa: 2006 excavations. *South African Archaeological Bulletin* 65, 132–147.
- Mackay, A. 2011. Nature and significance of the Howiesons Poort to post-Howiesons Poort transition at Klein Kliphuis rockshelter, South Africa. *Journal of Archaeological Science* 38, 1430–1440.
- Mackay, A. 2012. Report on excavations at Klipfonteinrand, 2011/12. Report submitted to Heritage Western Cape, Cape Town, South Africa.
- Mackay, A. 2016. Technological change and the importance of variability: the Western Cape of South Africa from MIS 5 to MIS 2. In: Jones, S. and Stewart, B.A. (eds.), *Africa from MIS 6-2: Population Dynamics and Paleoenvironments*. Springer, Dordrecht.
- Mackay, A., Jacobs, Z., and Steele, T.E. 2015. Pleistocene archaeology and chronology of Putslaagte 8 (PL8) rockshelter, Western Cape, South Africa. *Journal of African Archaeology* 13, 71–98.
- Mackay, A., Orton, J., Schwartz, S., and Steele, T.E. 2010. Soutfontein (SFT)-001: Preliminary report on an open-air site rich in bifacial points, southern Namaqualand, South Africa. *South African Archaeological Bulletin* 65, 84–95.
- Mackay, A., Stewart, B.A., and Chase, B.M. 2014a. Coalescence and fragmentation in the late Pleistocene archaeology of southernmost Africa. *Journal of Human Evolution* 72, 26–51.
- Mackay, A., Sumner, A., Jacobs, Z., Marwick, B., Bluff, K., and Shaw, M. 2014b. Putslaagte 1 (PL1), the Doring River, and the later Middle Stone Age in southern Africa's Winter Rainfall Zone. *Quaternary International* 350, 43–58.
- Mackay, A. and Welz, A. 2008. Engraved ochre from a Middle Stone Age context at Klein Kliphuis in the Western Cape of South Africa. *Journal of Archaeological Science* 35, 1521–1532.
- Manhire, A. 1993. A report on the excavations at Faraoskop Rock Shelter in the Graafwater district of the southwestern Cape. *Southern African Field Archaeology* 2, 2–23.
- Manning, J. 2008. *Namaqualand*. Briza Publications, Pretoria.
- Marean, C.W., Bar-Matthews, M., Bernatchez, J., Fisher, E., Goldberg, P., Herries, A.I.R., Jacobs, Z., Jerardino, A., Karkanas, P., Minichillo, T., Nilssen, P.J., Thompson, E., Watts, I., and Williams, H.M. 2007. Early human use of marine resources and pigment in South Africa during the Middle Pleistocene. *Nature* 448, 905–907.
- McPherron, S., Dibble, H.L., and Goldberg, P. 2005. *Z. Geoarchaeology* 20, 243–262.
- McPherron, S.P. and Dibble, H.L. 2002. *Using Computers in Archaeology: A Practical Guide*. McGraw-Hill, Boston.
- Mejdahl, V. 1979. Thermoluminescence dating: beta-dose attenuation in quartz grains. *Archaeometry* 21, 61–72.
- Miller, C.E. 2015. *Formation Processes, Paleoenvironments, and Settlement Dynamics at the Paleolithic Cave Sites of Hohle Fels and Geißenklösterle: A Geoarchaeological and Micro-morphological Perspective*. Kerns-Verlag: Tübingen.
- Miller, G.H., Beaumont, P.B., Deacon, H.J., Brooks, A.S., Hare, P.E., and Jull, A.J.T. 1999. Earliest modern humans in southern Africa dated by isoleucine epimerization in ostrich eggshell. *Quaternary Science Reviews* 18, 1537–1548.
- Miller, J.M. and Willoughby, P.R. 2014. Radiometrically dated ostrich eggshell beads from the Middle and Later Stone Age of Magubike Rockshelter, southern Tanzania. *Journal of Human Evolution* 74, 118–122.
- Minichillo, T. 2005. *Middle Stone Age Lithic Study, South Africa: An Examination of Modern Human Origins*. Department of Anthropology, University of Washington, Seattle.
- Mitchell, P. 1988a. Human adaptations in South Africa during the Last Glacial maximum. In: Bower, J. and Lubell, D. (eds.), *Prehistoric Cultures and Environments in the Late Quaternary of Africa*. British Archaeological Reports International Series, Oxford, pp. 163–196.
- Mitchell, P. 1988b. The Late Pleistocene Early Microlithic assemblages of southern Africa. *World Archaeology* 20, 27–39.
- Mitchell, P. 2014. The canine connection II: dogs and southern African herders. *Southern African Humanities* 26, 1–19.
- Monnier, G.F. and Missal, K. 2014. Another Mousterian debate? Bordian facies, chaîne opératoire technocomplexes, and patterns of lithic variability in the western European Middle and Upper Pleistocene. *Quaternary International* 350, 59–83.
- Mooney, S.D., Geiss, C., and Smith, M.A. 2003. The use of mineral magnetic parameters to characterize archaeological ochres. *Journal of Archaeological Science* 30, 511–523.
- Mourre, V., Villa, P., and Henshilwood, C.S. 2010. Early use of pressure flaking on lithic artifacts at Blombos Cave, South Africa. *Science* 330, 659–662.
- Murray, A.S. and Wintle, A.G. 2000. Luminescence dating of quartz using an improved single-aliquot regenerative-dose protocol. *Radiation Measurements* 32, 57–73.
- Murray, A.S. and Wintle, A.G. 2003. The single aliquot regenerative dose protocol: potential for improvements in reliability. *Radiation Measurements* 37, 377–381.

- Myers, N., Mittermeier, R.A., Mittermeier, C.G., da Fonseca, G.A.B., and Kent, J. 2000. Biodiversity hotspots for conservation priorities. *Nature* 403, 853–858.
- Nathan, R.P., Thomas, P.J., Jain, M., Murray, A.S., and Rhodes, E.J. 2003. Environmental dose rate heterogeneity of beta radiation and its implications for luminescence dating: Monte Carlo modelling and experimental validation. *Radiation Measurements* 37, 305–313.
- Odell, G.H. 1978. Préliminaires d'une analyse fonctionnelle des pointes microlithiques de Bergumermeer (Pays Bas). *Bulletin de la Société Préhistorique Française* 75, 37–49.
- Odell, G. and Odell-Vereecken, F. 1980. Verifying the reliability of lithic use wear assessment by 'blind tests': the low power approach. *Journal of Field Archaeology* 7, 87–120.
- Orton, J. 2006. The Later Stone Age lithic sequence at Elands Bay, Western Cape, South Africa: raw materials, artefacts and sporadic change. *Southern African Humanities* 18, 1–28.
- Orton, J. 2008a. A late Pleistocene microlithic Later Stone Age assemblage from coastal Namaqualand, South Africa. *Before Farming* 2008/1, article 3.
- Orton, J. 2008b. Later Stone Age ostrich eggshell bead manufacture in the Northern Cape, South Africa. *Journal of Archaeological Science* 35, 1765–1775.
- Orton, J. 2012. *Late Holocene archaeology in Namaqualand, South Africa: hunter-gatherers and herders in a semi-arid environment*. School of Archaeology. University of Oxford, Oxford.
- Orton, J. and Halkett, D. 2010. Stone tools, beads and a river: two Holocene microlithic sites at Jakkalsberg in the northwestern Richtersveld, Northern Cape. *South African Archaeological Bulletin* 65, 13–25.
- Orton, J. and Mackay, A. 2008. New excavations at Klein Kliphuis rock shelter, Cederberg Mountains, Western Cape, South Africa: the late Holocene deposits. *South African Archaeological Bulletin* 63, 69–76.
- Orton, J., Mackay, A., Schwartz, S., and Steele, T.E. 2011a. Archaeology in the Knersvlakte, Southern Namaqualand. Poster presentation. The Association of Southern African Professional Archaeologists, Mbabane, Swaziland.
- Orton, J., Mackay, A., Schwartz, S., and Steele, T.E. 2011b. Two Holocene rock shelter deposits from the Knersvlakte, southern Namaqualand, South Africa. *Southern African Humanities* 23, 109–150.
- Orton, J., Mitchell, P., Klein, R.G., Steele, T.E., and Horskburg, K.A. 2013. Early date for cattle from Namaqualand, South Africa: implications for the origins of herding in southern Africa. *Antiquity* 87, 108–120.
- Fernández-López de Pablo, J., Badal, E., Ferrer García, C., Martínez-Ortí, A., and Sanchis Serra, A. 2014. Land snails as a diet diversification proxy during the Early Upper Palaeolithic in Europe. *PLoS ONE* 9, e104898.
- Parkington, J., Poggenpoel, C., Rigaud, J.-P., and Texier, P.-J. 2006. From tool to symbol: the behavioural context of intentionally marked ostrich eggshell from Diepkloof, Western Cape. In: d'Errico, F. and Backwell, L. (eds.), *From Tools to Symbols: From Early Hominids to Modern Humans*. Witwatersrand University Press, Johannesburg, pp. 475–492.
- Parkington, J.E. 2003. Middens and moderns: shellfishing and the Middle Stone Age of the Western Cape, South Africa. *South African Journal of Science* 99, 243–247.
- Parkington, J.E. and Poggenpoel, C. 1971. Excavations at De Hangen 1968. *South African Archaeological Bulletin* 26, 3–36.
- Parkington, J.E. and Poggenpoel, C. 1987. Diepkloof Rock Shelter. In: Parkington, J.E. and Hall, M. (eds.), *Papers in the Prehistory of the Western Cape, South Africa*. British Archaeological Reports 332, Oxford, pp. 269–293.
- Plisson, H. 1985. *Etude fonctionnelle d'outillages lithiques préhistoriques par l'analyse des micro-usures : recherche méthodologique et archéologique*. Université Paris I, Paris.
- Plug, I. 2006. Aquatic animals and their associates from the Middle Stone Age levels at Sibudu. *Southern African Humanities* 18, 289–299.
- Popelka-Filcoff, R.S., Miksa, E.J., Robertson, J.D., Glascock, M.D., and Wallace, H. 2008. Elemental analysis and characterization of ochre sources from Southern Arizona. *Journal of Archaeological Science* 35, 752–762.
- Popelka-Filcoff, R.S., Robertson, J.D., Glascock, M.D., and Descantes, C. 2007. Trace element characterization of ochre from geological sources. *Journal of Radioanalytical and Nuclear Chemistry* 272, 17–27.
- Porráz, G., Igreja, M., and Texier, P.-J. 2015. Développement sur une discontinuité technique dans la séquence Howiesons Poort de l'Abri Diepkloof (Afrique du sud). In: Conard, N. and Delagnes, A. (eds.), *Settlement Dynamics of the Middle Paleolithic and Middle Stone Age* (vol. IV). Kerns Verlag Tubingen, pp. 77–103.
- Porráz, G., Parkington, J.E., Rigaud, J.-P., Miller, C.E., Poggenpoel, C., Tribolo, C., Archer, W., Cartwright, C.R., Charrié-Duhaut, A., Dayet, L., Igreja, M., Mercier, N., Schmidt, P., Verna, C., and Texier, P.-J. 2013a. The MSA sequence of Diepkloof and the history of southern African Late Pleistocene populations. *Journal of Archaeological Science* 40, 3542–3552.
- Porráz, G., Texier, P.-J., Archer, W., Piboule, M., Rigaud, J.-P., and Tribolo, C. 2013b. Technological successions in the Middle Stone Age sequence of Diepkloof Rock Shelter, Western Cape, South Africa. *Journal of Archaeological Science* 40, 3376–3400.
- Prescott, J.R. and Hutton, J.T. 1994. Cosmic ray contributions to dose rates for luminescence and ESR dating: large depths and long term variations. *Radiation Measurements* 23, 497–500.
- Rabenhorst, M.C. and Wilding, L.P. 1986. Pedogenesis on the Edwards Plateau, Texas: III. New model for the formation of petrocalcic horizons. *Soil Science Society of America Journal* 50, 693–699.
- Richter, D., Dibble, H., Goldberg, P., McPherron, S., Niven, L., Sandgathe, D., Talamo, S., and Turq, A. 2013. The late Middle Palaeolithic in Southwest France: new TL dates for the sequence of Pech de l'Azé IV. *Quaternary*

- International* 294, 160–167.
- Richter, D., Moser, J., Nami, M., Eiwanger, J., and Mikdad, A. 2010. New chronometric data from Ifri n'Ammar (Morocco) and the chronostratigraphy of the Middle Palaeolithic in the Western Maghreb. *Journal of Human Evolution* 59, 672–679.
- Riel-Salvatore, J. and Barton, M. 2004. Late Pleistocene technology, economic behavior, and land-use dynamics in southern Italy. *American Antiquity* 69, 257–274.
- Rigaud, J.-P., Texier, P.-J., Parkington, J.E., and Poggenpoel, C. 2006. Le mobilier Stillbay et Howiesons Poort de l'abri Diepkloof. La chronologie du Middle Stone Age sud-africain et ses implications. *Comptes Rendus Palevol* 5, 839–849.
- Rodnight, H. 2008. How many equivalent dose values are needed to obtain a reproducible distribution? *Ancient TL* 26, 3–10.
- Rose, J., Lee, J.A., Kemp, R.A., and Harding, P.A. 2000. Palaeoclimate, sedimentation and soil development during the Last Glacial Stage (Devensian), Heathrow Airport, London, UK. *Quaternary Science Reviews* 19, 827–847.
- Rudner, J. 1979. The use of stone artefacts and pottery among the Khoisan peoples in historic and proto-historic times. *South African Archaeological Bulletin* 34, 3–17.
- Rufer, D. and Preusser, F. 2009. Potential of autoradiography to detect spatially resolved radiation patterns in the context of trapped charge dating. *Geochronometria* 24, 1–13.
- Scerri, E.M.L. 2013. The Aterian and its place in the North African Middle Stone Age. *Quaternary International* 300, 111–130.
- Schmidt, C., Pettke, T., Preusser, F., Rufner, D., Kasper, H.U., and Hilgers, A. 2012. Quantification and spatial distribution of dose rate relevant elements in silex used for luminescence dating. *Quaternary Geochronology* 12, 65–73.
- Schmidt, C., Rufner, D., Preusser, F., Krbetschek, M., and Hilgers, A. 2013. The assessment of radionuclide distribution in silex by autoradiography in the context of dose rate determination for thermoluminescence dating. *Archaeometry* 55(3), 407–422.
- Schmidt, I., Ossendorf, G., Hensel, E., Bubenzer, O., Eichhorn, B., Gessert, L., Gwasira, G., Henselowsky, F., Imalwa, E., Kehl, M., Rethemeyer, J., Röpke, A., Sealy, J., Stengel, I., and Tussenius, M. 2016. New investigations at the Middle Stone Age site Pockenbank Rock Shelter, Namibia. *Antiquity Project Gallery* 90 (<https://doi.org/10.15184/aqy.2016.165>).
- Schmidt, P. and Mackay, A. 2016. Why was silcrete heat-treated in the Middle Stone Age? An early transformative technology in the context of raw material use at Mertenhof Rock Shelter, South Africa. *PLoS One* 11, e0149243.
- Schwartz, S., Orton, J., Mackay, A., and Steele, T.E. 2012. Middle Stone Age archaeology in open-air surface sites along the Varsche River (Southern Namaqualand, South Africa). Poster presentation, Society for American Archaeology, Memphis, Tennessee.
- Semenov, S.A. 1964. *Prehistoric Technology*. Adams and Dart, London.
- Singer, R. and Wymer, J. 1982. *The Middle Stone Age at Klasies River Mouth in South Africa*. The University of Chicago Press, Chicago.
- Skead, C.J. 1980. *Historical Mammal Incidence in the Cape Province*. Volume 1: *The Western and Northern Cape*. Department of Nature and Environmental Conservation, Cape Town.
- Soriano, S., Villa, P., and Wadley, L. 2007. Blade technology and tool forms in the Middle Stone Age of South Africa: the Howiesons Poort and post-Howiesons Poort at Rose Cottage Cave. *Journal of Archaeological Science* 34, 681–703.
- Steele, T.E. and Klein, R.G. 2005/06. Mollusk and tortoise size as proxies for stone age population density in South Africa: Implications for the evolution of human cultural capacity. *Munibe (Antropologia - Arkeologia)* 57, 221–237.
- Steele, T.E. and Klein, R.G. 2013. The Middle and Later Stone Age faunal remains from Diepkloof Rock Shelter, Western Cape, South Africa. *Journal of Archaeological Science* 40, 3453–3462.
- Steele, T.E., Mackay, A., Orton, J., and Schwartz, S. 2012. Varsche Rivier 003, a new Middle Stone Age site in southern Namaqualand, South Africa. *South African Archaeological Bulletin* 67, 108–119.
- Stoops, G. 2003. *Guidelines for Analysis and Description of Soil and Regolith Thin Sections*. Soil Science Society of America, Madison, WI.
- Stoops, G., Marcelino, V., and Mees, F. 2010. *Interpretation of Micromorphological Features of Soils and Regoliths*. Elsevier Science, Amsterdam.
- Szabó, K. and Koppel, B. 2015. Limpet shells as unmodified tools in Pleistocene Southeast Asia: an experimental approach to assessing fracture and modification. *Journal of Archaeological Science* 54, 64–76.
- Taylor, V.K., Barton, R.N.E., Bell, M., Bouzouggar, A., Collcutt, S.N., Black, S., and Hogue, J.T. 2011. The Epipaleolithic (Iberomaurusian) at Grotte des Pigeons (Taforalt), Morocco: a preliminary study of the land Mollusca. *Quaternary International* 244, 5–14.
- Team, R.D.C. 2014. *R: A Language and Environment for Statistical Computing*. Retrieved from <http://www.R-project.org/>.
- Texier, P.-J., Porraz, G., Parkington, J., Rigaud, J.-P., Poggenpoel, C., Miller, C., Tribolo, C., Cartwright, C., Coudenneau, A., Klein, R., Steele, T., and Verna, C. 2010. A Howiesons Poort tradition of engraving ostrich eggshell containers dated to 60,000 years ago at Diepkloof Rock Shelter, South Africa. *Proceedings of the National Academy of Sciences USA* 107, 6180–6185.
- Texier, P.-J., Porraz, G., Parkington, J., Rigaud, J.-P., Poggenpoel, C., and Tribolo, C. 2013. The context, form and significance of the MSA engraved ostrich eggshell collection from Diepkloof Rock Shelter, Western Cape, South Africa. *Journal of Archaeological Science* 40, 3412–

- 3431.
- Thackeray, J.F. 1979. An analysis of faunal remains from archaeological sites in southern South West Africa (Namibia). *South African Archaeological Bulletin* 34, 18–33.
- Thompson, J.C. and Henshilwood, C.S. 2014. Tortoise taphonomy and tortoise butchery patterns at Blombos Cave, South Africa. *Journal of Archaeological Science* 41, 214–229.
- Thomsen, K.J., Murray, A.S., and Bøtter-Jensen, L. 2005. Sources of variability in OSL dose measurements using single grains of quartz. *Radiation Measurements* 39, 47–61.
- Tribolo, C., Mercier, N., Douville, E., Joron, J.-L., Reyss, J.-L., Rufer, D., Cantin, N., Lefrais, Y., Miller, C.E., Porraz, G., Parkington, J., Rigaud, J.-P., and Texier, P.-J. 2013. OSL and TL dating of the Middle Stone Age sequence at Diepkloof Rock Shelter (South Africa): a clarification. *Journal of Archaeological Science* 40, 3401–3411.
- Tribolo, C., Mercier, N., Valladas, H., Joron, J.L., Guibert, P., Lefrais, Y., Selo, M., Texier, P.-J., Rigaud, J.-P., Porraz, G., Poggenpoel, C., Parkington, J.E., Texier, J.-P., and Lenoble, A. 2009. Thermoluminescence dating of a Stillbay-Howiesons Poort sequence at Diepkloof Rock Shelter (Western Cape, South Africa). *Journal of Archaeological Science* 36, 730–739.
- Tringham, R., Cooper, G., Odell, G., Voytek, B., and Whitman, A. 1974. Experimentation in the formation of edge damage: a new approach to lithic analysis. *Journal of Field Archaeology* 1, 171–196.
- Valladas, H., Wadley, L., Mercier, N., Tribolo, C., Reyss, J.-L., and Joron, J.-L. 2005. Contribution of thermoluminescence on lithics to the chronology of MSA layers of Rose Cottage Cave. *South African Journal of Science* 101, 169–174.
- van Rissen, W.J. and Avery, G. 1992. The late Holocene deposits at Klein Kliphuis Shelter, Cedarberg, Western Cape Province. *South African Archaeological Bulletin* 47, 34–43.
- van Vliet-Lanoë, B. 2010. Frost action. In: Stoops, G., Marcelino, V., and Mees, F. (eds.), *Interpretation of Micro-morphological Features of Soils and Regoliths*. Elsevier Science, Amsterdam, pp. 81–108.
- Vanhaeren, M., d’Errico, F., Stringer, C.B., James, S.L., Todd, J.A., and Mienis, H.K. 2006. Middle Paleolithic shell beads in Israel and Algeria. *Science* 312, 1785–1788.
- Vanhaeren, M., d’Errico, F., van Niekerk, K.L., Henshilwood, C.S., and Erasmus, R.M. 2013. Thinking strings: additional evidence for personal ornament use in the Middle Stone Age at Blombos Cave, South Africa. *Journal of Human Evolution* 64, 500–517.
- Villa, P., Soressi, M., Henshilwood, C.S., and Mourre, V. 2009. The Still Bay points of Blombos Cave (South Africa). *Journal of Archaeological Science* 36, 441–460.
- Villa, P., Soriano, S., Teyssandier, N., and Wurz, S. 2010. The Howiesons Poort and MSA III at Klasies River main site, Cave 1A. *Journal of Archaeological Science* 37, 630–655.
- Vogel, J.C. 2000. Radiometric dates for the Middle Stone Age in South Africa. In: Tobias, P.V.T., Raath, M.A., Moggi-Cecchi, J., and Doyle, G.A. (eds.), *Humanity from African Naissance to Coming Millennia*. University of Florence, Florence.
- Vogelsang, R. 1998. *Middle-Stone-Age-Fundstellen in Südwest-Namibia*. Heinrich Barth Institut, Köln.
- Vogelsang, R., Richter, J., Jacobs, Z., Eichhorn, B., Linseele, V., and Roberts, R.G. 2010. New excavations of Middle Stone Age deposits at Apollo 11 Rockshelter, Namibia: stratigraphy, archaeology, chronology and past environments. *Journal of African Archaeology* 8, 185–218.
- Volman, T.P. 1978. Early archaeological evidence for shellfish collecting. *Science* 201, 911–913.
- Volman, T.P., 1981. *The Middle Stone Age in the Southern Cape*. University of Chicago, Chicago.
- Wadley, L. 1993. The Pleistocene Later Stone Age south of the Limpopo River. *Journal of World Prehistory* 7, 243–296.
- Wadley, L. 2005a. Ochre crayons or waste products? Replications compared with MSA “crayons” from Sibudu Cave, South Africa. *Before Farming* 2005, 1–12.
- Wadley, L. 2005b. Putting ochre to the test: replication studies of adhesives that may have been used for hafting tools in the Middle Stone Age. *Journal of Human Evolution* 49, 587–601.
- Wadley, L. 2005c. A typological study of the Final Middle Stone Age stone tools from Sibudu Cave, Kwazulu-Natal. *South African Archaeological Bulletin* 60, 51–63.
- Wadley, L. 2007. Announcing a Still Bay industry at Sibudu Cave, South Africa. *Journal of Human Evolution* 52, 681–689.
- Wadley, L. 2012. Two ‘moments in time’ during Middle Stone Age occupations of Sibudu, South Africa. *Southern African Humanities* 24, 79–97.
- Wadley, L. and Harper, P. 1989. Rose Cottage Cave revisited: Malan’s Middle Stone Age collection. *South African Archaeological Bulletin* 44, 23–32.
- Watts, I. 2002. Ochre in the Middle Stone Age of Southern Africa: ritualised display or hide preservative? *South African Archaeological Bulletin* 57, 1–14.
- Webley, L.E. 2002. The re-excavation of Spoegrivier Cave on the west coast of South Africa. *Annals of the Eastern Cape Museums* 2, 19–49.
- Wendorf, F., Schild, R., Close, A.E., Donahue, D.J., Jull, A.J.T., Zabel, T.H., Wieckowska, H., Kobusiewicz, M., Issawi, B., and El Hadidi, N. 1984. New radiocarbon dates on the cereals from Wadi Kubbania. *Science* 225, 645–646.
- Wendorf, F., Schild, R., El Hadidi, N., Close, A.E., Kobusiewicz, M., Wieckowska, H., Issawi, B., and Haas, H. 1979. Use of barley in the Egyptian Late Paleolithic. *Science* 205, 1341–1347.
- Will, M., Mackay, A., and Phillips, N. 2015. Implications of Nubian-like core reduction systems in southern Africa for the identification of early modern human dispersals. *PLoS One* 10, e0131824.
- Wright, V.P. and Tucker, M.E. 1991. *Calcretes*. Blackwell Scientific Publications.

- Wurz, S. 1999. The Howiesons Poort backed artefacts from Klasies River: an argument for symbolic behavior. *South African Archaeological Bulletin* 54, 38–50.
- Wurz, S. 2002. Variability in the Middle Stone Age lithic sequence, 115,000–60,000 years ago at Klasies River, South Africa. *Journal of Archaeological Science* 29, 1001–1015.
- Wurz, S. 2012. The significance of MIS 5 shell middens on the Cape coast: a lithic perspective from Klasies River and Ysterfontein 1. *Quaternary International* 270, 61–69.
- Wurz, S. 2013. Technological trends in the Middle Stone Age of South Africa between MIS 7 and MIS 3. *Current Anthropology* 54, S305–S319.